Christof Weber

Electron energy loss spectroscopy with plasmonic nanoparticles

Diplomarbeit

zur Erlangung des akademischen Grades eines
Magisters
an der naturwissenschaftlichen Fakultät der
Karl-Franzens-Universität Graz

Betreuer: Ao. Univ. Prof. Mag. Dr. Ulrich Hohenester

Institut für Physik
Fachbereich Theoretische Physik
Karl-Franzens-Universität Graz

2011

Danksagung

Zuallererst möchte ich mich bei meinen Eltern **Karin Weber** und **Reinhold Weber** und Großeltern **Erika Raschke** und **Kurt Raschke** bedanken. Ohne deren Unterstützung wäre mein Studium unmöglich gewesen. Auch meiner Schwester **Tania Weber** und dem Rest meiner Familie gebührt ein außerordentlicher Dank.
Ein ganz spezieller und riesengroßer Dank geht an meine Freundin **Stefanie Judmaier**, die mich während der ganzen Diplomarbeitszeit unterstützt und motiviert hat. Vielen lieben Dank!
Natürlich geht ein riesengroßes Dankeschön an meinen Betreuer **Ao. Univ. Prof. Mag. Dr. Ulrich Hohenester**, einen großartigen Menschen und Physiker, der mich sehr gut durch die Diplomarbeitszeit geführt hat und von dem ich viel lernen durfte. Vielen Dank für die gute Betreuung und die hilfreichen Beantwortungen meiner hoffentlich nicht allzu lästigen Fragen!
Weiters möchte ich mich bei meinen Freund/innen und Kolleg/innen **Jürgen Waxenegger**, **Hajreta Softic**, **Andreas Trügler**, **Peter Leitner**, **Florian Wodlei**, **Faruk Geles**, **Gernot Schaffernak**, **Sudhir Sundaresan** und **Hannes Bergthaller** und vielen mehr für die moralische und sonstige Unterstützung, die mich gut durch´s Studium gebracht hat, bedanken.
Ein spezieller Dank für´s Durchlesen und Korrigieren meiner Arbeit, sowie wertvolle Tipps geht an **Andreas Trügler**, **Jürgen Waxenegger**, **Stefanie Judmaier** und **Florian Wodlei**.
Ich widme diese Diplomarbeit meiner verstorbenen Großmutter **Erika Raschke** und meinem verstorbenen Freund **Armin Fritz**.

Contents

1. Introduction 5
- 1.1. Definition of a nanoparticle . . . 6
- 1.2. Short introduction to electron energy loss spectroscopy . . . 9

2. Theoretical Basics 13
- 2.1. Fundamentals of Plasmonics . . . 13
  - 2.1.1. Dielectric function . . . 14
  - 2.1.2. Plasmons . . . 20
  - 2.1.3. Surface plasmons . . . 21
- 2.2. Basic elements of classical electrostatics . . . 31
  - 2.2.1. Poisson equation . . . 32
  - 2.2.2. Uniqueness of the solution of the Poisson equation . . . 34
  - 2.2.3. The Green function . . . 34
  - 2.2.4. Multipole expansion . . . 37
- 2.3. Boundary integral method . . . 38

3. Electron energy loss probability for a dielectric sphere 43
- 3.1. Theory of Electron Energy Loss Spectroscopy . . . 43
  - 3.1.1. Classical dielectric formalism . . . 43
- 3.2. Electron trajectory past sphere . . . 45
- 3.3. Electron trajectory penetrating sphere . . . 51
  - 3.3.1. Electron energy loss probability for an electron penetrating the sphere . . . 53

4. Numerical methods 55
- 4.1. Boundary element method . . . 55
- 4.2. External excitation . . . 58
  - 4.2.1. Electron beam passing by the nanoparticle . . . 58
  - 4.2.2. Electron beam penetrating the nanoparticle . . . 60
- 4.3. Energy loss . . . 61

5. Results 63
- 5.1. Comparison between Mie-theory and boundary element method . . . 63
  - 5.1.1. Plots against the energy . . . 63

5.1.2. Plots against the impact parameter 76
5.2. Drude versus full dielectric function 79

6. Summary and Outlook 86

A. Appendix 87
A.1. Laplace equation in spherical coordinates 87
A.2. Associated Legendre functions and spherical harmonics 88
A.2.1. Orthogonality relation, completeness and symmetry of the spherical harmonics 89
A.2.2. Expansion of functions in spherical harmonics 90
A.3. The law of Gauss 90
A.4. Maxwell equations 93

1. Introduction

Since the first years of the last century charged particles have been used to obtain information about the properties and nature of the materials under study [1]. In this diploma thesis we focus on the use of electrons as a probe for the determination of the characteristics of the materials under consideration. Other kinds of particles have been also used as a testing probe, e.g. photons (i.e. illumination with light). Since this thesis is about electron energy loss spectroscopy (EELS) it will be concerned with the usage of electrons as a testing probe. As we will see in the upcoming chapters the materials considered in this thesis are metallic nanoparticles or plasmonic nanoparticles respectively.

In this diploma thesis we aim at obtaining EELS-spectra for these metallic nanoparticles interacting with an electron beam. Due to this interaction the metallic nanoparticles exhibit plasmon excitations while the electrons lose energy in an inelastic process. They are also called plasmonic nanoparticles. We will only shortly mention the plasmon excitations at this stage and will go into further detail in the next chapter. Excitations of the bulk of the material correspond to bulk plasmon excitations. They correspond to collective excitations of the electron charge density in the bulk with the well-known plasma frequency $\omega_p = \sqrt{\frac{4\pi ne^2}{m}}$. e is the electron charge and m the electron mass. There also occur collective excitations corresponding to oscillations of the electron charge density at the interface between two dielectric media. They are known as surface plasmons. If they are confined in all three spatial dimensions to the particle surface they are called particle plasmons (see section 2.1.3 for further details).

In section 1.1 we provide the definition of a nanoparticle and in order to give motivation for the importance of the topic we will shortly focus on the usage of nanoparticles in various fields of application. Then we give a short and general introduction to EELS.

Let us start a short historical overview with Ernest Rutherford (* 30. August 1871), who used α-particles to study the structure of atoms, in the year 1911. In 1927 Clinton Joseph Davisson (* 22. October 1881) and Lester Germer (* 10. October 1896) [2] already used electrons as a testing probe [1]. Another example for the use of electrons is the famous experiment by James Franck (* 26. August 1882) and Gustav Ludwig Hertz (* 22. July 1887). In 1948 G. Rutherman already used electrons in transmission mode and he obtained electron energy loss spectra

in the range of a few eV ([1], [3]).
The first proposal and demonstration of EELS in TEMs (transmission electron microscopes) has already been made in the year 1944 by Hillier and Baker [4]. Notice that 1904 Leithäuser [5] was the first to exploit the energy loss of electrons during their transition through a thin foil [6].
Using electrons in transmission mode means that an electron beam is transmitted through a specimen. The electrons interact with the specimen while passing through it. From this interaction one obtains an image of the specimen. The energy losses of the electrons due to the inelastic scattering process caused by the interaction can be interpreted in terms of what caused the energy loss. The inelastic interactions include phonon excitations (phonons are the quanta of lattice vibrations of a solid), Cerenkov radiation or plasmon excitations. The latter are the ones relevant in this diploma thesis.
The device for the use of electrons in this way is the transmission electron microscope, TEM in short. In transmission electron microscopy the spatial resolution is much higher than in light microscopes because electrons have a small De Broglie wave length. A scanning transmission electron microscope (STEM) (see figure 1.1) uses spatially focalised electrons transmitted across the target. The electron beam is focussed into a narrow spot. It is scanned over the specimen in a raster (for further details see [1] and [7] and section 1.1).

1.1. Definition of a nanoparticle

Nanoparticles

Nanoparticles are small clusters of a few or several million atoms or molecules. Their name concerns their size which lies in the range of 1 up to 100 nanometers. 1 nanometer is 10^{-9} meters. The nanoparticle behaves as a whole unit in terms of its properties. There exists no strict dividing line between a nanoparticle and a non-nanoparticle. Nanoparticles have different properties compared to the bulk material. Properties that distinguish a nanoparticle from the bulk material typically emerge at a length scale under 100 nanometers. So the guiding line for the definition of a nanoparticle is certainly its length scale [8]. Examples for such structures are fullerenes or carbon nanotubes. Several types of metallic and semiconducting nanoparticles have been synthesized and there exist many more examples which won't be mentioned in this diploma thesis.

When dealing with nanoparticles we are situated at mesoscopic scales of physics. Objects belonging to this scale lie between the macroscopic and the microscopic world. At the macroscopic level one is dealing with bulk materials and the lower limit is roughly the size of single atoms. The microscopic world is subject to quantum mechanics. Mesoscopic and macroscopic objects both contain a large number of atoms. Macroscopic objects are described by classical mechanics whereas mesoscopic objects feel the influence of quantum effects and thus are subject of quantum mechanics. This means that a mesoscopic object - like a nanoparticle - has quantum mechanical properties, in contrast to a macroscopic object. An example for this is a conducting wire. Its conductance increases with its diameter when we are in macroscopic scales. But on the mesoscopic level the conductance of the wire is quantized; this means that the increase of the conductance occurs in discrete steps. In applied mesoscopic physics one aims at the construction of nano-devices. Since the systems under study in mesoscopic physics are usually of a size about 100 nanometers up to 1000 nanometers it has a close connection with nanotechnology. Nevertheless, in this diploma thesis we are going to use a classical or at least semiclassical formalism. The reason why we can do that and neglect the quantum mechanical effects will be further explained in chapter 2.

We already know that the approximate upper limit for the size of a nanoparticle is 100 nanometers which is still beyond the diffraction limit of light. This property is very practicable for applications in packaging, cosmetics or coatings. Nanoparticles are used in fields such as computer industry or the pharmaceutical industry. They are also used in biotechnology, microelectronics, interplanetary sciences or biochemistry [6]. But all these topics are too far off from this diploma thesis. For further details see [8], [9].

Metallic nanoparticles

This thesis focuses on plasmonic nanoparticles (metallic nanoparticles), i.e. particles which exhibit plasmon and surface plasmon excitations when they are excited. Surface plasmons occur at the interface of vacuum or a material with a positive dielectric constant and a material with a negative dielectric constant. The latter are usually metals.

Examples for applications of nanoparticles

Now let us start mentioning the various fields of application for nanoparticles. Although the focus of this work are metallic nanoparticles it is quite important to gain an introductory insight into the various possible applications of nanoparticles. The main scientific area where nanoparticles are used nowadays is nanotechnology. One of the best examples to illustrate the importance of science on the nanometer length scale is the future use of nanoparticles in medicine. Nanoparticles may be an important weapon in the fight against cancer. One could control the doses of medication used in chemotherapy much better. The dose would be lower but much more targeted at the position of the tumour. So there would be less side effects than for classical chemotherapy and one would not harm the healthy cells. A great advantage would be that the nanoparticles are biodegradable [10]. Scientists have already successfully tested this procedure on a culture of cancer cells [11].

Gold nanostructures are also used for pregnancy tests. The particles are spread along the test strip and coupled with antibodies, which marks the nanoparticles. This mark becomes visible through white light: the particles glow in colour. The antibody realizes a hormone which gives notice of a starting pregnancy. If this hormone is contained in the urine, the nano-gold-particles build up in the vision panel of the pregnancy test and produce a red stripe due to a shift of plasmon resonances through a change of the dielectric environment [12].

Another possible field of application for nanoparticles in the future could be the cleaning of wastewater. One wants to build nanoparticles for the detoxification of contaminated water. In this case detoxification means decomposition of halogenous organic materials into molecules which are not toxic and easily decomposable and organic. Since the risks and effects of nanoparticles for living cells and so for human beings are not fully understood this technique is not in use yet [13].

Nanotechnology or nanoparticles respectively are also used in car paint. Nanoparticles make the car paint more resistent against scratches. Mercedes for instance uses a car paint which shall look very new even if its very old. The small particles (ceramic particles mixed with the nano-car paint) form a much denser net structure as a usual car paint. The aim of the scientists is that one cannot permanently deform the car paint, i. e. that the net which forms the car paint dodges mechanical strain and goes back to the original form. One also thinks about self-repairing car paint. If it becomes scratched open then nanocapsules become scratched open too and set free a substance which restores the car paint. Even surfaces which are water- and oil-repellent are in process of planning. Dust does not stick to these surfaces [14].

Nanoparticles can also be found in food. Antibacterial silver particles, particles as an anticaking agent for packet soup or nanocapsules in vitamin compound are a few examples [15]. Reportedly nanoparticles in the milkshake make it more creamy and healthier [16].

Nanosilver in T-shirts or socks lowers the smell of sweat and has disinfecting effects. With modern washing agent one can make the clothes with 30 degrees as clean as with 60 degrees [17].

Nanoparticles are also used in sun tan lotion [9] to improve the protection of the skin. The solar radiation is reflected and the risks for skin cancer are lowered. They also prevent the generation of the white film which is present if one uses

standard sun tan lotion [18]. But there are discussions about the safety of this usage of nanoparticles because the effects of the nanoparticles in the sun tan lotion on the human body are not yet fully understood. Maybe they could have harmful effects for the cells in the human brain [19].
We won´t go into more detail about all this because these topics are too far off from the actual topic of this diploma thesis. As mentioned above it is about EELS, i.e. the aim of this diploma thesis is to derive electron energy loss spectra for the interaction of a metallic nanoparticle with an external electron beam. One will see more about the calculation of these EELS-spectra in chapter 3 and 4.
In the upcoming section we will give a definition of a nanoparticle and the nanometer length scale in order to know what such particles are and on which length scales we are operating.

1.2. Short introduction to electron energy loss spectroscopy

In electron energy loss spectroscopy (EELS) one shoots an electron beam onto a certain material under study. It´s aim is to study the characteristics and nature of electronic excitations in a solid body (metallic nanoparticle) [1]. The electrons of the beam lie in a narrow and known range of kinetic energy. When they collide with the specimen they undergo scattering. Some of them are inelastically scattered and therefore they lose energy. This energy loss can be measured with a spectrometer. By interpreting the spectrum one gets information about the structure of the material and its chemical properties [20]. This is often carried out in a transmission electron microscope (TEM). In other words one wants to get information about the properties of structured materials with low-energy-excitations by fast electrons [6] (kinetic energies of about 100 to 300 keV).
For EELS in STEM (Scanning transmission electron microscopy) one has two types of losses. One of them are excitations of the core electrons at well-defined energies, ranging from 100 to 2000 eV [1]. The spatial resolution is governed by the parameter $\frac{v}{\omega}$. This means that it lies on atomic scales and one can identify atoms in thin crystals or can gain chemical information of selected parts of the material under study [1]. Then there are the losses caused by excitations of valence electrons. They are more intense spectral losses and correspond to collective excitations. These excitations are equivalent to coherent oscillations of the electronic charge density in the bulk (bulk plasmons) and occur with the so-called plasma frequency $\omega_p = \sqrt{\frac{4\pi n e^2}{m}}$. Oscillations of the electronic charge density at the surface are surface plasmons [1]. Surface and bulk plasmons are excited at energies of a few eV to about 50 eV. The valence electron energy losses are produced by the

excitation of surface and bulk plasmons [1].

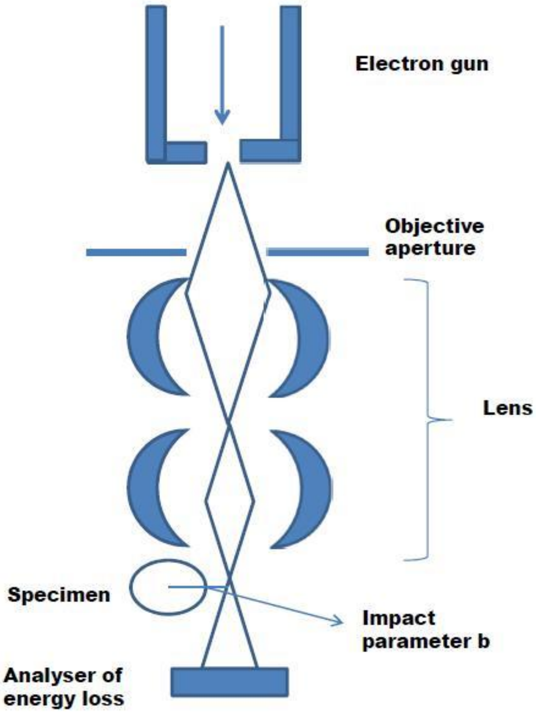

Figure 1.1.: Schematic representation of a STEM (Scanning Transmission Electron Microscope) [1].

Figure 1.1 shows a schematic representation of a STEM. At the top there is an emission source emanating electrons. This electron gun is connected to a high voltage source and with enough current it will begin to emit the electrons by so-called thermionic or field electron emission. The electron gun shoots the electrons through an objective aperture. The lense system of the microscope is used to focus the electron beam onto the specimen. The electrons are flying along the z-direction which lies perpendicular to the impact parameter b, which is defined as the distance from the center of the specimen to the electron beam. The electrons are collected in the analyser. It can be used in two different ways:

- Fixed energy ω: The specimen is scanned for different impact parameters b [1].
- Fixed impact parameter b: EELS is performed and one obtains different types of losses, mainly core and valence losses [1].

What is the main advantage of using electrons rather than light in the investigation of the nanoworld in nanotechnology? When using a simple light microscope one uses photons as a testing probe for the material under study. So a light microscopes maximum resolution is limited by the relatively large wavelength of the photons λ, and by the numerical aperture of the microscope [21]. Electrons have a short wavelength (about 0.1 nanometer for electrons of 100 keV) [1]. For electron microscopes the spatial resolution can be down to the atomic level (i.e. nanometer resolution) while the energy resolution usually is about 1 eV. One is able to make images with high resolution by scanning the probe with an extremely well focussed electron beam and by analysing the reflected and secondary emitted electrons [1]. It can be decreased to 0.1 eV if one makes the electron beam monochromatic. This is the best resolution one can get up to now ([6], [20]).

The electron microscope focuses the electron beams on points within the nanometer length scale onto the observed target (e.g. metallic nanoparticles). By the analysis of the electron energy loss and the detection of the emitted radiation one aims at:

- Making pictures of the nanoworld.
- Investigation of the excitations of the target (e.g. nanoparticles or bulk materials).

The last of these two points is important to learn something about how these small objects (i.e. the target) evolve dynamically. The excitations are relevant in fields such as encoding of and manipulating information and are applied in molecular biology. The **main goal** is to perform spectroscopy at the smallest possible length scale and at the highest possible energy resolution [6].

Electron microscopes are the best possibility to investigate localised and extended excitations with spatial details on a sub-nanometer length scale and with an energy resolution of less than 0.1 eV in each material [6]. These microscopes are very sensible for surfaces and lead to information about the bulk-properties of a material. Their main advantage is their high spatial resolution which currently cannot be achieved by any other technique [6].

EELS experiments lead to information of the electronical band structure, give information about plasmons in the regions of low energy and about the chemical identity with atomic resolution; this chemical identity is encoded in the core losses [6]. They are of great relevance in the following scientific areas for instance:

1. Biochemistry
2. Interplanetary science
3. Micro electronics

4. Medicine

The scattering of the electrons takes place due to interaction with atoms in the solid. This interaction is of Coulomb form because the nucleii in the atoms, the electrons in the atom and the incident electrons are all charged particles [20]. As mentioned above the incident electrons are either scattered elastically or inelastically. For quasi-elastic scattering the exchanged amount of energy is so small that it usually cannot be measured with a TEM-EELS-system. The reason for this is, that the electron is scattered by the nucleus of the atom. The mass of the nucleus is much higher than the electrons mass and so the energy exchange is small. What causes inelastic scattering is the interaction between the electrons in the atom and the incident electron. An example of an excitation in this case are plasmon excitations. Even before entering a specimen the electric charge of the incident electron polarizes the specimens surface which leads to surface plasmon excitations. If the electron beam penetrates the specimen there are also volume or bulk plasmon excitations present which constitutes a negative contribution to the energy loss probability of the electrons coming from the so-called **begrenzungs-effect**. In chapter 2 we will find out more about plasmons and surface plasmons and in chapter 3 the begrenzungs-effect will be mentioned again. More information about this effect can be found in [7] and [22].

In the upcoming chapters we will be concerned with the following forms of excitations:

Bulk plasmons in a source-free metal

- Their magnetic field is zero, $\boldsymbol{B} = 0$.
- Their electrical field is longitudinal, $\boldsymbol{\nabla} \times \boldsymbol{E} = 0$

Hence they fulfill the Maxwell equations trivially if the permittivity vanishes.

Surface plasmons

- They are confined to the interfaces between metals and dielectrics.
- Their magnetic fields are unequal to zero.
- They are transversal, i.e. $\boldsymbol{\nabla} \cdot \boldsymbol{E} = 0$ in each homogeneous region of space which is separated by the interface on which the plasmons are defined.

2. Theoretical Basics

In this chapter we will provide the mathematical and theoretical basics for this diploma thesis. Section 2.1 will be about the basic concepts of plasmonics. We are going to start with a general section about the dielectric function. In the last part of this section we will derive the dielectric function for a semiclassical model, the Drude model, which leads us to the Drude form of the dielectric function, valid for a free electron gas. The dielectric function is essential for the description of metallic nanoparticles. Then we will introduce surface plasmons and particle plasmons. The other two basic ingredients for the theoretical description of EELS are provided in chapter 3. There we will see how to describe the electron beam and the interaction between the electrons and the particle.
In section 2.2 we are going to introduce some basic concepts of classical field theory needed in chapter 3 for the calculation of the electron energy loss probability for an electron passing by a sphere or going through it. Some more basic concepts of classical electrodynamics can be found in the appendix.
The last part of this chapter is dedicated to the boundary integral method.

2.1. Fundamentals of Plasmonics

What we are going to do in this section is to describe basic concepts of an emerging scientific field known as "Plasmonics" (see [23] for further details). This field consists of the study of plasmon resonances and has influence on many experimental situations in nanotechnology. The first form of plasmon excitations with which we will be concerned are the volume or bulk plasmons, which are usually referred to as plasmons in the literature ([24], [25]). They are the collective excitations of the conduction electrons in a metal. Then we will introduce surface plasmons. They are plasmons confined to the surface between a dielectric and a metal. Finally, we will discuss particle plasmons which are most relevant for this diploma thesis. They are surface plasmons in metallic nanoparticles, such as gold or aluminium nanospheres. This section is based on [23].

2.1.1. Dielectric function

The dielectric function is one of the basic quantities in electrodynamics. It describes the response of a system (in our case a metallic nanoparticle) to external excitations (plane wave or electron beam), i.e. it describes the effect of an external electromagnetic field on a polarizable medium. In the dielectric formalism all the information about the target (the nanoparticle) in an EELS-experiment excited by the external electron beam is contained in this dielectric response function [7]. For vacuum or for a small frequency range a medium is non-dispersive. Otherwise a medium is dispersive and because of that a general dielectric function has to be momentum and frequency dependent: $\varepsilon = \varepsilon(\boldsymbol{k}, \omega)$ where ω is the frequency and $\boldsymbol{k}$ is the wave vector (momentum).
In this diploma thesis we consider the so-called optical approximation and neglect the dependence of ε on the momentum $\boldsymbol{k}$. This limit, i.e. $\boldsymbol{k} \to 0$, is the long wavelength limit and is also called quasi-static approximation. Then the dielectric function is $\varepsilon(0, \omega) \cong \varepsilon(\omega)$. The local approach $\varepsilon(\boldsymbol{k} = 0, \omega)$ can be used because the very fast electrons in the beam only transfer small momentum k in the inelastic interaction process [1], i.e.:

$$k = \frac{\omega}{v} \approx 0.1 \text{ nm}^{-1} \tag{2.1}$$

So we can neglect dispersion effects.
At this point it is convenient to mention that we will consider the electron as a classical point particle when deriving the energy loss probability (see chapter 3 for further details).

The Maxwell equations for macroscopic electromagnetism in Gaussian units are:

$$\boldsymbol{\nabla} \cdot \boldsymbol{D} = 4\pi \rho_{ext} \tag{2.2}$$

$$\boldsymbol{\nabla} \cdot \boldsymbol{B} = 0 \tag{2.3}$$

$$\boldsymbol{\nabla} \times \boldsymbol{E} = -\frac{1}{c}\frac{\partial \boldsymbol{B}}{\partial t} \tag{2.4}$$

$$\boldsymbol{\nabla} \times \boldsymbol{H} = \frac{4\pi}{c}\boldsymbol{j}_{ext} + \frac{1}{c}\frac{\partial \boldsymbol{D}}{\partial t} \tag{2.5}$$

The following table gives the definitions of the terms entering the Maxwell equations:

$\boldsymbol{B}$ ...	magnetic induction or magnetic flux density
$\boldsymbol{H}$ ...	magnetic field
$\boldsymbol{D}$ ...	dielectric displacement
$\boldsymbol{E}$ ...	electrical field
ρ_{ext} ...	external charge density
$\boldsymbol{j}_{ext}$ ...	external current density
c ...	speed of light

We are using Gaussian units throughout this diploma thesis. For a detailed discussion of unit systems in classical field theory consult the fabulous book of John David Jackson [26].

The total charge density is given by:

$$\rho_{tot} = \rho_{ext} + \rho \tag{2.6}$$

The total current density is given by:

$$\boldsymbol{j}_{tot} = \boldsymbol{j}_{ext} + \boldsymbol{j} \tag{2.7}$$

The external charge and current densities ρ_{ext} and $\boldsymbol{j}_{ext}$ drive the system. ρ and $\boldsymbol{j}$ are the responses of the system to the external excitation.

Now we introduce the polarisation $\boldsymbol{P}$ and the magnetisation $\boldsymbol{M}$. We get:

$$\boldsymbol{D} = E + 4\pi\boldsymbol{P} \tag{2.8}$$

$$\boldsymbol{H} = \boldsymbol{B} - 4\pi\boldsymbol{M} \tag{2.9}$$

Here we only consider non-magnetic media. Because of that we set $\boldsymbol{M} = 0$. $\boldsymbol{P}$ describes the electric dipole moment per unity volume in the material. $\boldsymbol{P}$ is caused by the alignment of microscopic dipoles with the electrical field.

$$\boldsymbol{\nabla} \cdot \boldsymbol{P} = -4\pi\rho \tag{2.10}$$

The continuity equation

$$\boldsymbol{\nabla} \cdot \boldsymbol{j} = -\frac{\partial \rho}{\partial t} \tag{2.11}$$

says that charge is conserved. From this charge conservation it follows that

$$4\pi\boldsymbol{j} = -\frac{\partial \boldsymbol{P}}{\partial t} \tag{2.12}$$

Now we plug

$$\boldsymbol{D} = \boldsymbol{E} + 4\pi\boldsymbol{P} \tag{2.13}$$

into

$$\boldsymbol{\nabla}\cdot\boldsymbol{D} = 4\pi\rho_{ext} \tag{2.14}$$

and get

$$\boldsymbol{\nabla}\cdot\boldsymbol{E} = 4\pi\rho_{tot} \tag{2.15}$$

In the following we will consider linear, isotropic and non-magnetic media.
We define:

$$\boldsymbol{D} = \varepsilon\boldsymbol{E} \tag{2.16}$$

$$\boldsymbol{B} = \mu\boldsymbol{H} \tag{2.17}$$

ε is the dielectric constant or relative permittivity and μ is the relative permeability of the non-magnetic medium ($\mu = 1$ throughout) [23].
We express $\boldsymbol{D} = \varepsilon\boldsymbol{E}$ through the dielectric susceptibility χ:

$$\boldsymbol{P} = \chi\boldsymbol{E} \tag{2.18}$$

$$\boldsymbol{E} + 4\pi\boldsymbol{P} = (1 + 4\pi\chi)\boldsymbol{E} = \varepsilon\boldsymbol{E} \tag{2.19}$$

$$4\pi\chi\cdot\left(\frac{1}{\chi} + 1\right) = \varepsilon \tag{2.20}$$

$$\varepsilon = 1 + 4\pi\chi \tag{2.21}$$

The current density can be expressed through the conductivity σ:

$$\boldsymbol{j} = \sigma\boldsymbol{E} \tag{2.22}$$

This relation, as well as

$$\boldsymbol{D} = \varepsilon\boldsymbol{E} \tag{2.23}$$

are only valid for linear media without dispersion in time and space.
The optical response of metals depends on the frequency ω and possibly on the wave vector $\boldsymbol{k}$ too. Because of that we have to take into account the non-locality in time and space by generalising the linear relations in the following way:

$$\boldsymbol{D}(\boldsymbol{r}, t) = \int dt' d\boldsymbol{r}' \varepsilon(\boldsymbol{r} - \boldsymbol{r}', t - t')\boldsymbol{E}(\boldsymbol{r}', t') \tag{2.24}$$

$$\boldsymbol{j}(\boldsymbol{r}, t) = \int dt' d\boldsymbol{r}' \sigma(\boldsymbol{r} - \boldsymbol{r}', t - t')\boldsymbol{E}(\boldsymbol{r}', t') \tag{2.25}$$

We assume homogeneity for our material system, i. e. the response functions only depend on the differences between the space and time coordinates $\boldsymbol{r}-\boldsymbol{r}'$ and $t-t'$. For a local response, the response functions are proportional to a δ-function. Then we get the original formulas without the integrals.
If we make a Fourier transformation with respect to $\int dt d\boldsymbol{r} e^{i(\boldsymbol{k}\boldsymbol{r}-\omega t)}$ of the above equations the convolutions are changed to multiplications. By doing this we split the fields into single plane wave parts with wave vector $\boldsymbol{k}$ and frequency ω.
We get:

$$\boldsymbol{D}(\boldsymbol{k},\omega) = \varepsilon(\boldsymbol{k},\omega)\boldsymbol{E}(\boldsymbol{k},\omega) \tag{2.26}$$

$$4\pi\boldsymbol{j}(\boldsymbol{k},\omega) = \sigma(\boldsymbol{k},\omega)\boldsymbol{E}(\boldsymbol{k},\omega) \tag{2.27}$$

Now we use

$$\boldsymbol{D} = \boldsymbol{E} + 4\pi\boldsymbol{P} \tag{2.28}$$

and

$$4\pi\boldsymbol{j} = \frac{\partial\boldsymbol{P}}{\partial t} \tag{2.29}$$

and equation (2.27) as well as the change from $\frac{\partial}{\partial t}$ to $-i\omega$ from the Fourier transform to get the final result for the frequency dependent dielectric function:

$$\boxed{\varepsilon(\boldsymbol{k},\omega) = 1 + \frac{4\pi i\sigma(\boldsymbol{k},\omega)}{\omega}} \tag{2.30}$$

For the limit of optical frequencies we have a spatially local response for metals:

$$\varepsilon(\boldsymbol{k}=0,\omega) = \varepsilon(\omega) \tag{2.31}$$

This is valid as long as the wave length λ is larger than characteristical dimensions (for instance the mean free path of the electrons) of the material. As we have already mentioned for the metallic nanoparticles considered in this diploma thesis the wavelength of light λ (the wavelength of the electromagnetic field interacting with the metallic nanoparticle) is larger than the particle dimensions thus justifying the usage of the quasistatic approximation, i.e. neglecting the dependence on momentum (equation (2.31)).
In general we have complex valued functions of the frequency ω:

$$\varepsilon(\omega) = \varepsilon_1(\omega) + i\varepsilon_2(\omega) \tag{2.32}$$

$$\sigma(\omega) = \sigma_1(\omega) + i\sigma_2(\omega) \tag{2.33}$$

$Re(\sigma)$ dictates the magnitude of the absorption and $Im(\sigma)$ contributes to ε_1, i.e. to the magnitude of the polarisation.
Now we combine the following two equations:

$$\nabla \times \boldsymbol{E} = -\frac{1}{c}\frac{\partial \boldsymbol{B}}{\partial t} \tag{2.34}$$

$$\nabla \times \boldsymbol{H} = \frac{4\pi}{c}\boldsymbol{j}_{ext} + \frac{1}{c}\frac{\partial \boldsymbol{D}}{\partial t} \tag{2.35}$$

where we assume that $\boldsymbol{j}_{ext} = 0$, i.e there is no external perturbation.
We get:

$$\nabla \times \nabla \times \boldsymbol{E} = -\frac{1}{c^2}\frac{\partial^2 \boldsymbol{D}}{\partial t^2} \tag{2.36}$$

After a Fourier transformation we have:

$$\boldsymbol{k} \cdot (\boldsymbol{k}\boldsymbol{E}) - k^2 \cdot \boldsymbol{E} - k^2 \cdot \boldsymbol{E} = -\varepsilon(\boldsymbol{k}, \omega)\frac{\omega^2}{c^2}\boldsymbol{E} \tag{2.37}$$

where c is the velocity of light in vacuum.

- transversal waves, $\boldsymbol{k} \cdot \boldsymbol{E} = 0$:

$$k^2 = \varepsilon(\boldsymbol{k}, \omega)\frac{\omega^2}{c^2} \tag{2.38}$$

- longitudinal waves:

$$\varepsilon(\boldsymbol{k}, \omega) = 0 \tag{2.39}$$

  Longitudinal collective oscillations only occur for frequencies that correspond to zeros of $\varepsilon(\omega)$.

Dielectric function of the free electron gas

In a wide frequency range one can describe the optical properties of metals with a "plasma model". In this model a gas of free electrons with number density n moves against the rigid background of positive ion cores.
The **plasma model** contains no details of the lattice potential or the interaction of electrons with electrons. Instead one plugs several aspects of the band structure into the effective optical mass of each electron [23]. The response of the system to the applied electromagnetic field results in an oscillation of the electrons. Their

movement is damped by collisions. These collisions occur with a certain characteristical collision frequency

$$\gamma = \frac{1}{\tau} \tag{2.40}$$

where τ is the relaxation time of the free electron gas. For room temperature it lies approximately at 10^{-14} seconds

$$\tau \approx 10^{-14}\ \mathrm{s} \tag{2.41}$$

From this it follows that

$$\gamma = 100\ \mathrm{THz} \tag{2.42}$$

The **equation of motion** for an electron of the plasma sea, which is exposed to an external electrical field $\boldsymbol{E}$ is

$$m\ddot{\boldsymbol{x}} + m\gamma \cdot \dot{\boldsymbol{x}} = -e \cdot \boldsymbol{E} \tag{2.43}$$

We assume that

$$\boldsymbol{E}(t) = \boldsymbol{E}_0 \cdot e^{-i\omega t} \tag{2.44}$$

From this we get a particular solution, which describes the oscillations of the electron:

$$\boldsymbol{x}(t) = \boldsymbol{x}_0 \cdot e^{-i\omega t}\boldsymbol{E}(t) \tag{2.45}$$

$\boldsymbol{x}_0$ is the complex amplitude. Via the following formula

$$\boldsymbol{x}(t) = \frac{e}{m\left(\omega^2 + i\gamma\omega\right)} \tag{2.46}$$

this amplitude contains all phase shifts between $\boldsymbol{E}$ and the response of the material system.

The electrons are displaced by the influence of the electrical field. The displaced electrons contribute to the macroscopic polarisation $\boldsymbol{P} = -ne\boldsymbol{x}$ through

$$\boldsymbol{P} = -\frac{e^2 n}{m\left(\omega^2 + i\gamma\omega\right)} \cdot \boldsymbol{E} \tag{2.47}$$

We plug this expression into $\boldsymbol{D} = \boldsymbol{E} + 4\pi\boldsymbol{P}$ and get

$$\boldsymbol{D} = \left(1 - \frac{\omega_p^2}{\omega^2 + i\gamma\omega}\right) \cdot \boldsymbol{E} \tag{2.48}$$

where ω_p is the plasma frequency:

$$\omega_p^2 = \frac{4\pi n e^2}{m} \tag{2.49}$$

where n is an electron charge density.
This yields the formula for the dielectric function of a free electron gas:

$$\varepsilon(\omega) = 1 - \frac{\omega_p^2}{\omega^2 + i\gamma\omega} \tag{2.50}$$

It has a real and an imaginary part:

$$\varepsilon(\omega) = \varepsilon_1(\omega) + i\varepsilon_2(\omega) \tag{2.51}$$

The real and imaginary parts are:

$$\begin{aligned} \varepsilon_1(\omega) &= 1 - \frac{\omega_p^2\tau^2}{1+\omega^2\tau^2} && (2.52) \\ \varepsilon_2(\omega) &= \frac{\omega_p^2 \cdot \tau}{\omega\left(1+\omega^2\tau^2\right)} && (2.53) \end{aligned}$$

Here we consider frequencies $\omega < \omega_p$ since the plasmon resonances which we consider lie below the bulk plasmon frequency ω_p.
For high frequencies near ω_p we have $\omega\tau >> 1$. Then damping is negligible and $\varepsilon(\omega)$ is mostly real

$$\varepsilon(\omega) = 1 - \frac{\omega_p^2}{\omega^2} \tag{2.54}$$

This is the dielectric function of the undamped free electron plasma.
For gold, silver and copper we have to extend the free electron model. This is caused by the fact that the d-band is close to the Fermi surface and generates a residual polarisation of the ion cores:

$$\boldsymbol{P}_\infty = (\varepsilon_\infty - 1)\,\boldsymbol{E} \tag{2.55}$$

ε_∞ lies in the following range:

$$1 \leq \varepsilon_\infty \leq 10 \tag{2.56}$$

$\varepsilon_\infty = 10$ is the value for gold. The modified Drude dielectric function then reads as follows:

$$\varepsilon(\omega) = \varepsilon_\infty - \frac{\omega_p^2}{\omega^2 + i\gamma\omega} \tag{2.57}$$

2.1.2. Plasmons

In subsubsection 2.1.1 we have introduced the plasma frequency ω_p (see equation (2.49)). This is the frequency with which the free electron gas oscillates under the influence of an external electromagnetic field.
Plasmons are collective excitations of the free conduction electrons in metals. They are the quanta of the collective vibrations of the electron gas, and they are so-called quasiparticles.

Volume plasmons

In the literature plasmons in bulk materials are also referred to as volume or bulk plasmons.
We look more closely at this collective oscillation of the conduction electrons against the fixed positive background (i.e. the ions). By the oscillation the electrons are displaced. Suppose that the electrons are displaced by a distance x. Because of the displacement a charge density ρ arises:

$$\rho = \pm 4\pi nex \tag{2.58}$$

This charge density generates an electric field of the following form:

$$E = 4\pi nex \tag{2.59}$$

This means that the oscillating electrons experience a restoring force. Thus the oscillations obey the following equation of motion:

$$nm\ddot{x} = -neE = 4\pi n^2 e^2 x \tag{2.60}$$

The plasma frequency ω_p was defined as

$$\omega_p^2 = \frac{4\pi ne^2}{m} \tag{2.61}$$

With this definition one can write the equation of motion in the following way:

$$\ddot{x} + \omega_p^2 x = 0 \tag{2.62}$$

Thus ω_p is the frequency of the oscillations of the conduction electrons, i.e. the electron gas. The plasmons are the quanta of these vibrations.

2.1.3. Surface plasmons

In this subsection we describe surface plasmon polaritons (i.e. surface plasmons interacting with an external electromagnetic field). Surface plasmons occur at the interface between a metal and a dielectric. We start with the derivation of the boundary conditions at the interface between two dielectric media.

Derivation of the boundary conditions between different media

This section is based on [26]. We start by depicting the interface between two dielectric media in figure 2.1.

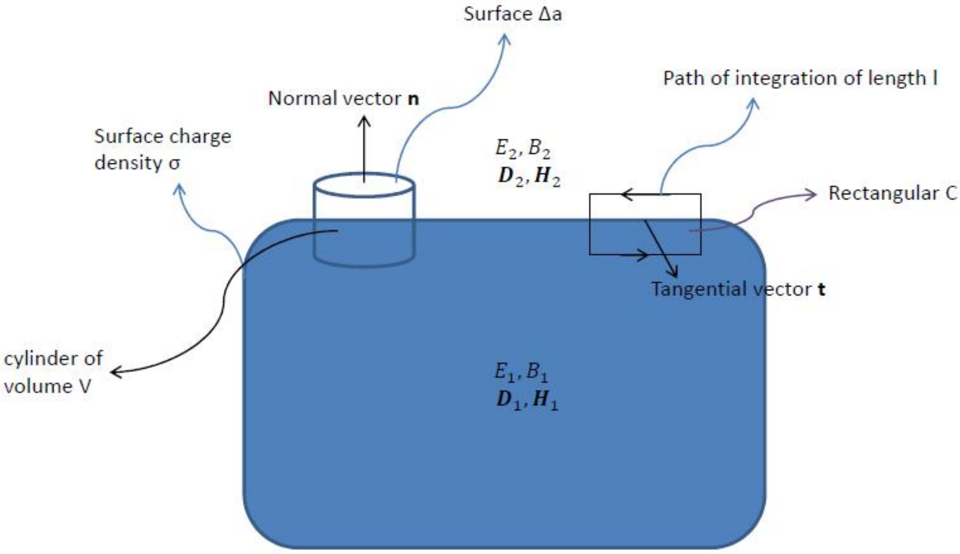

Figure 2.1.: Interface between two media. The normal vector $\boldsymbol{n}$ points from medium 1 (E_1, B_1) to medium 2 (E_2, B_2). The interface between medium 1 and medium 2 is occupied by a surface charge density σ.

In figure 2.1 the cylinder has a height h, the volume V and the surface S. The upper and lower areas of the cylinder are denoted by Δa.
The Maxwell equations in differential form are given in the appendix. By using the theorems of Gauss and Stoke we can transform them to integral form. Let V be a finite space element, confined by the surface S (see 2.1). $\boldsymbol{n}$ is the surface normal which points outwards from the surface element dA, i.e. from medium 1 to medium 2. We apply the theorem of Gauss to Coulomb´s law and the last of the Maxwell equations (the first and fourth Maxwell equation, see appendix A.4 or section 2.1.1) and get the following integral relations:

$$\oint_S \boldsymbol{D} \cdot \boldsymbol{n} dA = 4\pi \int_V \rho d^3x \tag{2.63}$$

$$\oint_S \boldsymbol{B} \cdot \boldsymbol{n} dA = 0 \tag{2.64}$$

The first of these two equations is the law of Gauss (see appendix A.3). The second equation is analogous to the first one but it is it´s magnetic analogon.
If we apply Stoke´s theorem to the second and third Maxwell equation (Ampere´s

law and Faraday´s induction law) we get

$$\begin{aligned}\oint_C \boldsymbol{H} \cdot d\boldsymbol{l} &= \int_{S'} \left[\boldsymbol{j} + \frac{\partial \boldsymbol{D}}{\partial t}\right] \cdot \boldsymbol{n}' dA \qquad (2.65)\\ \oint_C \boldsymbol{E} \cdot d\boldsymbol{l} &= -\int_{S'} \frac{\partial \boldsymbol{B}}{\partial t} \cdot \boldsymbol{n}' dA \qquad (2.66)\end{aligned}$$

From this form of the Maxwell equations we can derive the boundary conditions of the electromagnetic fields and the potentials at the interface between the two media. The interface is occupied with surface charges and surface currents. We apply the law of Gauss (2.63) and its magnetic analogon (2.64) to the volume V of the cylinder of height h and surface S. For an infinitesimal height h the surface of the cylinder jacket does not yield any contribution. Only the upper and lower circular areas denoted by Δa contribute to the integrals. We get:

$$\begin{aligned}\oint_S \boldsymbol{D} \cdot \boldsymbol{n} dA &= (\boldsymbol{D}_2 - \boldsymbol{D}_1) \cdot \boldsymbol{n} \Delta a \qquad (2.67)\\ \oint_S \boldsymbol{B} \cdot \boldsymbol{n} dA &= (\boldsymbol{B}_2 - \boldsymbol{B}_1) \cdot \boldsymbol{n} \Delta a \qquad (2.68)\end{aligned}$$

If the charge density ρ is singular on the interface and forms an idealized surface charge density σ on it, then we get for the right hand side of (2.63):

$$\int_V \rho d^3x = \sigma \Delta a \qquad (2.69)$$

This yields the relation between the normal components of $\boldsymbol{D}$ and $\boldsymbol{B}$, i.e. the boundary conditions for the normal components of the fields $\boldsymbol{D}$ and $\boldsymbol{B}$:

$$\begin{aligned}(\boldsymbol{D}_2 - \boldsymbol{D}_1) \cdot \boldsymbol{n} &= 4\pi\sigma \qquad (2.70)\\ (\boldsymbol{B}_2 - \boldsymbol{B}_1) \cdot \boldsymbol{n} &= 0 \qquad (2.71)\end{aligned}$$

In other words: the normal component of $\boldsymbol{B}$ is continuous at the interface, whereas the normal component of $\boldsymbol{D}$ has a jump.
Now we can apply Stoke´s theorem in an analogous way to the rectangular loop. This leads us to the boundary conditions for the tangential components of $\boldsymbol{E}$ and $\boldsymbol{H}$. Let Δl be the length of one of the longer sides of the rectangular and let the lateral sides be negligibly small. The integral on the left hand sides of equations (2.65) and (2.66) becomes:

$$\begin{aligned}\oint_C \boldsymbol{E} d\boldsymbol{l} &= (\boldsymbol{t} \times \boldsymbol{n}) \cdot (\boldsymbol{E}_2 - \boldsymbol{E}_1) \Delta l \qquad (2.72)\\ \oint_C \boldsymbol{H} d\boldsymbol{l} &= (\boldsymbol{t} \times \boldsymbol{n}) \cdot (\boldsymbol{H}_2 - \boldsymbol{H}_1) \Delta l \qquad (2.73)\end{aligned}$$

The right hand side of (2.66) vanishes because $\frac{\partial \boldsymbol{B}}{\partial t}$ is finite at the interface and the area spanned by C vanishes for infinitesimally small lateral sides. The right hand side of (2.65) does not vanish if there is an idealized surface current of density $\boldsymbol{K}$ flowing on the interface. The integral on the right hand side of (2.65) becomes

$$\int_{S'} \left[\boldsymbol{j} + \frac{\partial \boldsymbol{D}}{\partial t} \right] \cdot \boldsymbol{t} dA = \boldsymbol{K} \cdot \boldsymbol{t} \Delta l \tag{2.74}$$

Since $\frac{\partial \boldsymbol{D}}{\partial t}$ is finite on the interface too the second term of this integral also vanishes. The relation between the tangential components of $\boldsymbol{E}$ and $\boldsymbol{H}$ are:

$$\boldsymbol{n} \times (\boldsymbol{E}_2 - \boldsymbol{E}_1) = 0 \tag{2.75}$$
$$\boldsymbol{n} \times (\boldsymbol{H}_2 - \boldsymbol{H}_1) = \boldsymbol{K} \tag{2.76}$$

This means that the tangential components of $\boldsymbol{E}$ are continuous.
The boundary conditions for the potential Φ can be derived by using the relation $\boldsymbol{D} = \varepsilon \boldsymbol{E} = -\varepsilon \boldsymbol{\nabla} \Phi$ applied to our problem, i.e.:

$$\boldsymbol{D}_1 = \varepsilon_1 \boldsymbol{E}_1 = -\varepsilon_1 \boldsymbol{\nabla} \Phi_1 \tag{2.77}$$
$$\boldsymbol{D}_2 = \varepsilon_2 \boldsymbol{E}_2 = -\varepsilon_2 \boldsymbol{\nabla} \Phi_2 \tag{2.78}$$

We insert this into equation (2.70) and get:

$$(-\varepsilon_2 \boldsymbol{\nabla} \Phi_2 + \varepsilon_1 \boldsymbol{\nabla} \Phi_1) \cdot \boldsymbol{n} = 4\pi\sigma \tag{2.79}$$

and from this, using that $\boldsymbol{n}\boldsymbol{\nabla}\Phi$ is the normal derivative of Φ at the surface:

$$\varepsilon_1 \Phi_1'|_S = \varepsilon_2 \Phi_2'|_S \tag{2.80}$$

where the $'$ denotes the normal derivative and S denotes the surface.
In the case of a spherical nanoparticle with radius a and surface charge density σ in a dielectric medium with dielectric function ε_{out} one can transform this equation to spherical coordinates. The dielectric function of the sphere is ε_{in}. We get:

$$\varepsilon_{in} \frac{\partial \Phi_{in}}{\partial r}|_a - \varepsilon_{out} \frac{\partial \Phi_{out}}{\partial r}|_a = 4\pi\sigma \tag{2.81}$$
$$\frac{\partial \Phi_{in}}{\partial \theta}|_a - \frac{\partial \Phi_{out}}{\partial \theta}|_a = 0 \tag{2.82}$$

Surface Plasmon Polaritons

Surface plasmons are confined to the interface between a material with a positive dielectric constant and a material (metal) with a negative dielectric constant or at the interface between vacuum and a material with a negative dielectric constant. Because one of the materials has to have a negative dielectric function metals are a good candidate for this material. The dielectric function of the metal has to be more negative than the one of the dielectric (e.g. air):

$$|\varepsilon_2| > \varepsilon_1 \tag{2.83}$$

The reason for this will be explained below.

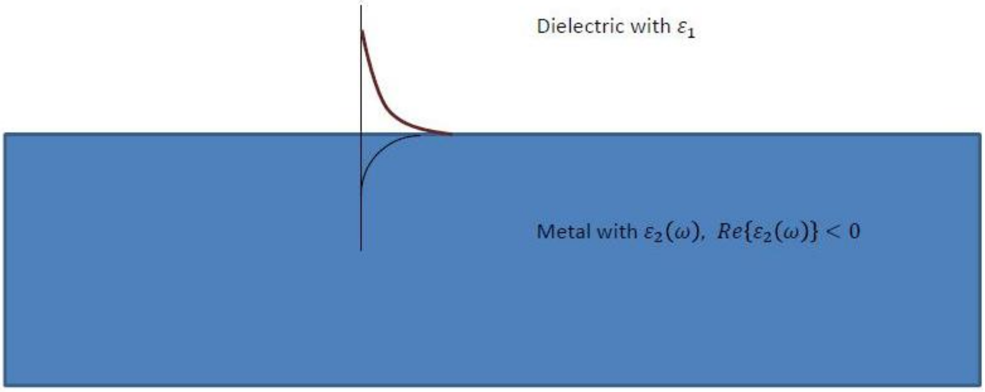

Figure 2.2.: Surface plasmons occur for instance at the interface between a metal (blue area) and a dielectric, where the dielectric function of the metal ε_2 is negative and the one from the dielectric (air, for instance), ε_1, is positive.

The electrical field associated with the surface plasmons $\boldsymbol{E}$ falls off exponentially in the metal and in the dielectric. It is called an evanescent field.

The evanescent fields have a strong spatial localisation and propagate along the interface. They are only present in the immediate vicinity of the object or interface. In figure 2.2 we see the exponential decay of the evanescent fields away from the metal-dielectric-interface. Later in this chapter we will see that an evanescent wave corresponds to a TM-(transversal magnetic) mode, propagating along the interface between the metal and the dielectric.

After these introductory words about evanescent waves we will now go into detail about surface plasmon polaritons at the interface between a non-absorbing dielectric and a conductor. Surface plasmon polaritons are electromagnetic excitations

which are confined to the interface between a dielectric (air for instance) and a conductor (a metal for instance) and they only propagate along this interface falling off exponentially in the direction perpendicular to the interface. This exponential fall-off means that they have evanescent character [23].
In figure 2.2 a typical geometry for the occurrence of surface plasmon polaritons is depicted.
We start by applying the Maxwell equations to a flat interface between a conductor and a dielectric. We consider the case without external charge and current densities, i.e. $\rho_{ext} = 0$ and $\boldsymbol{j}_{ext} = 0$. Then we can combine the following two Maxwell equations

$$\begin{aligned} \boldsymbol{\nabla} \times \boldsymbol{E} &= -\frac{1}{c}\frac{\partial \boldsymbol{B}}{\partial t} \\ \boldsymbol{\nabla} \times \boldsymbol{H} &= \frac{1}{c}\frac{\partial \boldsymbol{D}}{\partial t} \end{aligned}$$

which yields the wave equation

$$\boldsymbol{\nabla} \times \boldsymbol{\nabla} \times \boldsymbol{E} = \frac{1}{c^2}\frac{\partial^2 \boldsymbol{D}}{\partial t^2} \tag{2.84}$$

Now we use the following relations:

$$\begin{aligned} \boldsymbol{\nabla} \times \boldsymbol{\nabla} \times \boldsymbol{E} &= \boldsymbol{\nabla}(\boldsymbol{\nabla} \cdot \boldsymbol{E}) - \nabla^2 \cdot \boldsymbol{E} && (2.85) \\ \boldsymbol{\nabla}(\varepsilon \cdot \boldsymbol{E}) &= \boldsymbol{E} \cdot \boldsymbol{\nabla}\varepsilon + \varepsilon \boldsymbol{\nabla} \cdot \boldsymbol{E} && (2.86) \end{aligned}$$

Since there are no external charges present we also have $\boldsymbol{\nabla} \cdot \boldsymbol{D} = 0$.
All this yields the following wave equation:

$$\boldsymbol{\nabla}\left(-\frac{1}{\varepsilon}\boldsymbol{E} \cdot \boldsymbol{\nabla}\varepsilon\right) - \nabla^2 \boldsymbol{E} = -\frac{1}{c^2}\varepsilon\frac{\partial^2 \boldsymbol{E}}{\partial t^2} \tag{2.87}$$

If $\varepsilon(\boldsymbol{r})$ has only negligible variation with respect to its argument we get the following form of the wave equation:

$$\nabla^2 \boldsymbol{E} - \frac{\varepsilon}{c^2}\frac{\partial^2 \boldsymbol{E}}{\partial t^2} = 0 \tag{2.88}$$

Now we assume that the time-dependence is harmonic, i.e.:

$$\boldsymbol{E}(\boldsymbol{r}, t) = \boldsymbol{E}(\boldsymbol{r})e^{-i\omega t} \tag{2.89}$$

We plug this into equation (2.88) and get:

$$\nabla^2 \boldsymbol{E} + k_0^2 \cdot \varepsilon \cdot \boldsymbol{E} = 0 \tag{2.90}$$

This is the so-called Helmholtz-equation. $k_0 = \frac{\omega}{c}$ is the wave number of the propagating wave in vacuum.

Now we want to consider the special case of an one-dimensional geometry, i.e. ε only depends on one spatial direction, $\varepsilon = \varepsilon(z)$. The interface in which the evanescent wave is propagating equals the plane $z = 0$. We can describe the wave in the following way:

$$\boldsymbol{E}(x, y, z) = \boldsymbol{E}(z) \cdot e^{ik_x \cdot x} \tag{2.91}$$

k_x is the component of the wave vector $\boldsymbol{k}$ in the direction of propagation and is called propagation constant [23].

We plug this into the Helmholtz equation and get:

$$\frac{\partial^2 \boldsymbol{E}(z)}{\partial z^2} + (k_0^2 \varepsilon - k_x^2)\boldsymbol{E} = 0 \tag{2.92}$$

An analogous equation holds for the magnetic field $\boldsymbol{H}$. To get this equation one starts again with the assumption of harmonic time dependence and follows basically the same steps as above.

We use again the equations

$$\begin{aligned} \boldsymbol{\nabla} \times \boldsymbol{E} &= -\frac{1}{c}\frac{\partial \boldsymbol{B}}{\partial t} && (2.93) \\ \boldsymbol{\nabla} \times \boldsymbol{H} &= \frac{1}{c}\frac{\partial \boldsymbol{D}}{\partial t} && (2.94) \end{aligned}$$

to find explicit expressions for the field components $\boldsymbol{E}$ and $\boldsymbol{H}$.

Since we assume harmonic time dependence we get the following system of coupled equations:

$$\begin{aligned} \frac{\partial E_z}{\partial y} - \frac{\partial E_y}{\partial z} &= i\omega H_x && (2.95) \\ \frac{\partial E_x}{\partial z} - \frac{\partial E_z}{\partial x} &= i\omega H_y && (2.96) \\ \frac{\partial E_y}{\partial x} - \frac{\partial E_x}{\partial y} &= i\omega H_z && (2.97) \\ \frac{\partial H_z}{\partial y} - \frac{\partial H_y}{\partial z} &= -i\omega\varepsilon E_x && (2.98) \\ \frac{\partial H_x}{\partial z} - \frac{\partial H_z}{\partial x} &= -i\omega\varepsilon E_y && (2.99) \\ \frac{\partial H_y}{\partial x} - \frac{\partial H_x}{\partial y} &= -i\omega\varepsilon E_z && (2.100) \end{aligned}$$

We have propagation along the x-direction and assume homogeneity in y-direction.

Then the system of equations takes the following form:

$$\begin{aligned}
\frac{\partial E_y}{\partial z} &= -i\omega H_x \qquad (2.101)\\
\frac{\partial E_x}{\partial z} - ik_x E_z &= i\omega H_y \qquad (2.102)\\
ik_x E_y &= i\omega H_z \qquad (2.103)\\
\frac{\partial H_y}{\partial z} &= i\omega\varepsilon E_x \qquad (2.104)\\
\frac{\partial H_x}{\partial z} ik_x H_z &= -i\omega\varepsilon E_y \qquad (2.105)\\
ik_x H_y &= -i\omega\varepsilon E_z \qquad (2.106)
\end{aligned}$$

From this set of equations one gets two sets of solutions:

- TM-modes, i.e. only E_x, E_y and H_y are unequal to zero
- TE-modes, i.e. only H_x, H_z and E_y are unequal to zero

TM stands for "transversal magnetic" and TE stands for "transversal electric". The solutions for the TM-modes are:

$$\begin{aligned}
E_x &= -i\frac{1}{\omega\varepsilon} \cdot \frac{\partial H_y}{\partial z} \qquad (2.107)\\
E_z &= -\frac{k_x}{\omega\varepsilon} \cdot H_y \qquad (2.108)
\end{aligned}$$

The corresponding wave equation is:

$$\frac{\partial^2 H_y}{\partial z^2} + (k_0^2\varepsilon - k_x^2)H_y = 0 \qquad (2.109)$$

The solutions for the TE-modes are of the following form:

$$\begin{aligned}
H_x &= i\frac{1}{\omega} \cdot \frac{\partial E_y}{\partial z} \qquad (2.110)\\
H_z &= \frac{k_x}{\omega} \cdot E_y \qquad (2.111)
\end{aligned}$$

and the corresponding wave equation is:

$$\frac{\partial^2 E_y}{\partial z^2} + (k_0^2\varepsilon - k_x^2)E_y = 0 \qquad (2.112)$$

Now we come to the description of surface plasmon polaritons for the simple case depicted in figure 2.2, i.e. we consider a single flat interface between a conductor and a dielectric. The dielectric has a constant $\varepsilon_1 > 0$ which is real. The conductor has a dielectric constant $\varepsilon_2(\omega)$ with $Re(\varepsilon_2) < 0$. For metals the condition $Re(\varepsilon_2) < 0$ is fulfilled for $\omega < \omega_p$.
The solutions we are searching for are propagating waves with an evanescent field falling off in the z-direction (perpendicular to the interface) and are thus confined to the interface.
For $z > 0$ the TM-solutions for this case are:

$$\begin{aligned} H_y(z) &= A_2 e^{ik_x x} e^{-k_{2z}} && (2.113)\\ E_x(z) &= iA_2 \frac{1}{\omega\varepsilon_1} k_2 e^{ik_x x} e^{-k_{2z}} && (2.114)\\ E_z(z) &= -A_1 \frac{k_x}{\omega\varepsilon_1} e^{ik_x x} e^{-k_{2z}} && (2.115) \end{aligned}$$

For $z < 0$ we get:

$$\begin{aligned} H_y(z) &= A_1 e^{ik_x x} e^{k_{1z}} && (2.116)\\ E_x(z) &= -iA_1 \frac{1}{\omega\varepsilon_2} k_1 e^{ik_x x} e^{k_{1z}} && (2.117)\\ E_z(z) &= -A_1 \frac{k_x}{\omega\varepsilon_2} e^{ik_x x} e^{k_{1z}} && (2.118) \end{aligned}$$

k_{iz} with $i = 1, 2$ are the components of the wave vector perpendicular to the interface in the two media.
Now we use the boundary conditions which we have obtained in the beginning of this subsection. The continuity of H_y and $\varepsilon_i E_z$ at the interface leads to the condition

$$A_1 = A_2 \tag{2.119}$$

This leads to

$$\frac{k_2}{k_1} = -\frac{\varepsilon_1}{\varepsilon_2} \tag{2.120}$$

For confinement at the interface the following must hold:

$$Re(\varepsilon_2) < 0 \text{ if } \varepsilon_1 > 0 \tag{2.121}$$

This means that surface plasmon polaritons only exist at the interface between materials with opposite signs of the real parts of their dielectric constants, i.e.

between insulators and conductors.
The expression $H_y(z) = A_1 e^{ik_1 x} \cdot e^{k_{1z}}$ has to fulfill the wave equation

$$\frac{\partial^2 H_y}{\partial z^2} + (k_0^2 \varepsilon - k_x^2) H_y = 0 \tag{2.122}$$

From this we get the following relations:

$$k_1^2 = k_x^2 - k_0^2 \varepsilon_1 \tag{2.123}$$

$$k_2^2 = k_x^2 - k_0^2 \varepsilon_2 \tag{2.124}$$

Now we combine this equation with equation (2.120). This yields the dispersion relation for the surface plasmon polaritons:

$$k_x = k_0 \sqrt{\frac{\varepsilon_1 \varepsilon_2}{\varepsilon_1 + \varepsilon_2}} \tag{2.125}$$

The expression in the square root has to be larger than 0 because then the wave is confined to the interface. Because of that $|\varepsilon_2| > \varepsilon_1$ (the dielectric function of the metal has to be more negative than the one of the dielectric). Now we look at the TE-solutions. For $z > 0$ the TE-solutions for this case are:

$$E_y(z) = A_2 e^{ik_x x} e^{-k_{2z}} \tag{2.126}$$

$$H_x(z) = -iA_2 \frac{1}{\omega} k_2 e^{ik_x x} e^{-k_{2z}} \tag{2.127}$$

$$H_z(z) = A_2 \frac{k_x}{\omega} e^{ik_x x} e^{-k_{2z}} \tag{2.128}$$

For $z < 0$ we get:

$$E_y(z) = A_1 e^{ik_x x} e^{k_{1z}} \tag{2.129}$$

$$H_x(z) = iA_1 \frac{1}{\omega} k_1 e^{ik_x x} e^{k_{1z}} \tag{2.130}$$

$$H_z(z) = A_1 \frac{k_x}{\omega} e^{ik_x x} e^{k_{1z}} \tag{2.131}$$

Since E_y and H_x are continuous at the interface (see first part of this section about surface plasmons) we get

$$A_1(k_1 + k_2) = 0 \tag{2.132}$$

Confinement at the interface means that $Re(k_1) > 0$ and $Re(k_2) < 0$. From this we get:

$$A_1 = 0 \tag{2.133}$$

$$A_2 = A_1 = 0 \tag{2.134}$$

This means that for TE-polarization there do not exist surface-plasmon-polariton-modes. Surface plasmon polaritons only exist for TM-polarization.
For large wave vectors the frequency of the surface plasmon polaritons reaches the surface plasmon frequency [23]:

$$\omega_{SP} = \frac{\omega_p}{\sqrt{1+\varepsilon_1}} \tag{2.135}$$

To prove this we insert the expression for the dielectric function in the Drude model

$$\varepsilon(\omega) = 1 - \frac{\omega_p^2}{\omega^2 + i\gamma\omega} \tag{2.136}$$

into the dispersion relation of the surface plasmon polaritons (equation (2.125)). If the damping of the oscillation of the conduction electrons is negligible, i.e. if $Im(\varepsilon_2(\omega)) = 0$, then k_x goes to infinity while the frequency reaches the surface plasmon frequency $\omega \rightarrow \omega_{SP}$ and the group velocity goes to zero, $v_g \rightarrow 0$. This means that we have an electrostatic mode and this mode is called surface plasmon.

Particle Plasmons

Particle plasmons are the modes of excitation of a metallic nanoparticle. Thus these plasmon modes are the ones of interest in this diploma thesis. Like for surface plasmons we should also talk about particle plasmon polaritons because they are so-to-say the particle plasmons in interaction with an electromagnetic field. If an electromagnetic field impinges on a metallic nanoparticle the particle becomes polarized and this polarization generates a restoring force. From this restoring force we again get a plasmon mode. Particle plasmons are surface plasmons which are confined in all three spatial dimensions to the particle surface ([23],[27]).

2.2. Basic elements of classical electrostatics

In this section we start with the Poisson equation which will be used in chapter 3 and 4 to get the potential of the interaction between the electron beam and the metallic spherical nanoparticle. Then we shortly mention Dirichlet and Neumann boundary conditions because we need them for the discussion about Green´s functions and to show the uniqueness of the solution of the Poisson equation. The Green function technique is used to solve the Poisson equation in the following chapters. Finally we introduce the multipole expansion because the solutions of chapter 3 will follow from such an expansion of the Green function, imposing the boundary conditions of 2.1.3 to obtain the coefficients of the expansion. In this section we follow closely the book of [26].

2.2.1. Poisson equation

This subsection introduces the Poisson equation for the electrostatic case in order to give the foundation for the calculations of chapter 3 where we use the Poisson equation for dielectric media.
The electrostatic field is described by the following two differential equations:

$$\begin{aligned} \boldsymbol{\nabla} \cdot \boldsymbol{E} &= 4\pi\rho \qquad (2.137) \\ \boldsymbol{\nabla} \times \boldsymbol{E} &= 0 \qquad (2.138) \end{aligned}$$

These are the Maxwell equations for the static case.
From the last of these two equations it follows that $\boldsymbol{E}$ is representable by the gradient of a scalar function. This function is the so-called scalar potential Φ:

$$\boldsymbol{E} = -\boldsymbol{\nabla}\Phi \qquad (2.139)$$

We plug this equation into the differential form of Gauss´ law (equation (2.137)). Formula (2.137) and Gauss´ law are discussed in appendix A.3.
This yields:

$$\begin{aligned} \boldsymbol{\nabla}(-\boldsymbol{\nabla}\Phi) &= 4\pi\rho \qquad (2.140) \\ \boldsymbol{\nabla}^2\Phi &= \Delta\Phi = -4\pi\rho \qquad (2.141) \end{aligned}$$

This is the **Poisson equation** for the static case and for $\rho \neq 0$. For $\rho = 0$ it reduces to the so-called **Laplace equation**.
The Poisson equation is a partial differential equation for the scalar potential $\Phi(\boldsymbol{x})$. Its solution for a spatially restricted charge density ρ is

$$\Phi(\boldsymbol{x}) = \int \frac{\rho(\boldsymbol{x}')}{|\boldsymbol{x} - \boldsymbol{x}'|} d^3x' \qquad (2.142)$$

This solution goes to zero for large distance $|\boldsymbol{x} - \boldsymbol{x}'|$ and only holds for infinite media.
Now we have to show that $\Phi(\boldsymbol{x})$ fulfills the Poisson equation and the Laplace equation respectively. To manage that we apply the Laplace operator Δ on both sides of the solution (2.142):

$$\Delta\Phi(\boldsymbol{x}) = \int \Delta \frac{\rho(\boldsymbol{x}')}{|\boldsymbol{x} - \boldsymbol{x}'|} d^3x' \qquad (2.143)$$

The integrand is singular. To avoid too much writing one renames $|\boldsymbol{x} - \boldsymbol{x}'|$ to r. The following relation holds:

$$\Delta \frac{1}{|\boldsymbol{x} - \boldsymbol{x}'|} = \Delta \left(\frac{1}{r}\right) = -4\pi \cdot \delta(\boldsymbol{x} - \boldsymbol{x}') \qquad (2.144)$$

We have to proof this equation. $\frac{1}{r}$ is singular at $r = 0$. This function is first replaced by a smooth function:

$$\begin{aligned} \chi_\epsilon(r) &= \frac{1}{\sqrt{r^2+\epsilon^2}} &(2.145)\\ \lim_{\epsilon\to 0}\chi_\epsilon(r) &= \frac{1}{r} &(2.146) \end{aligned}$$

Because of its symmetry we will treat the problem in spherical coordinates. The Laplace operator in spherical coordinates is (see appendix):

$$\Delta = \frac{1}{r}\frac{\partial^2}{\partial r^2}r + \frac{1}{r^2}\left[\frac{1}{\sin\vartheta}\frac{\partial}{\partial\vartheta}\left(\sin\vartheta\frac{\partial}{\partial\vartheta}\right) + \frac{1}{\sin^2\vartheta}\frac{\partial^2}{\partial\varphi^2}\right] \tag{2.147}$$

In our case we only need the radial part, i. e. $\frac{1}{r}\frac{\partial^2}{\partial r^2}r$. We get:

$$\begin{aligned} \Delta\chi_\epsilon(r) &= \frac{1}{r}\frac{\partial^2}{\partial r^2}\frac{r}{\sqrt{r^2+\epsilon^2}} = \\ &= \frac{1}{r}\frac{\partial}{\partial r}\left(\frac{1}{\sqrt{r^2+\epsilon^2}} - \frac{r^2}{\sqrt[3]{r^2+\epsilon^2}}\right) = \\ &= \frac{1}{r}\frac{\partial}{\partial r}\left(\frac{r^2+\epsilon^2}{\sqrt{r^2+\epsilon^2}\cdot(r^2+\epsilon^2)} - \frac{r^2}{\sqrt[3]{r^2+\epsilon^2}}\right) = \\ &= \frac{\epsilon^2}{r}\frac{\partial}{\partial r}\left(\frac{1}{(r^2+\epsilon^2)^{\frac{3}{2}}}\right) = \\ &= -3\cdot\frac{\epsilon^2}{(r^2+\epsilon^2)^{\frac{5}{2}}} =: \mu_\epsilon(r) &(2.148) \end{aligned}$$

Integration yields:

$$\begin{aligned} \int d^3r\mu_\epsilon(r) &= 4\pi\int drr^2\mu_\epsilon(r) = \\ &= 4\pi\int drr^2\Delta\underbrace{\chi_\epsilon(r)}_{r\frac{\partial^2}{\partial r^2}r\chi_\epsilon(r)} = \\ \text{Now we use partial integration:} &= -4\pi\int_0^\infty dr\left(\frac{\partial}{\partial r}r\chi_\epsilon(r)\right) = \\ &= -4\pi\frac{r}{\sqrt{r^2+\epsilon^2}}|_0^\infty = -4\pi &(2.149) \end{aligned}$$

The parameter ϵ does not play any role and because of that we have the desired proof. We get

$$\Delta\left(\frac{1}{r}\right) = -4\pi\delta(r) \tag{2.150}$$

Therefore

$$\Phi(\boldsymbol{x}) = \int \frac{\rho(\boldsymbol{x}')}{|\boldsymbol{x}-\boldsymbol{x}'|} d^3x' \tag{2.151}$$

is a solution of the Poisson equation.

2.2.2. Uniqueness of the solution of the Poisson equation

There exist two kinds of boundary conditions which hold for the potential and proof its uniqueness within a volume V enclosed by a surface S.

Dirichlet boundary conditions

Φ is given on the boundary S of a closed volume V.
We assume that the Poisson equation has two different solutions Φ_1 and Φ_2 in the volume V. One can show (see [26]) that on the boundary of the volume V enclosed by S, they shall fulfill the following condition:

$$\Phi_1(\boldsymbol{x}) = \Phi_2(\boldsymbol{x}) \ \forall \ \boldsymbol{x} \in \partial V \tag{2.152}$$

This condition is derived and can be found in the usual textbooks of classical Electrodynamics, like the highly recommended books from **Jackson** and **Griffiths** ([26],[28]).

Neumann boundary conditions

Here the potential in the direction normal to the area S is given, i. e. $\frac{\partial\Phi}{\partial n}$.
The condition which has to be fulfilled by now is:

$$\frac{\partial\Phi_1(\boldsymbol{x})}{\partial n} = \frac{\partial\Phi_2(\boldsymbol{x})}{\partial n} \tag{2.153}$$

where $x \in V$ and $\frac{\partial}{\partial n}$ denotes the normal derivative.

2.2.3. The Green function

In chapter 3 we use the method of Green functions to solve the Poisson equation. In this subsection we will give a short overview of Green´s functions.
In order to get the solution of the Poisson or Laplace equation in a finite volume V

with Dirichlet or Neumann boundary conditions on the boundary area S enclosing V, one uses the second Green identity

$$\int_V dV(\psi\Delta\Phi + \boldsymbol{\nabla}\psi\boldsymbol{\nabla}\Phi) = \oint_{\partial V} dA\left(\psi\frac{\partial}{\partial n}\Phi\right) \tag{2.154}$$

and the Green function.
Equation (2.154) is subtracted from the first Green identity

$$\int_V (\boldsymbol{\nabla}\Phi\boldsymbol{\nabla}\psi + \Phi\Delta\psi)dV = \oint_{\partial V} dA\left(\Phi\frac{\partial\Psi}{\partial n}\right) \tag{2.155}$$

This leads to

$$\int_V dV(\Phi\Delta\psi - \psi\Delta\Phi) = \oint_{\partial V} dA\left(\Phi\frac{\partial}{\partial n}\psi - \psi\frac{\partial}{\partial n}\Phi\right) \tag{2.156}$$

One makes the following choice for ψ:

$$\psi = \frac{1}{|\boldsymbol{x} - \boldsymbol{x}'|} \tag{2.157}$$

We apply the Laplace operator to this equation:

$$\Delta\left(\frac{1}{|\boldsymbol{x} - \boldsymbol{x}'|}\right) = -4\pi\delta(\boldsymbol{x} - \boldsymbol{x}') \tag{2.158}$$

$\frac{1}{|\boldsymbol{x}-\boldsymbol{x}'|}$ is only one function from a whole class of functions which fulfill this equation. They are called **Green´s functions**.
In general they fulfill the following equation:

$$\Delta G(\boldsymbol{x}, \boldsymbol{x}') = -4\pi\delta(\boldsymbol{x} - \boldsymbol{x}') \tag{2.159}$$

with

$$G(\boldsymbol{x}, \boldsymbol{x}') = \frac{1}{|\boldsymbol{x} - \boldsymbol{x}'|} + F(\boldsymbol{x}, \boldsymbol{x}') \tag{2.160}$$

F fulfills the Laplace equation:

$$\Delta F = 0 \tag{2.161}$$

$G(\boldsymbol{x}, \boldsymbol{x}')$ is symmetric with respect to its arguments:

$$G(\boldsymbol{x}, \boldsymbol{x}') = G(\boldsymbol{x}', \boldsymbol{x}) \tag{2.162}$$

This relation is a result of the translational invariance of space and is called reciprocity theorem.

The Green function fulfills the Poisson equation from above but it does not fulfill the Dirichlet and Neumann boundary conditions. Only if the surface S lies at infinity it fulfills these boundary conditions. By choosing $F(\boldsymbol{x}, \boldsymbol{x}')$ properly one can achieve the fulfillment of the boundary conditions.
One uses the second Green identity and chooses $\psi = G(\boldsymbol{x}, \boldsymbol{x}')$:

$$\begin{aligned} \Phi(\boldsymbol{x}) &= \int_V d^3x' \rho(\boldsymbol{x}') G(\boldsymbol{x}, \boldsymbol{x}') + \\ &+ \oint_{\partial V} dA' \left[G(\boldsymbol{x}, \boldsymbol{x}') \frac{\partial \Phi}{\partial n'} - \Phi \frac{\partial}{\partial n'} G(\boldsymbol{x}, \boldsymbol{x}') \right] \end{aligned} \tag{2.163}$$

Now we have two cases:

Green function for Dirichlet boundary conditions

We choose

$$G(\boldsymbol{x}, \boldsymbol{x}') = G_D(\boldsymbol{x}, \boldsymbol{x}') \tag{2.164}$$

Therefore

$$G_D(\boldsymbol{x}, \boldsymbol{x}') = 0 \tag{2.165}$$

if $\boldsymbol{x}'$ lies on the boundary ∂V. Then the term proportional to $\frac{\partial \Phi}{\partial n'}$ disappears. The solution is:

$$\Phi(\boldsymbol{x}) = \int_V \rho(\boldsymbol{x}') G_D(\boldsymbol{x}, \boldsymbol{x}') d^3x' - \frac{1}{4\pi} \oint_{\partial V} dA' \left(\Phi(\boldsymbol{x}' \frac{\partial G_D}{\partial n'}) \right) \tag{2.166}$$

Green function for Neumann boundary conditions

One could be tempted to use the ansatz $\frac{\partial}{\partial n'} G(\boldsymbol{x}, \boldsymbol{x}') = 0$. With this ansatz the second term of the surface integral of the over-determined problem

$$\Phi(\boldsymbol{x}') = \int_V dV \frac{\rho(\boldsymbol{x}')}{R} - \frac{1}{4\pi} \oint_{\partial V} dA \left(\Phi \frac{\partial}{\partial n} \frac{1}{R} - \frac{1}{R} \frac{\partial \Phi}{\partial n} \right) \tag{2.167}$$

disappears. The ansatz leads to a wrong result because it does not fulfill the conditions of Gauss law for the unit charge. The result is:

$$\oint_{\partial V} dA' \frac{\partial}{\partial n'} G_N(\boldsymbol{x}, \boldsymbol{x}') = \oint_{\partial V} dA' \boldsymbol{n}' \boldsymbol{\nabla}' G_N(\boldsymbol{x}, \boldsymbol{x}') = \int_V d^3x' \Delta' G_N(\boldsymbol{x}, \boldsymbol{x}') = -4\pi \tag{2.168}$$

The law of Gauss says that the expression on the right hand side has to be $4\pi q$ and not -4π.
The simplest choice which leads to a fulfillment of Gauss law would be:

$$\frac{\partial}{\partial n'} G(\boldsymbol{x}, \boldsymbol{x}') = -\frac{4\pi}{S} \tag{2.169}$$

if S is the total area and for $\boldsymbol{x}'$ lying on the boundary ∂V.
This is plugged into the over-determined relation (2.167) for $\Phi(\boldsymbol{x})$ where

$$\frac{1}{R} = \frac{1}{|\boldsymbol{x} - \boldsymbol{x}'|} \tag{2.170}$$

The result is:

$$\Phi(\boldsymbol{x}) = \int_V d^3x' \rho(\boldsymbol{x}') G_N(\boldsymbol{x}, \boldsymbol{x}') + \frac{1}{4\pi} \oint_{\partial V} dA' G_N(\boldsymbol{x}, \boldsymbol{x}') \frac{\partial \Phi}{\partial n'} + \frac{1}{S} \oint_{\partial V} dA' \Phi \tag{2.171}$$

where

$$\frac{1}{S} \oint_{\partial V} \Phi dA' = \langle \Phi \rangle_{\partial V \equiv S} \tag{2.172}$$

is the average value of the potential on the surface. If $S \to \infty$ the average value disappears if Φ falls off faster than $\frac{1}{\boldsymbol{x}}$ for $\boldsymbol{x} \to \infty$.

Interpretation of $F(\boldsymbol{x}, \boldsymbol{x}')$

F fulfills the Laplace equation in the volume V: $\Delta F = 0$. Therefore it represents the potential of a charge distribution outside of V. Together with the potential of a point charge at $\boldsymbol{x}'$, $\frac{1}{|\boldsymbol{x}-\boldsymbol{x}'|}$,the Green function has exactly the following values:

$$G_D(\boldsymbol{x}, \boldsymbol{x}') = 0 \text{ and } \frac{\partial}{\partial n'} G_N(\boldsymbol{x}, \boldsymbol{x}') + \frac{4\pi}{S} = 0 \text{ for } \boldsymbol{x} \in S \tag{2.173}$$

The external charge distribution shall exactly compensate the point charge at $\boldsymbol{x}'$ on the surface S. Therefore the outer charge distribution depends on $\boldsymbol{x}'$. $\boldsymbol{x}'$ is the position of the point charge.

2.2.4. Multipole expansion

To connect this section about the basic concepts of electrostatics with the upcoming chapters 3 and 4 we introduce the so-called multipole expansion. This will be used in chapter 3 for the calculation of the energy loss probability. Again we follow closely the book of Jackson [26].
We use spherical coordinates, referring the reader to appendix A.1 and A.2 for further details about spherical harmonics and spherical coordinates.
A localized charge distribution is described by a charge density $\rho(\boldsymbol{x}')$ which is only not vanishing inside of a sphere of radius R around a certain point of origin. If ρ decreases faster than every power of the spheres radius then the multipole expansion is valid for sufficiently large distances. The potential outside of the sphere can be written as an expansion in spherical harmonics (see appendix A.2):

$$\Phi(\boldsymbol{x}) = \sum_{l=0}^{\infty} \sum_{m=-l}^{l} \frac{4\pi}{2l+1} q_{lm} \frac{Y_{lm}(\theta, \varphi)}{r^{l+1}} \tag{2.174}$$

This is the so-called multipole expansion. The term with $l = 0$ equals a monopole, the one with $l = 1$ a dipole and so on. Now we need to determine the constants q_{lm}. We use

$$\Phi(\boldsymbol{x}) = \int \frac{\rho(\boldsymbol{x}')}{|\boldsymbol{x} - \boldsymbol{x}'|} d^3x' \tag{2.175}$$

We use the expansion of $\frac{1}{|\boldsymbol{x}-\boldsymbol{x}'|}$

$$\frac{\rho(\boldsymbol{x}')}{|\boldsymbol{x} - \boldsymbol{x}'|} = 4\pi \sum_{l=0}^{\infty} \sum_{m=-l}^{l} \frac{1}{2l+1} \frac{r_<^l}{r_>^{l+1}} Y_{lm}^\star(\theta', \varphi') Y_{lm}(\theta, \varphi) \tag{2.176}$$

The definition of $r_<$ and $r_>$ can be found in [26]. For our case $r_< = r'$ and $r_> = r$ since we are interested in the potential outside of the charge distribution. From this we get

$$\Phi(\boldsymbol{x}) = \sum_{lm} \frac{1}{2l+1} \left[\int Y_{lm}^\star(\theta', \varphi') r'^l \rho(\boldsymbol{x}') d^3x' \right] \frac{Y_{lm}(\theta, \varphi)}{r^{l+1}} \tag{2.177}$$

The term in the square brackets equals q_{lm}. These coefficients are called multipole moments.

2.3. Boundary integral method

For spherical nanoparticles calculations can be performed analytically without too much effort. If the systems under study become more complicated (e.g. coupled spheres or sphere-plane-system) an analytical calculation would be too elaborate and a numerical method is needed. In this section we introduce the boundary integral method (BIM). One goes over from integrals over surfaces (boundary integrals) to sums over surface elements (see section 4.1) for numerical computational calculations. In this approach we need to solve the Poisson equation 2.178. The aim is to find the induced surface charge density σ induced by an external charge density ρ_{ext}. The section is based on [1] (in chapter 4 we are going to make a boundary element method approach out of this boundary integral approach by discretizing the particles surface by small surface elements and going over from boundary integrals to sums over these elements).

We use the approximation of a local response of the system under consideration. Then the dielectric function of the medium depends on space too, $\varepsilon(\boldsymbol{r}, \omega)$. If we have a homogeneous medium we have no space dependency. The Poisson equation for inhomogeneous media can be written in this approximation in the following way:

$$\boldsymbol{\nabla} \left[\varepsilon(\boldsymbol{r}, \omega) \boldsymbol{\nabla} \Phi(\boldsymbol{r}, \omega) \right] = -4\pi \rho_{ext}(\boldsymbol{r}, \omega) \tag{2.178}$$

Here $\Phi(\boldsymbol{r},\omega)$ is the scalar potential and $\rho_{ext}(\boldsymbol{r},\omega)$ is the external charge density distribution.
The dielectric response is described by an arbitrary function of space $\boldsymbol{r}$ and frequency ω. This function is the dielectric function $\varepsilon(\boldsymbol{r},\omega)$.
Using the product rule we get:

$$\boldsymbol{\nabla}\varepsilon\boldsymbol{\nabla}\Phi + \varepsilon\Delta\Phi = -4\pi\rho_{ext} \tag{2.179}$$

The potential of the Poisson equation reads as follows:

$$\Phi(\boldsymbol{r},\omega) = \Phi^{\infty}(\boldsymbol{r},\omega) + \Phi^{boundary}(\boldsymbol{r},\omega) \tag{2.180}$$

The first term is the Coulomb term coming from the second term of equation (2.179). $\Phi(\boldsymbol{r},\omega)$ follows from the Poisson equation (2.178) in a similar way as equation (2.142). The explicit expressions for the two terms are:

$$\Phi^{\infty}(\boldsymbol{r},\omega) = \int d\boldsymbol{r}' \frac{\rho_{ext}(\boldsymbol{r}',\omega)}{\varepsilon(\boldsymbol{r}',\omega)|\boldsymbol{r}-\boldsymbol{r}'|} \tag{2.181}$$

$$\Phi^{boundary}(\boldsymbol{r},\omega) = \frac{1}{4\pi}\int d\boldsymbol{r}' \frac{\boldsymbol{\nabla}\Phi(\boldsymbol{r}',\omega)\boldsymbol{\nabla}\varepsilon(\boldsymbol{r}',\omega)}{\varepsilon(\boldsymbol{r}',\omega)|\boldsymbol{r}-\boldsymbol{r}'|} \tag{2.182}$$

In infinitely extended and homogeneous media $\Phi^{\infty}(\boldsymbol{r},\omega)$ reduces to the screened potential of the bulk of the material or particle under consideration. One gets

$$\Phi^{\infty}(\boldsymbol{r},\omega) = \frac{1}{\varepsilon\,(\omega)}\int d\boldsymbol{r}' \frac{\rho_{ext}(\boldsymbol{r}',\omega)}{|\boldsymbol{r}-\boldsymbol{r}'|} \tag{2.183}$$

The term $\Phi^{boundary}(\boldsymbol{r},\omega)$ results from the inhomogeneity of the response function. $\Phi^{boundary}(\boldsymbol{r},\omega)$ reduces to surface integrals for homogeneous dielectrics separated by abrupt interfaces. From now on we will only consider this case. We get

$$\Phi^{boundary}(\boldsymbol{r},\omega) \equiv \frac{1}{4\pi\varepsilon}\int d(\text{surface})\frac{\text{surface charge density}}{|\boldsymbol{r}-\boldsymbol{r}'|} \tag{2.184}$$

If we have ν different homogeneous dielectrics we have the dielectric function $\varepsilon_{\nu}(\omega)$ for the medium ν, where ν labels the different dielectrics.
This yields

$$\varepsilon(\boldsymbol{r},\omega) = \sum_{\nu}\varepsilon_{\nu}(\omega)\theta_{\nu}(\boldsymbol{r}) \tag{2.185}$$

This is the total dielectric function, depending on the frequency ω. The function $\theta_{\nu}(\boldsymbol{r})$ is 1 if $\boldsymbol{r}$ lies in medium ν and 0 otherwise [1].
The term under the integral in $\Phi^{boundary}$ is unequal to zero only at the interfaces. At the interfaces ε changes abruptly. This fact is described by so-called surface

delta functions which ensure that the integrand is unequal to zero only on the interfaces. This means that one can write

$$\frac{1}{4\pi}\frac{\boldsymbol{\nabla}\Phi \boldsymbol{\cdot} \nabla\varepsilon}{\varepsilon} = \frac{1}{4\pi}\boldsymbol{D}\cdot\boldsymbol{\nabla}\frac{1}{\varepsilon} = \sigma\delta_S \tag{2.186}$$

δ_S is a surface delta function which defines the interface. This term can be derived by using the following relations

$$\boldsymbol{D} = \varepsilon\boldsymbol{E} \tag{2.187}$$

$$\boldsymbol{\nabla}\cdot\boldsymbol{E} = 4\pi\rho = -\boldsymbol{\nabla}\Phi \tag{2.188}$$

$$\boldsymbol{\nabla}\cdot\boldsymbol{D} = 4\pi\rho \tag{2.189}$$

σ is the induced surface charge density of the boundary and the expression for it follows from the boundary condition $(\boldsymbol{D}_2 - \boldsymbol{D}_1)\boldsymbol{n} = 4\pi\sigma$.

$$\sigma(\boldsymbol{s},\omega) = \frac{1}{4\pi}\left(\frac{1}{\varepsilon_{\nu_2}(\omega)} - \frac{1}{\varepsilon_{\nu_1}(\omega)}\right)\boldsymbol{n}_s\cdot\boldsymbol{D} \tag{2.190}$$

$$= \frac{1}{4\pi}\frac{\varepsilon_{\nu_1}(\omega) - \varepsilon_{\nu_2}(\omega)}{\varepsilon_{\nu_1}(\omega)\varepsilon_{\nu_2}(\omega)}\boldsymbol{n}_s\cdot\boldsymbol{D}(\boldsymbol{s},\omega) \tag{2.191}$$

$\boldsymbol{s}$ is the coordinate vector along the interface and $\boldsymbol{n}_s$ is the normal to the interface at the vector $\boldsymbol{s}$. The index ν_1 labels the medium which is orientated against the direction of the normal to the interface and ν_2 labels the medium which is orientated in the direction of the normal to the interface (see Figure 2.3).

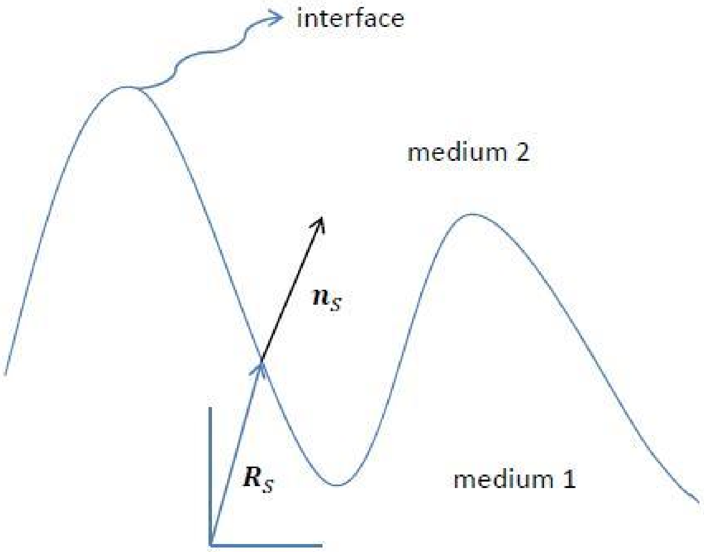

Figure 2.3.: The curve represents an interface between two dielectric media. The normal to the interface $\boldsymbol{n}_s$ points from medium 1 to medium 2. $\boldsymbol{R}_s$ is the position vector to the point where we calculate the potential. It is plotted inside a little coordinate system with y-axis (vertical) and x-axis (horizontal), where the z-axis points inside of the page [1].

ν_1 and ν_2 can depend on the vector $\boldsymbol{s}$. The surface delta function δ_S is uniquely defined because the component of the dielectric displacement normal to the interface, $\boldsymbol{n}_s \cdot \boldsymbol{D}$, is continuous. $\Phi_{boundary}$ becomes

$$\Phi_{boundary}(\boldsymbol{r},\omega) = \int d\boldsymbol{s} \frac{\sigma(\boldsymbol{s},\omega)}{|\boldsymbol{r}-\boldsymbol{s}|} \tag{2.192}$$

For the derivation of this equation we have used the law of Gauss. It is discussed in A.3. Here we will only shortly mention it.
The law of Gauss is in general:

- For a single point charge:

$$\oint_S \boldsymbol{E}\cdot\boldsymbol{n}da = \begin{cases} 4\pi q, & \text{if } q \text{ lies in} S \\ 0, & \text{if } q \text{ lies outside of} S \end{cases}$$

- For several charges:

$$\oint_S \boldsymbol{E}\cdot\boldsymbol{n}da = 4\pi \sum_i q_i \tag{2.193}$$

  in the volume enclosed by S.

- For a continuous charge distribution $\rho(\boldsymbol{x})$:

  $$\oint_S \boldsymbol{E} \cdot \boldsymbol{n} da = 4\pi \int_V \rho(\boldsymbol{x}) d^3x \tag{2.194}$$

  where V is the volume enclosed by S.

Its differential form is:

$$\oint_S \boldsymbol{A} \cdot \boldsymbol{n} da = \int_V \boldsymbol{\nabla} \boldsymbol{A} d^3x \tag{2.195}$$

From this we get:

$$\int_V \left(\boldsymbol{\nabla} \cdot \boldsymbol{E} - 4\pi\rho\right) d^3x = 0 \tag{2.196}$$

V is an arbitrary volume.
Finally we get:

$$\boldsymbol{\nabla} \cdot \boldsymbol{E} \overset{!}{=} 4\pi\rho \tag{2.197}$$

Now we consider the electric field at a point in medium ν_2 infinitesimally close to the interface. Owing to Gauss´ theorem the electrical field near the interface can be written as a sum of the contributions from the electrical field generated by all external charges plus the contribution from the charge density [7]:

$$\boldsymbol{E} = -\boldsymbol{n}_s \cdot \boldsymbol{\nabla}\Phi(\boldsymbol{s}, \omega) + 2\pi\sigma(\boldsymbol{s}, \omega) \tag{2.198}$$

The normal component of the dielectric displacement is:

$$\boldsymbol{n}_s \cdot \boldsymbol{D}(\boldsymbol{s}, \omega) = \varepsilon_{\nu_2}(\omega) \left[-\boldsymbol{n}_s \cdot \boldsymbol{\nabla}\Phi(\boldsymbol{n}_s, \omega) + 2\pi\sigma(\boldsymbol{n}_s, \omega)\right] \tag{2.199}$$

because $\boldsymbol{D} = \varepsilon \cdot \boldsymbol{E}$.
We can insert $\sigma(\boldsymbol{n}_s, \omega)$ in this equation. Furthermore we use equation (2.181) and equation (2.192) to get

$$\Lambda(\omega) \cdot \sigma(\boldsymbol{s}, \omega) = \boldsymbol{n}_S \cdot \boldsymbol{\nabla}\Phi^{\infty}(\boldsymbol{s}, \omega) + \int d\boldsymbol{s}' F(\boldsymbol{s}, \boldsymbol{s}') \cdot \sigma(\boldsymbol{s}', \omega) \tag{2.200}$$

where

$$\Lambda(\omega) = 2\pi \frac{\varepsilon_{\nu_2}(\omega) + \varepsilon_{\nu_1}(\omega)}{\varepsilon_{\nu_2}(\omega) - \varepsilon_{\nu_1}(\omega)} \tag{2.201}$$

and

$$F(\boldsymbol{s}, \boldsymbol{s}') = -\frac{\boldsymbol{n}_S \cdot (\boldsymbol{s} - \boldsymbol{s}')}{|\boldsymbol{s} - \boldsymbol{s}'|^3} \tag{2.202}$$

Equation (2.200) is the desired integral equation for the surface charge distribution σ. The problem has now only 2 dimensions instead of three. This means that the number of points needed to solve the equation numerically is reduced ([1], [29]).

3. Electron energy loss probability for a dielectric sphere

In this chapter we are going to calculate the energy loss probabilities for an electron passing by a dielectric metallic nanosphere or going through it. The general concept is presented and it can be applied in more complex situations. We use the Poisson equation (see section 2.2) for this derivation of the probability. The solution of it will lead us to the potential needed for the analytical calculation of the energy loss probability. Considering the spherical geometry allows to model the form of nanoparticles in experiments [1].

3.1. Theory of Electron Energy Loss Spectroscopy

In this section we present the classical theory of Electron Energy Loss Spectroscopy used in this diploma thesis. The basic equations needed in the subsequent sections are provided.

3.1.1. Classical dielectric formalism

Enrico Fermi´s famous work about the stopping of fast charged particles in dielectric materials [30] lead to the application of classical electrodynamics for the description of the interaction of fast electrons with matter [6].
The energy loss of a fast electron moving with constant velocity $\boldsymbol{v}$ along a straight line trajectory $\boldsymbol{r} = \boldsymbol{r}_e(t)$ is related or equivalent respectively to the force which is exerted from the induced electrical field $\boldsymbol{E}_{ind}$ of the material and acts back on the electron.

$$\Delta E = \int dt \cdot \boldsymbol{v} \cdot \boldsymbol{E}_{ind}(\boldsymbol{r}_e(t), t) = \int_0^\infty \omega \cdot P(\omega) \tag{3.1}$$

where $P(\omega)$ is the classical electron energy loss probability.

$$P(\omega) = \frac{1}{\pi} \int dt \cdot Im \left\{ \boldsymbol{v} \cdot e^{-i\omega t} \cdot \boldsymbol{E}_{ind}(\boldsymbol{r}_e(t), t) \right\} \tag{3.2}$$

Non-retarded case

In the quasistatic case considered in this diploma thesis we neglect the retardation of the electromagnetic signal which mediates the interaction between the electron and the probe.
The electrical field is given by

$$\boldsymbol{E}(\boldsymbol{r},\omega) = -\boldsymbol{\nabla}\Phi(\boldsymbol{r},\omega) \tag{3.3}$$

Without retardation we have no magnetic response and so one can neglect the magnetic field $\boldsymbol{H}$.
We express the electric potential Φ by the screened interaction $W(\boldsymbol{r},\boldsymbol{r}',\omega)$, i.e. the Green function of the Poisson equation of our problem (see chapter 2 and this chapter). W is the potential generated at $\boldsymbol{r}$ by a unit charge at position $\boldsymbol{r}'$. Attention has to be paid to the implicit $e^{-i\omega t}$-dependence. W has to be combined with the charge density for an electron with a straight trajectory, moving along the z-direction with constant velocity $\boldsymbol{v}$. The trajectory is:

$$\boldsymbol{r} = \boldsymbol{r}_0 + \boldsymbol{v}\cdot t \tag{3.4}$$

The electron charge density in frequency space becomes:

$$\rho(\boldsymbol{r},\omega) = -\int dt e^{i\omega t}\delta(\boldsymbol{r}-\boldsymbol{r}_0-\boldsymbol{v}\cdot t) = -\frac{1}{v}\delta(\boldsymbol{R}-\boldsymbol{R}_0)\cdot e^{i\omega(z-z_0)/v} \tag{3.5}$$

The convention for the Fourier transformation to the ω-space is given in the next section. Here $\boldsymbol{R}_0$ is the impact parameter, i.e. the two-dimensional vector (b_x, b_y). It describes the distance from the center of the metallic nanoparticle to the electron beam in the direction perpendicular to the direction of motion of the electrons.
The potential is:

$$\Phi(\boldsymbol{r},\omega) = \frac{1}{v}\int dz' W(\boldsymbol{r},\boldsymbol{R}_0,z',\omega)e^{i\omega(z'-z_0)/v} \tag{3.6}$$

If we plug this into equation 3.3 we get the following expression for the energy loss probability:

$$P(\boldsymbol{R}_0,\omega) = \frac{1}{\pi v^2}\int dz dz' Im\left\{-W(\boldsymbol{R}_0,z,\boldsymbol{R}_0,z',\omega)e^{i\omega(z'-z_0)/v}\right\} \tag{3.7}$$

In this chapter we are going to derive this quantity and W for the case of a spherical metallic nanoparticle.

Classical vs. quantum formalism

This work uses the classical formalism to describe the electrons and nanoparticles involved in the interaction processes of an EELS experiment. The validity of the classical approximation (considering electrons as point particles with a constant velocity v) has already been studied in the literature (see [1], [22] and [31]). If we describe the electron beam by the following wave function

$$\Psi_0(\boldsymbol{r}) \propto \Phi(\boldsymbol{r}_\perp - \boldsymbol{b}) e^{ik_0 z} \tag{3.8}$$

where $\boldsymbol{b}$ is the position of the center of the electron probe and $\boldsymbol{r}_\perp$ is the transversal projection of the position vector, we can describe the total energy loss as an incoherent sum over all trajectories of the losses of the classical electrons:

$$P_{qm}(\omega) = \int d\boldsymbol{r}_\perp |\Phi(\boldsymbol{r}_\perp - \boldsymbol{b})|^2 P(\omega, \boldsymbol{r}_\perp) \tag{3.9}$$

Here P is the classical electron energy loss probability. The condition for the validity of this formula is that all inelastically scattered electrons are collected in the analyser of the scanning transmission electron microscope [1]. The quantum corrections are small. Elastic scattering processes and recoil are neglected. The interaction can also be described classically because we neglect recoil effects. For further details see [1], [22] and [31].

3.2. Electron trajectory past sphere

Electron energy loss probabilities have been calculated for various geometries. EELS-spectra have been calculated for thin films [22] and the cases of hemispherical particles, cylindrical interfaces, systems of coupled spheres or hyperbolic wedges have been discussed in [1] and the corresponding references in this work.
The most simple particle geometry to consider is that of an isolated small sphere. The sphere is described by a dielectric function $\varepsilon(\omega)$. The electron energy loss probability can be derived analytically for this case, using Mie theory ([32], [33]). Other works considering the electron energy loss for an isolated sphere are [7], [34], [35] or [36]. In chapter 5 results for the EELS-spectrum of an electron beam exciting a spherical metallic nanoparticle will be presented, obtained by a Mathematica-routine for the analytical (Mie-) case and with MATLAB using a numerical method known as boundary element method (see chapter 2 and 4). The aim of this diploma thesis is to compare the analytical results obtained with Mie-theory with the ones obtained by the boundary element method. Two cases will be considered.
If the electron beam does not penetrate the sphere the geometry of the problem looks as follows:

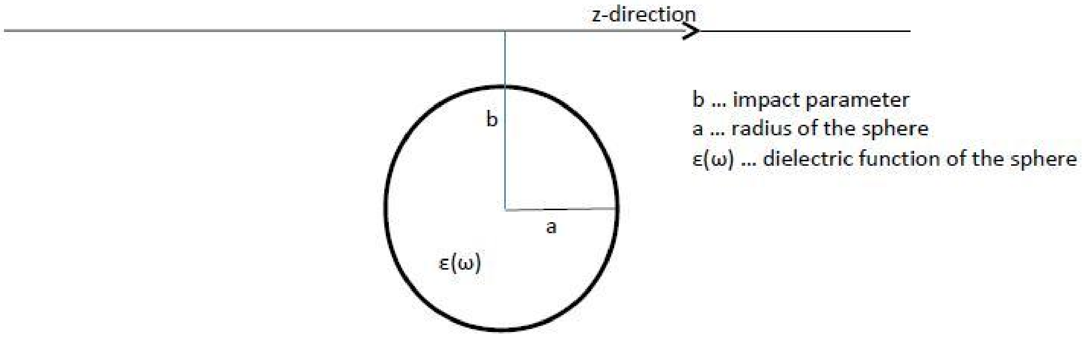

Figure 3.1.: Dielectric sphere with electron beam passing by distance b from the its center. The impact parameter is defined as the distance from the center of the sphere to the electron beam. The sphere is described by the dielectric function $\varepsilon(\omega)$. The electron passes the sphere in the z-direction with a constant velocity v_z.

b is the impact parameter defined as the distance between the center of the sphere and the electron trajectory. It´s dielectric function is $\varepsilon(\omega)$.
The inelastic scattering process takes place in the following way: the external electron beam is described by an external charge density ρ_{ext} which corresponds to an external potential Φ_{ext}. The electrons induce a potential $\Phi_{ind}(\boldsymbol{r})$ in the probe which acts back onto them. The interaction is given by the characteristics of the trajectory, i.e. v and b, the composition of the medium, i.e. $\varepsilon(\omega)$ and the geometry of the structure, e.g. a sphere in our case. We get Φ_{ind} from a solution of the Poisson equation in frequency space.
We want to calculate the energy loss probability $P(\omega)$ for the electron along the whole trajectory. $P(\omega)$ is the probability of losing the energy ω per unit energy and unit path length [1]. To do this derivation we have to calculate the total potential of this problem first. The general equation has already been introduced in chapter 2.2. For our problem we make a Fourier transformation of the Poisson equation to the frequency space. The Poisson equation was:

$$\Delta\Phi(\boldsymbol{r},t) = -\frac{4\pi}{\varepsilon}\rho(\boldsymbol{r},t) \tag{3.10}$$

This equation has to be Fourier transformed. The convention for the transformation is:

$$f(\boldsymbol{k},\omega) = \int\limits_{-\infty}^{\infty} d\boldsymbol{r} \int\limits_{-\infty}^{\infty} dt e^{-i(\boldsymbol{kr}-\omega t)} f(\boldsymbol{r},t) \tag{3.11}$$

$$f(\boldsymbol{k},\omega) = \frac{1}{(2\pi)^4} \int\limits_{-\infty}^{\infty} d\boldsymbol{k} \int\limits_{-\infty}^{\infty} d\omega e^{i(\boldsymbol{kr}-\omega t)} f(\boldsymbol{k},\omega) \tag{3.12}$$

The Poisson equation in frequency space becomes

$$\Delta\Phi(\boldsymbol{r},\omega) = -\frac{4\pi}{\varepsilon(\omega)}\rho(\boldsymbol{r},\omega) \tag{3.13}$$

if we make the Fourier transformation only with respect to t. The charge density ρ is given by:

$$\rho(\boldsymbol{r},\omega) = -\frac{1}{v}e^{\frac{i\omega z}{v}}\delta(y-b)\delta(x-b) \tag{3.14}$$

where v is the component of the velocity of the electron in its direction of motion. The lateral extension of the beam is small [1] and thus the electron is considered as a classical point particle, moving with velocity $\boldsymbol{v}$ along the z-direction.
The Fourier transformation of the charge density reads as follows:

$$\rho(\boldsymbol{r},t) = -\delta(\boldsymbol{r}-\boldsymbol{v}t) = -\delta(z-vt)\delta(y-b)\delta(x-b) \tag{3.15}$$

Now we make a partial Fourier transformation with respect to t:

$$\rho(\boldsymbol{r},\omega) = -\delta(y-b)\delta(z-b)\int\limits_{-\infty}^{\infty} dt e^{i\omega t}\delta(z-vt) \tag{3.16}$$

We solve this integral by substitution: $z = vt \longrightarrow t = \frac{z}{v}$. Then we exactly get equation (3.14).
To solve the Poisson equation we define its Green´s function $W(\boldsymbol{r},\boldsymbol{r}',\omega)$. This function is the screened interaction of the problem.

$$\Delta W(\boldsymbol{r},\boldsymbol{r}',\omega) = -\frac{4\pi}{\varepsilon(\omega)}\delta(\boldsymbol{r}-\boldsymbol{r}') \tag{3.17}$$

We interpret this equation as the Poisson equation for a point charge which is situated at r'. With this assumption we can use the usual electrostatics as found in [7], [26], [28] and [37]. We can express the solution of (3.13) with $W(\boldsymbol{r},\boldsymbol{r}',\omega)$:

$$\Phi(\boldsymbol{r},\omega) = \int\limits_{-\infty}^{\infty} d^3\boldsymbol{r}' W(\boldsymbol{r},\boldsymbol{r}',\omega)\rho(\boldsymbol{r}',\omega) \tag{3.18}$$

$W(\boldsymbol{r},\boldsymbol{r}',\omega)$ consists of an induced part and a Coulomb part:

$$W(\boldsymbol{r},\boldsymbol{r}',\omega) = W_{ind}(\boldsymbol{r},\boldsymbol{r}',\omega) + \frac{1}{|\boldsymbol{r}-\boldsymbol{r}'|} \tag{3.19}$$

We want to expand $W_{ind}(\boldsymbol{r},\boldsymbol{r}',\omega)$ as a regular solution of the Laplace equation. This means that for now we only consider the homogeneous part of the above Poisson equation, which equals the Laplace equation

$$\begin{aligned} \Delta W_{ind}(\boldsymbol{r},\boldsymbol{r}',\omega) = 0 &= \frac{1}{r^2} r^2 \partial_r W_{ind} + \\ \frac{1}{r^2 \sin\theta} \partial_\theta \sin\theta W_{ind} &+ \frac{1}{r^2 \sin\theta} \partial_\varphi \end{aligned} \tag{3.20}$$

The ansatz for the particular solution is the same as in appendix A.1 (see equation (A.2)):

$$W_{ind} = R(r)P(\theta)Q(\varphi) \tag{3.21}$$

Analogous to the appendix we set $z = \cos\theta \longrightarrow dz = -\sin\theta d\theta$. Like in section A.1 we plug the separation ansatz into the Laplace equation. The resulting equation has a left hand side which only depends on r and a right hand side depending on θ and φ. The left hand side and the right hand side are both equal to a constant which we call λ. Finally we get three equations for the three variables r, θ and φ. The solution for the φ-part leads to

$$Q(\varphi) = e^{im\varphi} \tag{3.22}$$

The solution for the θ-part is:

$$P(\theta) = P_l^m(x) \tag{3.23}$$

These are the so-called Legendre polynomials (see appendix).
The solution for the r-part is of the form r^l within the sphere and $\frac{1}{r^{l+1}}$ outside of the sphere.
The final solution for the induced part of the screened interaction is:

$$W_{ind}(\boldsymbol{r},\boldsymbol{r}',\omega) = \sum_{l=0}^{\infty} \sum_{m=-l}^{l} \frac{4\pi}{2l+1} \frac{1}{r^{l+1} r'^{l+1}} \gamma_l(\omega) \cdot a^{2l+1} \cdot Y_{lm}^{\star}(\theta',\varphi') Y_{lm}(\theta,\varphi) \tag{3.24}$$

(compare the expression for the multipole expansion (equation (2.174)))
a is the radius of the sphere. γ_l are the associated response functions of the sphere and are given by

$$\gamma_l(\omega) = \frac{l(1-\varepsilon)}{l(\varepsilon+1)+1} \tag{3.25}$$

(see [7] for details)
The full screened interaction is therefore:

$$W(\boldsymbol{r},\boldsymbol{r}',\omega)=\frac{1}{|\boldsymbol{r}-\boldsymbol{r}'|}+\sum_{l=0}^{\infty}\sum_{m=-l}^{l}\frac{4\pi}{2l+1}\frac{a^{2l+1}}{r^{l+1}r'^{l+1}}\gamma_l(\omega)\cdot Y^{\star}_{lm}(\theta',\varphi')Y_{lm}(\theta,\varphi)\quad(3.26)$$

$W(\boldsymbol{r},\boldsymbol{r}',\omega)$ can be interpreted as the total energy loss or in other words as the work done against the electric field which acts on the electron along the whole trajectory [38].
We can express the energy loss with the energy loss probability $P(\omega)$:

$$W(\boldsymbol{r},\boldsymbol{r}',\omega)=\int_{0}^{\infty}d\omega\omega P(\omega)\quad(3.27)$$

$P(\omega)$ is given by

$$P(\omega)=\frac{1}{\pi v^2}\int_{-\infty}^{\infty}dz'dzIm\left\{W_{ind}(\boldsymbol{r},\boldsymbol{r}',\omega)\cdot e^{-i\omega(z-z')/v}\right\}\quad(3.28)$$

We have to insert $W_{ind}(\boldsymbol{r},\boldsymbol{r}',\omega)$ into this equation and then perform the integral along the electron trajectory. To perform the integration we need the following result:

$$\int_{-\infty}^{\infty}dx\frac{P_l^m\left(\frac{z}{\sqrt{b^2+z^2}}\right)}{\sqrt{b^2+z^2}^{\,l+1}}e^{ikz}=2\cdot\left(\frac{ik}{|k|}\right)^{l-m}\frac{|k|^l}{(l-m)!}K_m(|k|\cdot b)\quad(3.29)$$

with spherical coordinates $r=\sqrt{b^2+z^2}$ and $\cos\theta=\frac{z}{r}$. $k=\frac{\omega}{v}$ is the wave number. Details of this non-trivial result can be found in [39].
Putting all this into (3.28) yields the expression for the energy loss probability for an electron passing by the sphere without penetrating it:

$$P(\omega)=\frac{4a}{\pi v^2}\sum_{l=1}^{\infty}\sum_{m=0}^{l}Im(\gamma_l(\omega))\left(\frac{\omega a}{v}\right)^{2l}\frac{2-\delta_{m0}}{(l+m)!(l-m)!}K_m^2\left(\frac{\omega b}{v}\right)\quad(3.30)$$

K_m stands for the modified Bessel function of order m and δ_{m0} is the Kronecker delta. A plot of $P(\omega)$ against the frequency ω can be seen below.

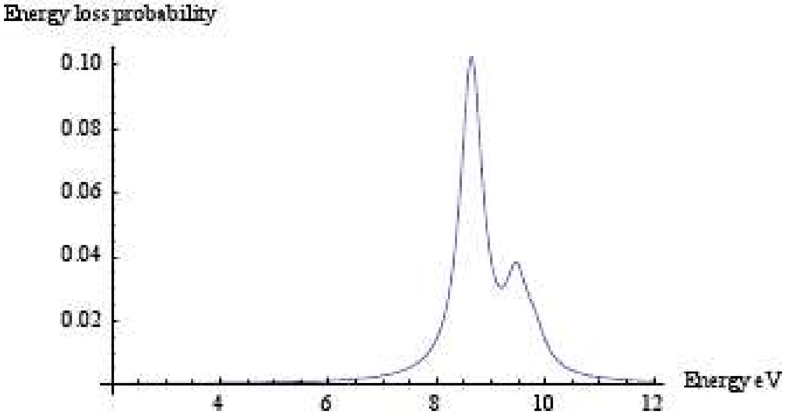

Figure 3.2.: Plot of the electron energy loss probability $P(\omega)$ on the y-axis against the energy ω on the x-axis for an aluminium nanosphere. The plot has been obtained with a Mathematica-routine and for two values of l in the sum.

The radius of the particle was chosen to be $a = 5$ nm ad the impact parameter $b = 6$ nm. We see two peaks. The first one corresponds to $l = 1$ in the sum and the second one to $l = 2$. In general the poles of the response function give a discrete set of l-modes [1]:

$$\omega_l = \sqrt{\frac{l}{2l+1}}\omega_p \tag{3.31}$$

from $\omega = \frac{\omega_p}{\sqrt{3}}$ for $l = 1$ (Mie-frequency) till $\omega = \frac{\omega_p}{\sqrt{2}}$ for $l \to \infty$ [1] (the surface modes of the energy loss probability for thin films as obtained by Ritchie [22]). For large radius a (a large enough in comparison with $\frac{v}{\omega}$) high multipolar terms are strongly excited which correspond to energy losses near $\frac{\omega_p}{\sqrt{2}}$ [1]. For $a \to \infty$ $P(\omega)$ converges to the energy loss probability for a plane (see [1] and [22]). Otherwise the classical dipole excitation for $l = 1$ is the main excitation. The resolution is given by a and b [1].
The analytical results for gold are presented in figure 3.3:

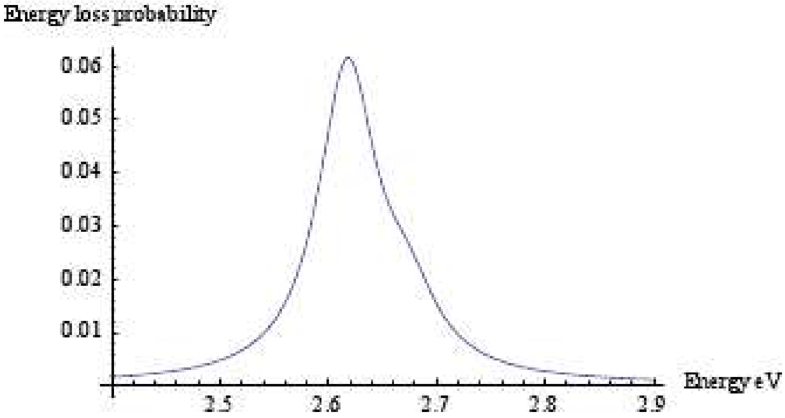

Figure 3.3.: Plot of the electron energy loss probability $P(\omega)$ on the y-axis against the energy ω on the x-axis. The plot has been obtained with a Mathematica-routine and for two values of l in the sum. The material of the nanosphere is gold in this case.

The radius was $a = 5$ nm and $b = 6$ nm.

3.3. Electron trajectory penetrating sphere

If the electron goes through the sphere we have the following geometry:

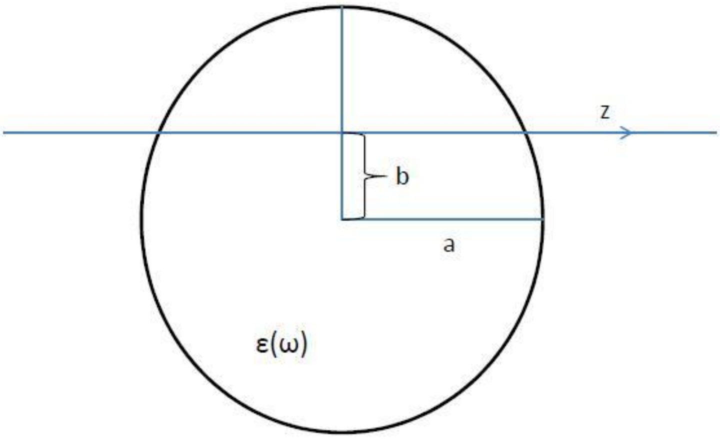

Figure 3.4.: Electron beam penetrating the dielectric nanosphere. The definitions are the same as in figure 3.1.

The calculation is performed basically in the same way as for the previous case. Again we want to solve the Poisson equation

$$\Delta\Phi(\boldsymbol{r},\omega) = -\frac{4\pi}{\varepsilon(\omega)}\rho(\boldsymbol{r},\omega) \tag{3.32}$$

with the charge density

$$\rho(\boldsymbol{r},\omega) = -\frac{1}{v}e^{\frac{i\omega x}{v}}\delta(y-b)\delta(z-b) \tag{3.33}$$

and again we define the Green function for this problem to be the screened interaction W, obeying the following Poisson equation

$$\Delta W(\boldsymbol{r},\boldsymbol{r}',\omega) = -\frac{4\pi}{\varepsilon(\omega)}\delta(\boldsymbol{r}-\boldsymbol{r}') \tag{3.34}$$

The relation between Φ and W is again given by

$$\Phi(\boldsymbol{r},\omega) = \int_{-\infty}^{\infty} d^3\boldsymbol{r}' W(\boldsymbol{r},\boldsymbol{r}',\omega)\rho(\boldsymbol{r}',\omega) \tag{3.35}$$

Again we are interested in the induced part of W. To calculate the screened interaction one has to expand W in a multipolar series (see section 2.2.4). This expansion has to be performed separately in each region of space. For our geometry (sphere) we have three regions. If both points r and r' lie inside of the sphere the first of the three terms holds. If both points lie outside of the sphere the second term holds. The coefficients of the expansions can be obtained by the appropriate boundary conditions (see section 2.1.3).

$$W_{ind}(\boldsymbol{r},\boldsymbol{r}',\omega) = \sum_{l=0}^{\infty}\sum_{m=-l}^{l}\frac{4\pi}{2l+1}\frac{r^l r'^l}{a^{2l+1}}\alpha_l(\omega)Y^\star_{lm}(\theta',\varphi')Y_{lm}(\theta,\varphi) \quad r,r' \le a \tag{3.36}$$

$$W_{ind}(\boldsymbol{r},\boldsymbol{r}',\omega) = \sum_{l=0}^{\infty}\sum_{m=-l}^{l}\frac{4\pi}{2l+1}\frac{r^l_<}{r^{l+1}_>}\beta_l(\omega)Y^\star_{lm}(\theta',\varphi')Y_{lm}(\theta,\varphi) \quad r_< \le a, r_> \ge a \tag{3.37}$$

$$W_{ind}(\boldsymbol{r},\boldsymbol{r}',\omega) = \sum_{l=0}^{\infty}\sum_{m=-l}^{l}\frac{4\pi}{2l+1}\frac{a^{2l+1}}{r^{l+1}r'^{l+1}}\gamma_l(\omega)Y^\star_{lm}(\theta',\varphi')Y_{lm}(\theta,\varphi) \quad r,r' \ge a \tag{3.38}$$

Here $r_<$ is the smallest of r and $r_>$ the biggest of r. The response functions γ_l, α_l

and β_l are given by

$$\begin{aligned}
\alpha_l(\omega) &= \frac{(l+1)(\varepsilon-1)}{\varepsilon(l\varepsilon+l+1)} && (3.39)\\
\beta_l(\omega) &= \frac{2l+1}{l\varepsilon+l+1} && (3.40)\\
\gamma_l(\omega) &= \frac{l(1-\varepsilon)}{l\varepsilon+l+1} && (3.41)
\end{aligned}$$

where $\varepsilon(\omega) = 1 - \frac{\omega_p^2}{(\omega i\gamma)}$ is the dielectric function of Aluminium. For more details about the derivation of these terms and about the response functions we refer to [40] and [41].

3.3.1. Electron energy loss probability for an electron penetrating the sphere

As mentioned above the derivation of the electron energy loss probability for an electron penetrating the sphere is done in the same way as in the case for an electron passing by the sphere. More details can be found in [7], [41] and [40]. Here we only give the final result:

$$\begin{aligned}
P(\omega) &= \frac{4a}{\pi v^2}\sum_{l=0}\sum_{m=0}(2-\delta_{m0})\frac{(l-m)!}{(l+m)!}\left\{Im\{\gamma_l(\omega)\}\left(A^o_{lm}\right)^2 + \right.\\
&+ \left. Im\left\{2\beta_l(\omega) - \frac{1}{\varepsilon(\omega)}\right\}A^i_{lm}A^o_{lm} + Im\left\{\alpha_l(\omega)\right\}\left(A^i_{lm}\right)^2\right\} \qquad (3.42)
\end{aligned}$$

where the functions A_{lm} are defined in the following way:

$$\begin{aligned}
B^o_{lm}(\omega) &= a^l\int_{z_a}^{\infty} dz\frac{1}{r^{l+1}}P_l^m\left(\frac{z}{r}\right)g_{lm}\left[\frac{\omega z}{v}\right] && (3.43)\\
B^i_{lm}(\omega) &= \frac{1}{a^{l+1}}\int_0^{z_a} dz r^l P_l^m\left(\frac{z}{r}\right)g_{lm}\left[\frac{\omega z}{v}\right] && (3.44)
\end{aligned}$$

where $z_a = \sqrt{a^2-b^2}$ and $r = \sqrt{z^2+b^2}$. $P_l^m(x)$ are the Legendre polynomials and

$$g_{lm}(z) = \begin{cases}\cos(z) & \text{if } (l+m) \text{ even}\\ \sin(z) & \text{if } (l+m) \text{ odd}\end{cases}$$

Now we come to the definition of the functions A_{lm}:

$$A^{i,o}_{lm} = \begin{cases}B^{i,o}_{lm} & \text{if } (l+m) \text{ even}\\ i^{-(l+m)}B^{i,o}_{lm} & \text{if } (l+m) \text{ odd}\end{cases}$$

This equation contains all the bulk terms. These terms are the ones proportional to $Im(-1/\varepsilon(\omega))$.
The energy loss W has two contributions; the contribution from the surface comes from the induced parts of the potential and has been calculated above (equation (3.42)). The contribution from the Coulomb part is the energy loss experienced by a classical particle travelling the distance $2z_a$ through an unbounded medium with the dielectric function $\varepsilon(\omega)$. It yields the bulk energy loss probability:

$$P(\omega) = 4z_a \frac{1}{\pi v^2} Im \left\{ -\frac{1}{\varepsilon(\omega)} \right\} \ln \frac{2v^2}{\omega_p} \tag{3.45}$$

For details of the derivation of this term we refer to [7] and [41]. ω_p is the bulk plasmon energy. The peaks of $P(\omega)$ in an infinite medium, i.e. from the bulk loss probability, are given by the poles of $Im\left\{-\frac{1}{\varepsilon(\omega)}\right\}$. They correspond to an excitation at the bulk plasmon energy ω_p for a free electron without damping.
In the introduction we mentioned the so-called begrenzungs-effect or boundary effect. In equation (3.42) the term proportional to ε^{-1} is exactly this contribution. It is a negative correction to the bulk plasmon excitation probability due to the presence of the boundary, i.e. the interface ([7], [36]). It reduces the bulk losses compared to the case of an electron travelling through an unbounded medium. The first description of it has been performed in [22] for thin films and occurs for penetrating electron beams. The physical meaning of this effect is that the excitation of surface modes takes place at the expense of the excitation of bulk modes [7]. The total energy loss is thus smaller than that of an infinite medium. To get a bulk plasmon excitation probability which is positive, the negative bulk correction from the boundary effect has to be balanced by the infinite bulk term [7].

4. Numerical methods

This chapter provides the basics used in the program for the numerical determination of the energy loss spectra. We are using a boundary element method approach whereby the surface of the metallic nanoparticle is discretized by small triangular surface elements. The form of the boundary element method used here is based on [34] and [42]. We assume homogeneous dielectric surroundings and isotropic dielectric functions for the materials and particles under consideration, which are separated by abrupt interfaces [27]. The advantage is that one only has to discretize the boundaries between the different dielectric media and not the whole volume [27].

Since the potentials caused by σ and $\boldsymbol{j}$ have a weaker spatial dependence for our approach we can assume that the surface charges and currents are located at the centers of each surface element. In this approach we write the potentials as a sum over all surface elements. In the program the particles are stored as faces ad vertices. The faces are the areas of the triangles and the vertices are their edge points.

4.1. Boundary element method

In this thesis we use a boundary element method approach for the numerical determination of the energy loss spectra. For details about the topic of this section we refer to [6], [27], [34] and [42]. In our approach we aim at the determination of the surface charge density σ such that the boundary conditions of the Maxwell equations are fulfilled. Thus the BEM (boundary element method) approach consists of solving the Maxwell equations by calculating the surface charge densities σ and surface currents $\boldsymbol{j}$ on the boundary of the particle for a given external excitation. For spherical particles we can compare the results with the ones obtained by Mie theory.

The BEM approach is appropriate for dielectric environments consisting of bodies which can be described by homogeneous and isotropic dielectric functions. The dielectric bodies have to be separated by sharp boundaries. The volume of the bodies (particles) is denoted by V and their boundary by ∂V. The outer surface normal $\boldsymbol{n}$ defines the interior and exterior of the particle. The direction in which it points is the outside direction. The dielectric functions are denoted by ε_1 (outside)

and ε_2 (inside).
We are using the quasistatic approximation. Quasistatic means that we are using a frequency dependent dielectric function $\varepsilon(\omega)$ and not the static limit ε. The arguments justifying the usage of the quasistatic limit and thus neglecting the dependence on momentum have already been introduced in chapter 2. The electrical field is expressed by the gradient of a scalar potential Φ as in classical electrostatics (see section 2.2).
The main idea of the BEM approach is that one can easily write down the solutions of the Poisson equation (or Laplace equation without any external sources) as an ad-hoc solution. For restricted regions these solutions still fulfill the Laplace or Poisson equation but with the wrong boundary conditions. To correct this we artificially add a surface charge distribution σ on the boundary such that the boundary conditions are fulfilled. The ad-hoc solutions for the case of an unbounded medium and the contributions from the surface charges then fulfill the equations with the right boundary conditions. Thus they are the proper and unique solutions of our problem.
For the solution of the Poisson equation we introduce the Green function (see 2.2.3):

$$\Delta G(\boldsymbol{r}-\boldsymbol{r}') = -4\pi\delta(\boldsymbol{r}-\boldsymbol{r}') \tag{4.1}$$

where G is defined as

$$G = \frac{1}{|\boldsymbol{r}-\boldsymbol{r}'|} \tag{4.2}$$

This solves the Poisson equation in an unbounded and homogeneous region for a pointlike source. For the external excitation Φ_{ext} we can write the scalar potential in the following form (ad hoc):

$$\Phi(\boldsymbol{r}) = \int_{\partial V} G(\boldsymbol{r}-\boldsymbol{s}')\sigma(\boldsymbol{s}')dA' + \Phi_{ext}(\boldsymbol{r}) \tag{4.3}$$

σ is the surface charge density. The solution is constructed in such a way that the Laplace-equation is automatically fulfilled in the media and σ has to be determined such that the Maxwell equations are fulfilled. The continuity of the potential at the boundary implies continuity of the tangential electrical field $\boldsymbol{E}$. This is fulfilled if the surface charge density is the same in- and outside of the boundaries. The perpendicular component of $\boldsymbol{D}$ is also continuous at the boundaries. If we want to use this condition we have to evaluate the following:

$$\lim_{\boldsymbol{r}\to\boldsymbol{s}} \boldsymbol{n}\cdot\boldsymbol{\nabla}\Phi(\boldsymbol{r}) \equiv \lim_{\boldsymbol{r}\to\boldsymbol{s}} \frac{\partial\Phi(\boldsymbol{r})}{\partial n} = \lim_{\boldsymbol{r}\to\boldsymbol{s}} \int_{\partial V} \frac{\partial G(\boldsymbol{r}-\boldsymbol{s}')}{\partial n}\sigma(\boldsymbol{s}')dA' + \frac{\partial\Phi_{ext}(\boldsymbol{r})}{\partial n} \tag{4.4}$$

We have to be cautious with the limes in the integral. Assuming a coordinate system with $\boldsymbol{n}$ in the z-direction and σ being constant in a small circle with radius

R we get

$$\lim_{z\to\pm 0} \boldsymbol{n} \int \frac{\boldsymbol{r}-\boldsymbol{s}'}{|\boldsymbol{r}-\boldsymbol{s}'|^3} dA' \longrightarrow \lim_{z\to\pm 0} 2\pi z \int\limits_0^R \frac{\rho d\rho}{(\rho^2+z^2)^{\frac{3}{2}}} = 2\pi \tag{4.5}$$

We have a +-sign if we come from the outside. We get for the normal derivative of Φ:

$$\frac{\partial\Phi(\boldsymbol{s})}{\partial n} = \pm 2\pi\sigma(\boldsymbol{s}) + \int_{\partial V} F(\boldsymbol{s}-\boldsymbol{s}')\sigma(\boldsymbol{s}')dA' + \frac{\partial\Phi_{ext}(\boldsymbol{s})}{\partial n} \tag{4.6}$$

where

$$F(\boldsymbol{s}-\boldsymbol{s}') = \frac{\partial G(\boldsymbol{s}-\boldsymbol{s}')}{\partial n} \tag{4.7}$$

is the normal derivative of the Green function. $\frac{\partial}{\partial n}$ denotes the derivative along the outer surface normal.

Now we convert the boundary integrals to boundary elements. In order to do that we discretize the surface of the metallic nanoparticle by small surface elements and we assume that the surface charges are at the centers of the elements. We get

$$\left(\frac{\partial\Phi}{\partial n}\right)_i = \pm 2\pi\sigma_i + \sum_i F_{ij}\sigma_j + \left(\frac{\partial\Phi_{ext}}{\partial n}\right)_i \tag{4.8}$$

$F_{ij} = \left(\frac{\partial G}{\partial n}\right)_{ij}$ connects the surface elements i and j.

In a compact matrix notation equation (4.8) reads as follows:

$$\frac{\partial\Phi}{\partial n} = \pm 2\pi\sigma + F\sigma + \frac{\partial\Phi_{ext}}{\partial n} \tag{4.9}$$

The continuity of the dielectric displacements perpendicular component implies

$$\varepsilon_2 \left(2\pi\sigma + F\sigma + \frac{\partial\Phi_{ext}}{\partial n}\right) = \varepsilon_1 \left(-2\pi\sigma + F\sigma + \frac{\partial\Phi_{ext}}{\partial n}\right) \tag{4.10}$$

From this we get for σ:

$$(\Lambda + F)\sigma = -\frac{\partial\Phi_{ext}}{\partial n} \tag{4.11}$$

where

$$\Lambda = 2\pi\frac{\varepsilon_2+\varepsilon_1}{\varepsilon_2-\varepsilon_1} \tag{4.12}$$

From this we can determine σ by matrix inversion for a given external excitation.

We can make an eigenmode expansion of F:

$$FX = X\lambda, \quad \widetilde{X}F = \lambda\widetilde{X}, \quad X\widetilde{X} = \widetilde{X}X = 1 \tag{4.13}$$

where X and $\widetilde{X}$ are the matrices of the left and right eigenvectors. λ is the diagonal matrix with the corresponding eigenvectors. This eigenmode expansion is useful if we only need a certain range of eigenmodes for the description of the problem, e.g. for the excitation with plane waves.
We assume that we have a particle with ε_2 and ε_1 such that the matrix Λ becomes scalar:

$$\widetilde{X}(\Lambda + F)\sigma = (\Lambda + \lambda)\widetilde{X}\sigma = -\widetilde{X}\frac{\partial \Phi_{ext}}{\partial n} \tag{4.14}$$

From this we get for σ:

$$\sigma = -X(\Lambda + \lambda)^{-1}\widetilde{X}\frac{\partial \Phi_{ext}}{\partial n} \tag{4.15}$$

The eigenmodes (eigenenergies) correspond to particle plasmons. The eigenmodes of a sphere are the spherical harmonics.

4.2. External excitation

In our quasistatic approximation the surface derivative of the external potential describes the excitation. The excitation is the same inside and outside of the boundary. In chapter 2 we said that we use the quasistatic limit if the particle is significantly smaller than the wavelength of light λ (optical approximation). For a metallic sphere radii of a smaller than 50 nm are small enough to use this approximation.

4.2.1. Electron beam passing by the nanoparticle

For an electron beam passing by the nanoparticle without penetrating the sphere and moving along the z-direction we have the following external charge density:

$$\rho_{ext}(\boldsymbol{r}, \omega) = -\delta(r - b) \cdot \frac{e^{\frac{i(z-z_0)}{v}}}{v} \tag{4.16}$$

b is the impact parameter, defined as the distance from the center of the nanosphere to the electron beam.
The external potential calculated along the trajectory of the electron in z-direction is:

$$\Phi_{ext} = -\int \frac{\rho_{ext}(\boldsymbol{r}, \omega)}{\varepsilon|\boldsymbol{r} - \boldsymbol{r}'|}dz = -\frac{e^{-\frac{i\omega z_0}{v}}}{\varepsilon \cdot v}\int_{-\infty}^{\infty} \frac{e^{\frac{i\omega z}{v}}}{\sqrt{b^2 + z^2}}dz = -\frac{2}{\varepsilon \cdot v}K_0\left(\frac{\omega b}{v}\right)e^{-iz_0\frac{\omega}{v}} \tag{4.17}$$

K_0 is the modified Bessel-function. Here we have used the relation

$$K_\nu(z) = \frac{\sqrt{\pi} z^\nu}{2^\nu \Gamma\left(\nu + \frac{1}{2}\right)} \int_1^\infty e^{-zt} \left(t^2 - 1\right)^{\nu - \frac{1}{2}} dt \tag{4.18}$$

where $\Gamma\left(\nu + \frac{1}{2}\right) = \sqrt{\pi}$ for $\nu = 0$ ([43], [44]).
Now we want to calculate the quantity which is directly needed in the program. It is the gradient of Φ_{ext}:

$$-\boldsymbol{\nabla}\Phi_{ext} = -\left(\hat{r}\frac{\partial}{\partial r} + \hat{z}\frac{\partial}{\partial z}\right)\Phi_{ext} = -\frac{2}{\varepsilon v}\left\{K_1\left(\frac{\omega r}{v}\right)\hat{r} + iK_0\left(\frac{\omega r}{v}\right)\hat{z}\right\}\frac{\omega}{v}e^{-\frac{\omega z}{v}} \tag{4.19}$$

We insert this quantity into equation (4.15). The surface charge density enters into the equation which we need for the calculation of the energy loss probability. This equation is:

$$\Phi_{ind}(\boldsymbol{r}) = \int_{\partial\Omega} G(\boldsymbol{r} - \boldsymbol{s})\sigma(\boldsymbol{s})da = \sum_i G(\boldsymbol{r} - \boldsymbol{s}_i)\sigma_i \cdot A_i = \sum_i \frac{1}{|\boldsymbol{r} - \boldsymbol{s}_i|}\sigma_i A_i \tag{4.20}$$

where the sum over i runs over all triangles of the discretized surface of the nanosphere. This is the potential induced by the external excitation.

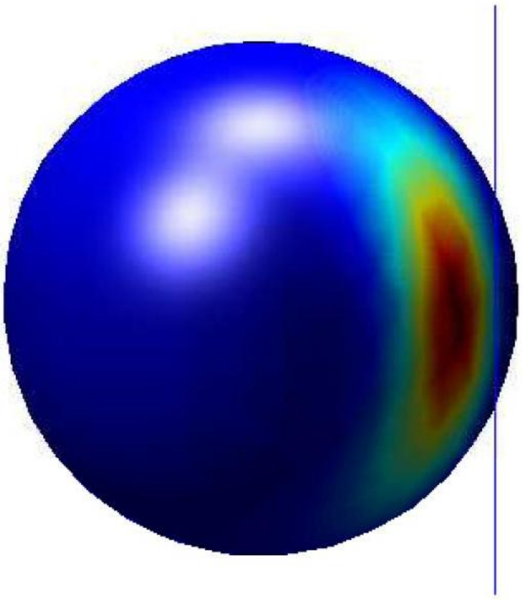

Figure 4.1.: Plot of a gold nanoparticle. The colour of the sphere shows the normal derivative of the external potential which has its highest value for red colour and the lowest value for blue colour. The line represents the electron beam passing by the sphere.

Figure 4.1 shows a plot of our spherical metallic nanoparticle. The blue line represents the electron beam. The regions of highest external potential are the ones close to the electron beam, i.e. the interaction is strongest in this region. To be correct not the potential is plotted in colour onto the surface of the particle. It is the normal derivative of the external potential induced on the surface of the sphere but we will refer to it as the potential keeping in mind that it actually is its normal derivative.

4.2.2. Electron beam penetrating the nanoparticle

For the case of penetrating electrons the only difference in the calculation lies in the external potential. Now we have to calculate it numerically by using the following formula:

$$\Phi_{ext}(\boldsymbol{r},\omega) = \int d\boldsymbol{r}' \frac{\rho_{ext}(\boldsymbol{r}',\omega)}{\varepsilon(\boldsymbol{r}',\omega)\cdot|\boldsymbol{r}-\boldsymbol{r}'|} \tag{4.21}$$

$\Phi_{ext}(\boldsymbol{r},\omega)$ is analogous to Φ_∞ of section 2.3 (see equation (2.181)). Again we use

$$\rho_{ext}(\boldsymbol{r}',\omega) = -\delta(x'-x_0)\delta(y'-y_0)\frac{e^{\frac{i\omega z'}{v}}}{v} \tag{4.22}$$

The potential becomes:

$$\Phi_{ext} = -\int dz' \frac{1}{v} \frac{e^{\frac{i\omega z'}{v}}}{\varepsilon\cdot\sqrt{(x-x_0)^2+(y-y_0)^2+(z-z')^2}} \tag{4.23}$$

Again we form the gradient of Φ:

$$\boldsymbol{\nabla}\Phi_{ext} = \left(\frac{\partial}{\partial x}\hat{x} + \frac{\partial}{\partial y}\hat{y} + \frac{\partial}{\partial z}\hat{z}\right)\Phi_{ext} \tag{4.24}$$

The three terms resulting from the gradient are:

$$\left(\frac{\partial}{\partial x}\right)\Phi_{ext} = \int dz' \frac{1}{2v\varepsilon} \frac{e^{\frac{i\omega z'}{v}}}{[(x-x_0)^2+(y-y_0)^2+(z-z')^2]^{\frac{3}{2}}}(2x-2x_0) \tag{4.25}$$

$$\left(\frac{\partial}{\partial y}\right)\Phi_{ext} = \int dz' \frac{1}{2v\varepsilon} \frac{e^{\frac{i\omega z'}{v}}}{[(x-x_0)^2+(y-y_0)^2+(z-z')^2]^{\frac{3}{2}}}(2y-2y_0) \tag{4.26}$$

$$\left(\frac{\partial}{\partial z}\right)\Phi_{ext} = \int dz' \frac{1}{2v\varepsilon} \frac{e^{\frac{i\omega z'}{v}}}{[(x-x_0)^2+(y-y_0)^2+(z-z')^2]^{\frac{3}{2}}}(2z-2z') \tag{4.27}$$

ε is the dielectric function of the particle.

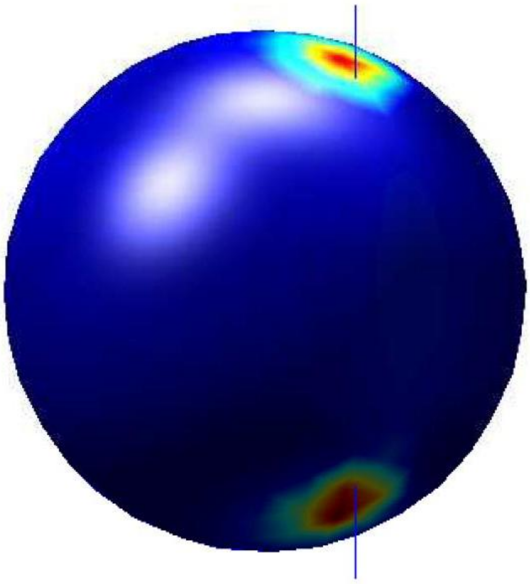

Figure 4.2.: The line through the nanosphere represents again the electron beam. We see that the potential has its highest values close to the intrusion points of the electron beam.

Figure 4.2 shows the nanoparticle with the electron beam going through it. The enhancement of the potential in the vicinity of the points of intrusion of the electron beam is clearly visible. One sees that the two red spots are not exactly symmetric (i.e. not exactly of the same size).

4.3. Energy loss

The quantity which lies at the heart of this diploma thesis is the so-called electron energy loss probability of the electron passing by or penetrating the sphere. It is:

$$P(\omega) = \frac{1}{v} \int Im \left\{ \rho^{\star}_{ext} \cdot \Phi_{ind} \right\} dz \tag{4.28}$$

It will be derived in what follows.

The electron beam interacts with the particle in the following way: the external potential of the electron beam induces a surface charge density on the sphere and thus an induced potential Φ_{ind} arises. This induced potential acts back on the electron or electrons, exerting an electric field which is acting on the electrons along the whole trajectory. The electrons experience an energy loss which can be calculated as the work done against the already mentioned electric field [38]:

$$W = \int_{-\infty}^{\infty} \frac{\partial \Phi_{ind}}{\partial z} dz = \int_{-\infty}^{\infty} d\Phi_{ind} dz - \int_{-\infty}^{\infty} \frac{\partial \Phi_{ind}}{\partial t} dt \tag{4.29}$$

If the induced potential is the same at both ends of the electrons trajectory (this is the case when we avoid the elastic contributions to W; they vanish when considering the whole trajectory [7]) this formula becomes

$$W = -\frac{1}{v} \int_{-\infty}^{\infty} \frac{\partial \Phi_{ind}}{\partial z} dz \tag{4.30}$$

All the derivatives of Φ_{ind} are evaluated at the trajectory. A more detailed discussion about the equality of the potentials at both ends of the trajectory ($\Phi(z = -\infty) = \Phi(z = \infty)$) can be found in [7].
The expression for the work W can be expressed via the loss probability (see equation (4.28) for instance):

$$W = \int_{0}^{\infty} d\omega P(\omega) \tag{4.31}$$

Since $W(\boldsymbol{r}, \boldsymbol{r'}, \omega) = W(\boldsymbol{r'}, \boldsymbol{r}, \omega)$ we get for the loss probability:

$$P(\omega) = \frac{1}{\pi v^2} \int_{-\infty}^{\infty} dz' \int_{-\infty}^{\infty} dz Im \left\{ W_{ind}(\boldsymbol{r}, \boldsymbol{r'}, \omega) \right\} e^{-i\omega(z-z')/v} \tag{4.32}$$

One can express this formula in terms of the charge density ρ (see equation (4.16)). This yields:

$$P(\omega) = \frac{1}{\pi} \int_{-\infty}^{\infty} d\boldsymbol{r'} \int_{-\infty}^{\infty} d\boldsymbol{r} Im \left\{ \rho^*(\boldsymbol{r}, \omega) W_{ind}(\boldsymbol{r}, \boldsymbol{r'}, \omega) \right\} \rho(\boldsymbol{r'}, \omega) \tag{4.33}$$

For an electron moving along the z-direction we only integrate over z and can bring this equation to the form which was encountered in equation (4.28).

5. Results

In this chapter we start with a comparison between Mie-theory and the BEM approach. We have divided the chapter into sections with plots of the energy loss against the energy and on the impact parameter and considered aluminium, silver and gold nanospheres for non-penetrating and penetrating trajectories.

5.1. Comparison between Mie-theory and boundary element method

In this section we compare the results from Mie-theory with the ones from the BEM approach. We start with plots of the energy loss against the energy and then give plots against the impact parameter. The energy axes are all in eV.

5.1.1. Plots against the energy

Non-penetrating trajectories

At first we consider the case of trajectories passing by the nanosphere (see figures 3.1 and 4.1). We show plots for aluminium, silver and gold for different radii and impact parameters.

Aluminium

In the following plots the red line corresponds to the Mie-theory-results and the blue line to the results from the BEM approach.
It is convenient here to mention that we have only considered two l-values in the sums of the analytical formulae for the energy loss probability in nearly all of our plots. We will explicitly mention if this is not the case. More accurate results could be obtained by taking into account more l-values. As was mentioned in the literature ([35], [39], [41], [45]) one has to consider many l-values for more accurate results. In the plots for aluminium we usually have taken three l-values in the sum.

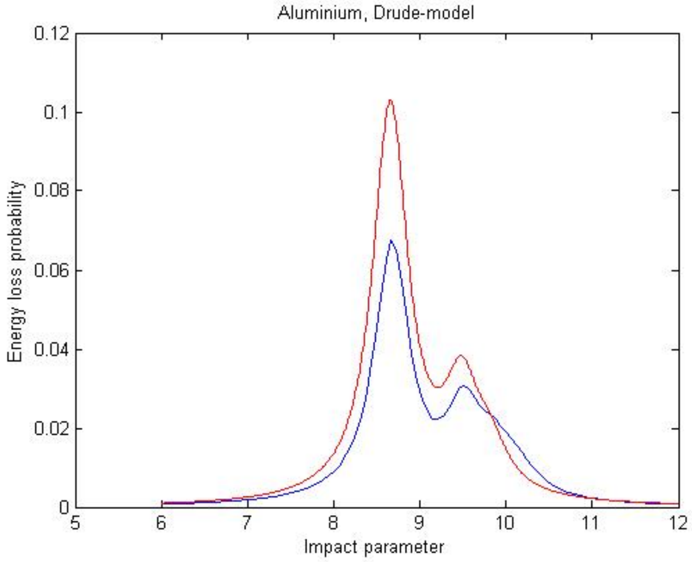

Figure 5.1.: Plot of the energy loss probability against the energy in eV for an aluminium nanosphere of radius $a = 5$ nm and an impact parameter of $b = 6$ nm.

For $a = 10$ nm and $b = 11$ nm we see a good qualitative agreement between the dipolar peak of the Mie and the BEM results. Here we already see a quantitative difference of the spectra. This difference becomes larger for larger spheres. This behaviour may be caused by the fact that retardation effects become more important for larger spheres. The reason for the quantitative difference has to be attributed to a mistake in the programs.

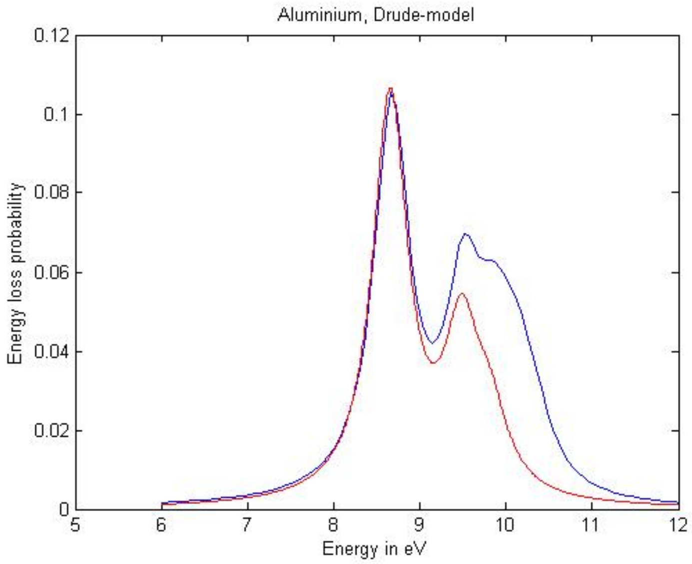

Figure 5.2.: Plot of the energy loss probability against the energy in eV for an aluminium nanosphere of radius $a = 10$ nm and an impact parameter of $b = 11$ nm.

In all of the figures for aluminium we see two main excitation peaks, one near 9 eV and another peak near 10 eV.

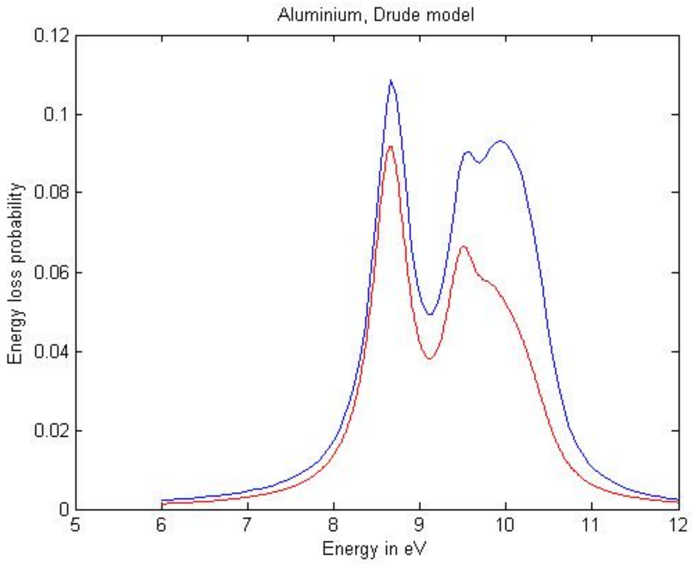

Figure 5.3.: Plot of the energy loss probability against the energy in eV for an aluminium nanosphere of radius $a = 15$ nm and an impact parameter of $b = 16$ nm.

Figure 5.3 shows a plot with 20 l-values in the sum.
The spectra can be interpreted as particle plasmon excitations. In chapter 3 we have determined the energy loss probability from the induced potential by making a multipolar expansion of the Green function W. For the plots within Mie-theory (red lines) we have taken into account two values of l in the sum. The dominant peaks in the plots correspond to the $l = 1$ contribution and the smaller peaks near 10 eV correspond to $l = 2$ (or higher multipolar terms, $l > 2$). There we also mentioned that the dipole excitation corresponds to the frequency $\omega = \frac{\omega_p}{\sqrt{3}}$. For aluminium $\omega_p = 15$ and $15/\sqrt{3} \approx 8.6603$. The dipole peaks lie near to that value. The agreement between Mie theory and BEM is best for $a = 15$ nm (figure 5.3). For the sphere with $a = 30$ we see that the higher multipolar terms (corresponding to the peak near 10 eV) are stronger excited than for the other radii considered here.

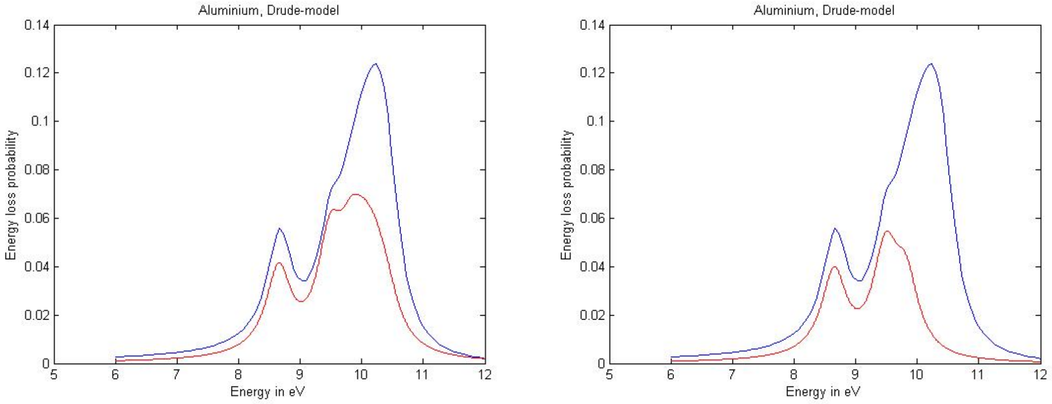

(a) (b)

Figure 5.4.: Plots of the energy loss probability against the energy in eV for an aluminium nanosphere of radius $a = 30$ nm and an impact parameter of $b = 31$ nm for 20 l-values (a) and 3 l-values (b).

In figure 5.4 we have again considered 20 l-values. To illustrate the point of the better agreement for more l-values we show a plot with only 3 values in this figure. We can see that the heights of the peaks do not differ that much for more (20) l-values.

For all of the aluminium plots we have used a Drude dielectric function.

The following plots are for two different impact parameters and a sphere of radius 10 nm and again 20 values of l.

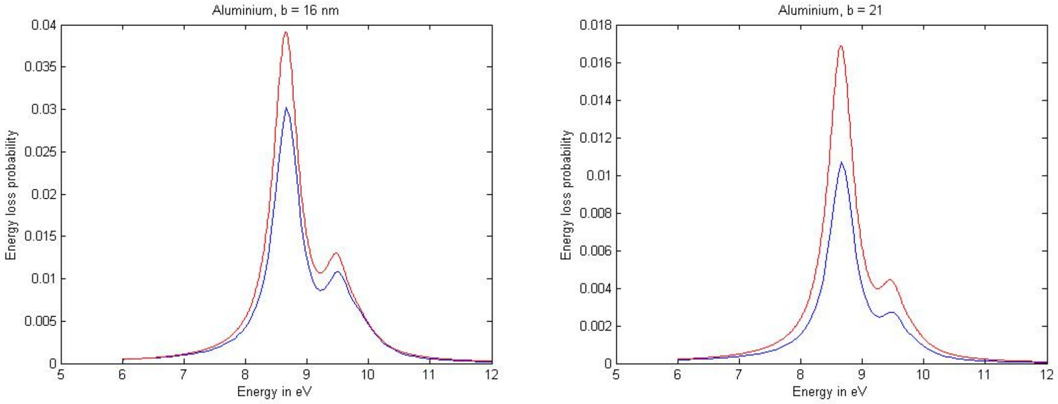

(a) (b)

Figure 5.5.: Plots of the energy loss probability against the energy in eV for an aluminium nanosphere of radius $a = 10$ nm and an impact parameter of $b = 16$ nm (a) and $a = 10$ nm and $b = 21$ nm (b).

We see that for higher values of the impact parameter the multipolar terms are not as strongly excited as for small b. Since the electron beam is farther away from the particle in this case this behaviour is expected.

Silver

From now on all of the plots only take into account 2 values of l in the analytical expressions for $P(\omega)$.
All three plots for a silver nanosphere clearly show two excitation peaks which can be interpreted analogously as for aluminium.

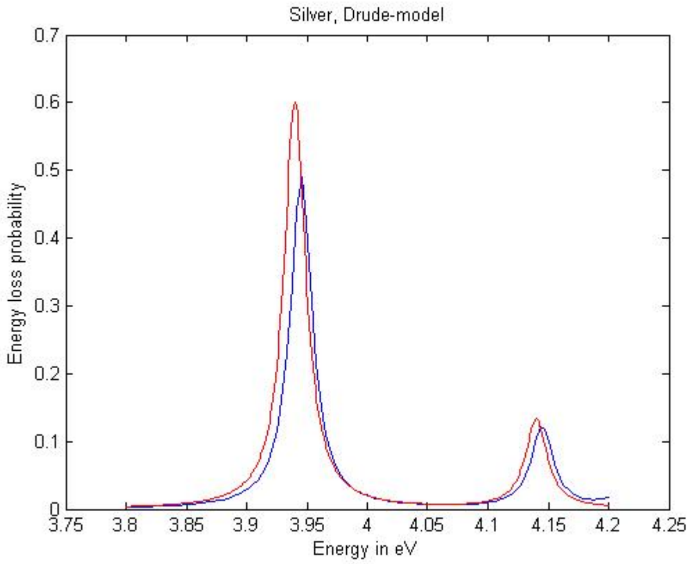

Figure 5.6.: Plot of the energy loss probability against the energy in eV for a silver nanosphere of radius $a = 5$ nm and an impact parameter of $b = 6$ nm.

The first peak lies around 3.95 eV and the second one around 4.15 eV.

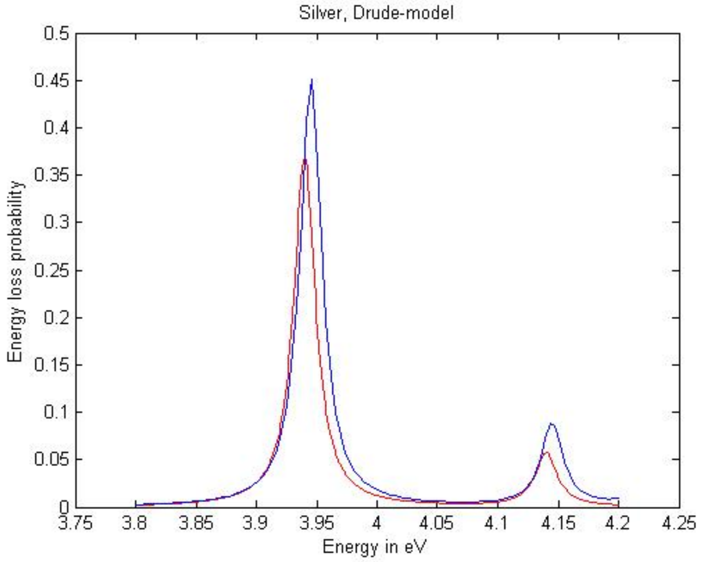

Figure 5.7.: Plot of the energy loss probability against the energy in eV for a silver nanosphere of radius $a = 10$ nm and an impact parameter of $b = 15$ nm.

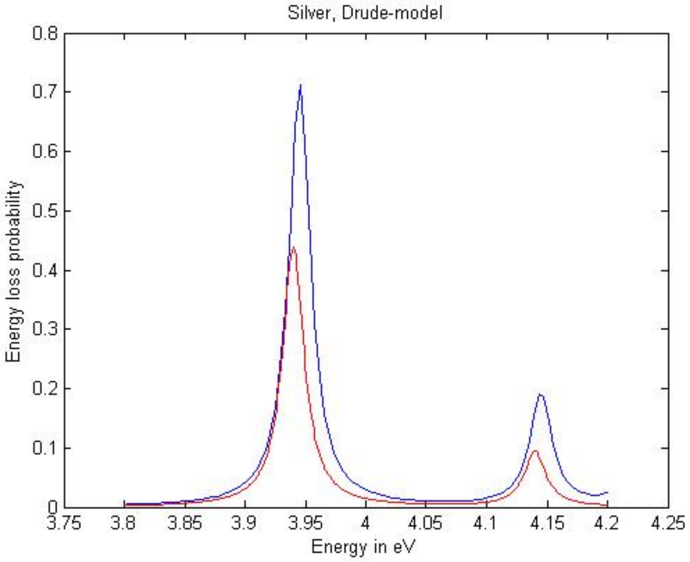

Figure 5.8.: Plot of the energy loss probability against the energy in eV for a silver nanosphere of radius $a = 15$ nm and an impact parameter of $b = 20$ nm.

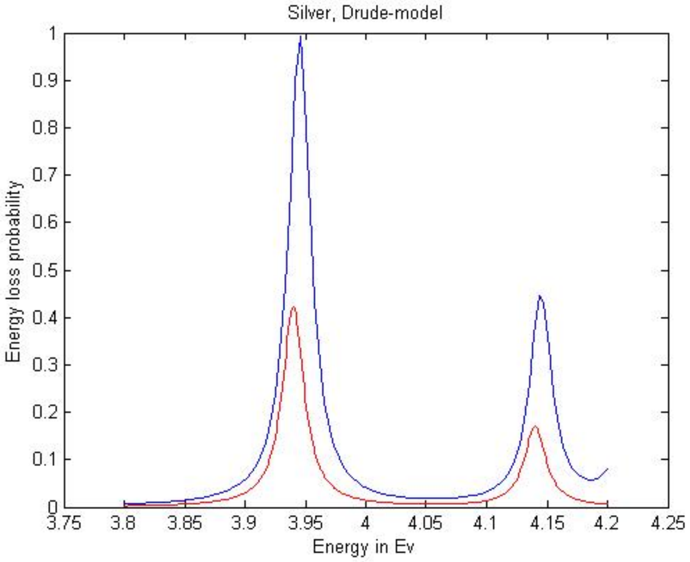

Figure 5.9.: Plot of the energy loss probability against the energy in eV for a silver nanosphere of radius $a = 30$ nm and an impact parameter of $b = 35$ nm.

Again we show plots for the same radius but different impact parameters ($a = 10$ nm in this case). We see that the quantitative agreement for a larger impact parameter is better.

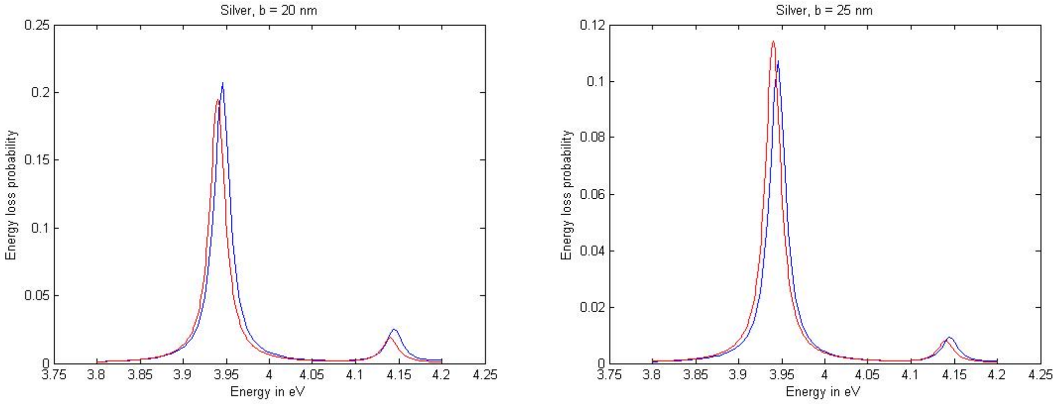

(a) (b)

Figure 5.10.: Plots of the energy loss probability against the energy in eV for a silver nanosphere of radius $a = 10$ nm and an impact parameter of $b = 20$ nm (a) and $a = 10$ nm and $b = 25$ nm (b).

For the largest of the considered impact parameters the quantitative agreement is best.

Gold

For gold, using a Drude dielectric function, we see that for larger spheres the agreement between BEM and Mie-theory is not as good as for the sphere with radius $a = 5$ nm. The main feature which all the plots have in common are again the excitation peaks around a certain resonance frequency for which particle plasmons are excited.

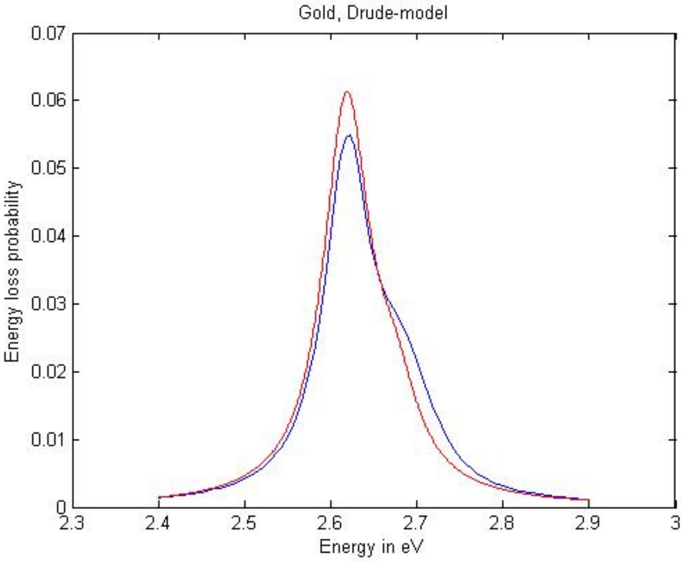

Figure 5.11.: Plot of the energy loss probability against the energy in eV for an aluminium nanosphere of radius $a = 5$ nm and an impact parameter of $b = 6$ nm.

We see that for gold the excitation peaks lie scarcely above 2.6 eV. For $a = 5$ nm we see a good agreement between the results from Mie theory and the numerical results.

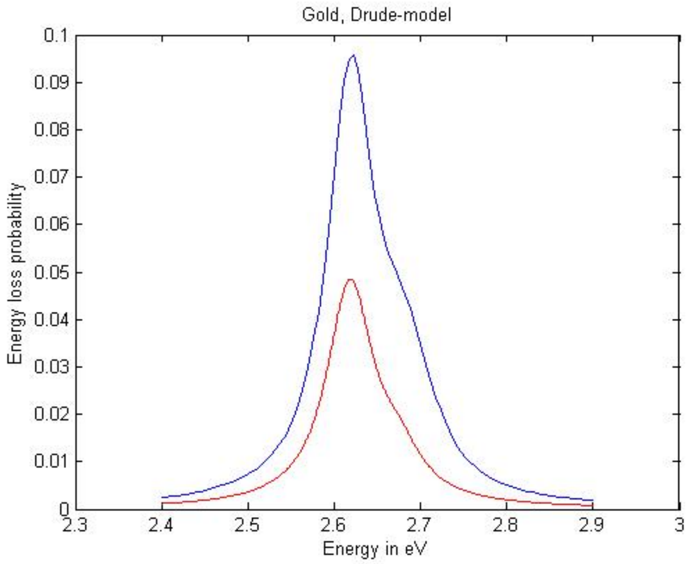

Figure 5.12.: Plot of the energy loss probability against the energy in eV for an aluminium nanosphere of radius $a = 15$ nm and an impact parameter of $b = 20$ nm.

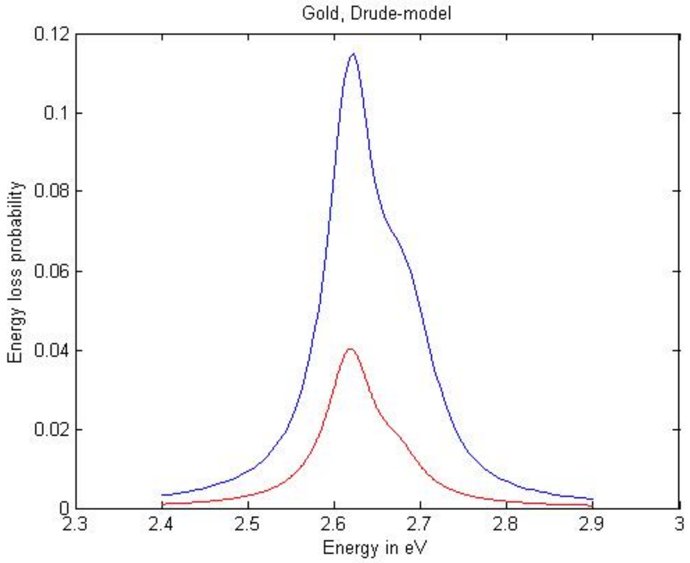

Figure 5.13.: Plot of the energy loss probability against the energy in eV for a gold nanosphere of radius $a = 30$ nm and an impact parameter of $b = 40$ nm.

Again a better agreement could be obtained by considering much more than 2 l-values in the sum.
At this stage it is crucial to mention that Johnson and Christy [46] have pointed out that the free Drude-model fails in the visible and ultraviolet region. Absorption in these regions comes from d-band transitions to the sp-conduction bands. The energies of the incident electrons have to lie lower than the threshold for the occurrence of interband transitions for the Drude expression of the dielectric function to be valid. The free-electron behaviour is dominant in the infrared region because there n is small and k is large [46] ($\varepsilon = n + ik$). As already mentioned in 2 the Drude model does not work as well for gold as for aluminium and silver.

Penetrating trajectories

In this section we provide loss-probability-vs.-energy-plots for penetrating trajectories. One of the main aims of this work was to obtain an EELS-spectrum for the case of an electron beam penetrating the nanoparticle.

Aluminium

The impact parameter in all of the cases is $b = 3$ nm and the radius is $a = 5$ nm.

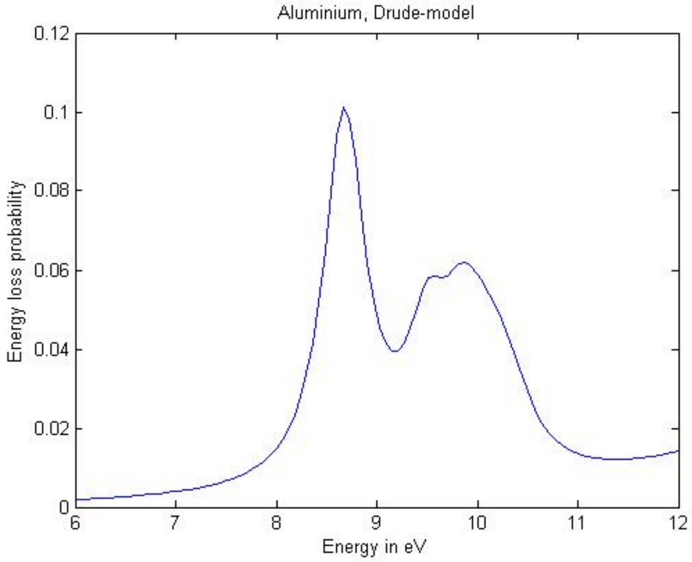

Figure 5.14.: Plot of the energy loss probability against the impact parameter for an aluminium nanosphere of radius $a = 5$ nm and an impact parameter of $b = 3$ nm.

Silver

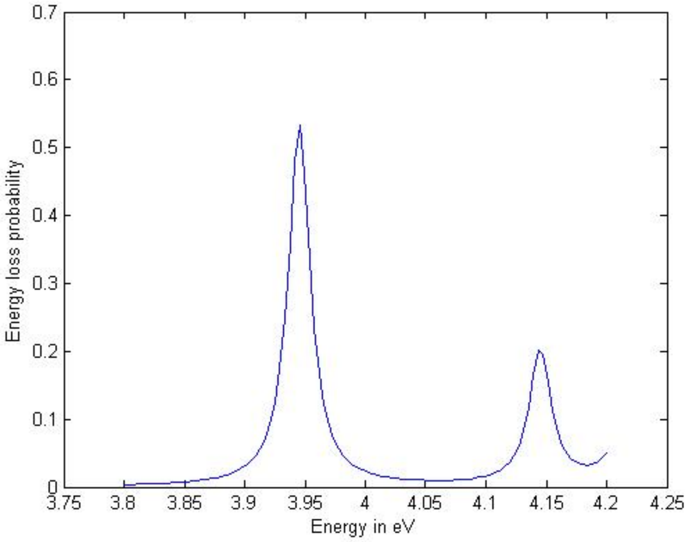

Figure 5.15.: Plot of the energy loss probability against the impact parameter for a silver nanosphere of radius $a = 5$ nm and an impact parameter of $b = 3$ nm.

For silver as well as for aluminium we see the main excitation peaks at the same energy values as for the case of non-penetrating trajectories. For both materials the Drude model is a good approximation.

Gold

In figure 5.16 we see a high peak near 2.9 eV. We have already mentioned the problem with d-band transitions when using the Drude dielectric function for gold. This peak can probably be caused by these transitions.

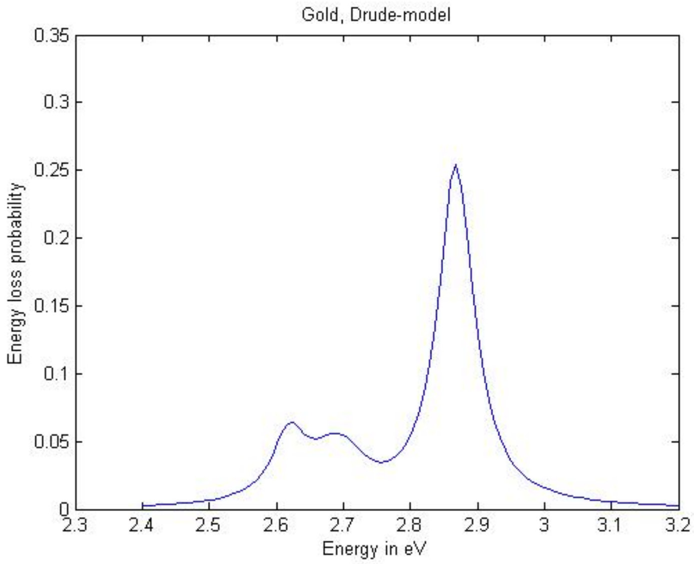

Figure 5.16.: Plot of the energy loss probability against the impact parameter for a gold nanosphere of radius $a = 5$ nm and an impact parameter of $b = 3$ nm.

5.1.2. Plots against the impact parameter

This section provides the most important results of this work.

Aluminium

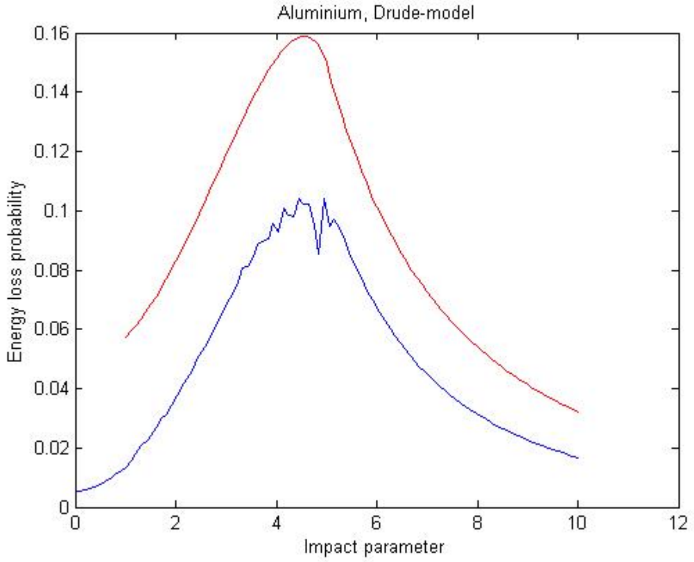

Figure 5.17.: Plot of the energy loss probability against the impact parameter for an aluminium nanosphere of radius $a = 5$ nm.

Figure 5.17 is one of the main results of this diploma thesis. It shows the energy loss spectrum of the electron beam penetrating an aluminium nanosphere. In this figure the impact parameter b is plotted against the energy loss probability $P(\omega)$. For values of $b < a$ we are within the sphere, namely the electron beam is going through it. For values of $b > a$ the electron beam passes the sphere without penetrating it. For $b = a$ we have grazing incidence, i.e. the electron beam does not penetrate the sphere but exactly touches its surface.

Silver

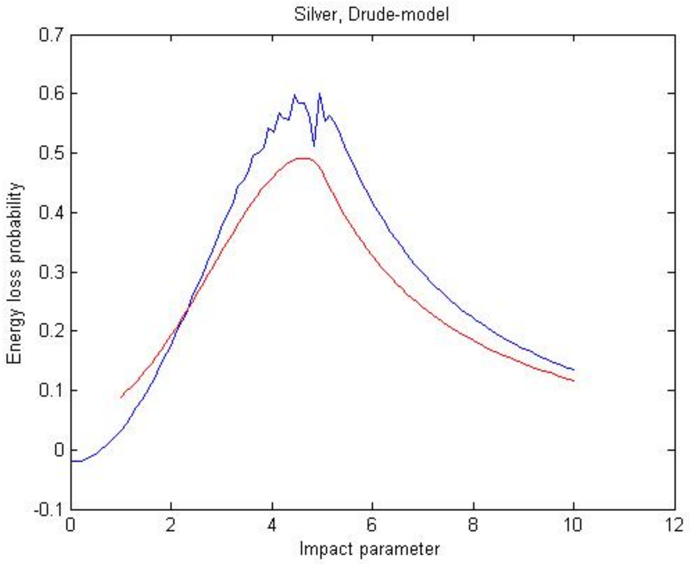

Figure 5.18.: Plot of the energy loss probability against the impact parameter for a silver nanosphere of radius $a = 5$ nm.

Gold

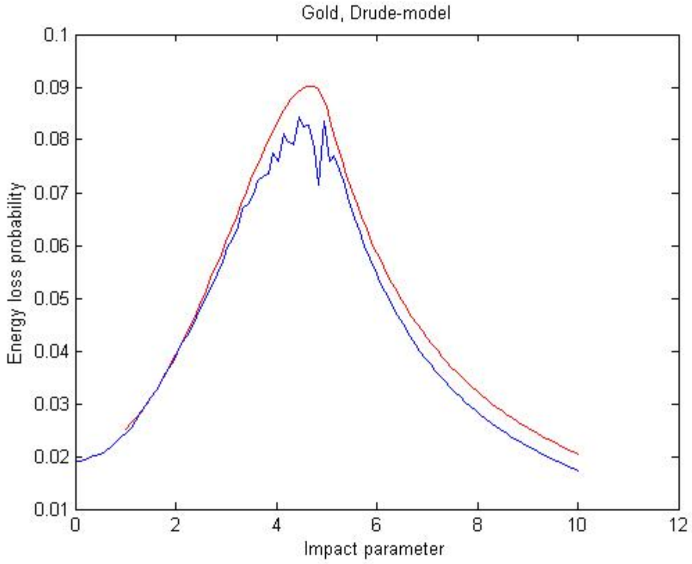

Figure 5.19.: Plot of the energy loss probability against the impact parameter for a gold nanosphere of radius $a = 5$ nm.

The agreement between the analytical results and the numerical results is best for gold. What one sees in all the plots is that the curve from the numerical results is not smooth. The reason for this is probably as follows. The surface of the nanosphere is discretized by small triangles in the BEM approach which we are using here. In our program we took the two triangles which are penetrated by the electron beam and their nearest neighbours and evaluated the mean value of the normal derivative of the external potential on them. In general one should have to integrate over these triangles to obtain a more accurate result. In conclusion we can say that the qualitative agreement between Mie theory and BEM approach is good but there is still work to be done to get a better quantitative agreement.

5.2. Drude versus full dielectric function

In chapter 2 we have derived the dielectric function from classical Maxwell´s theory and in the second subsubsection of 2.1.1 we have derived it for the classical Drude model for metals. There we have also mentioned a problem with this model for the case of gold caused by the fact that the density of states in the d-band is pronounced. The relatively high value $\varepsilon_0 = 10$ is also caused by this fact. The

plots that follow now show the real and imaginary parts of the dielectric function for two different media.
Figures 5.20 and 5.21 show the dielectric functions for aluminium in the Drude form. The real part of the dielectric function is depicted in 5.20 and the imaginary part in 5.21. The dielectric function is:

$$\varepsilon(\omega) = \varepsilon_\infty - \frac{\omega_p^2}{\omega \cdot (\omega + i\gamma)} \tag{5.1}$$

where ε_∞ is 1 for aluminium. γ describes the dissipative effects of the system and is an effective damping.

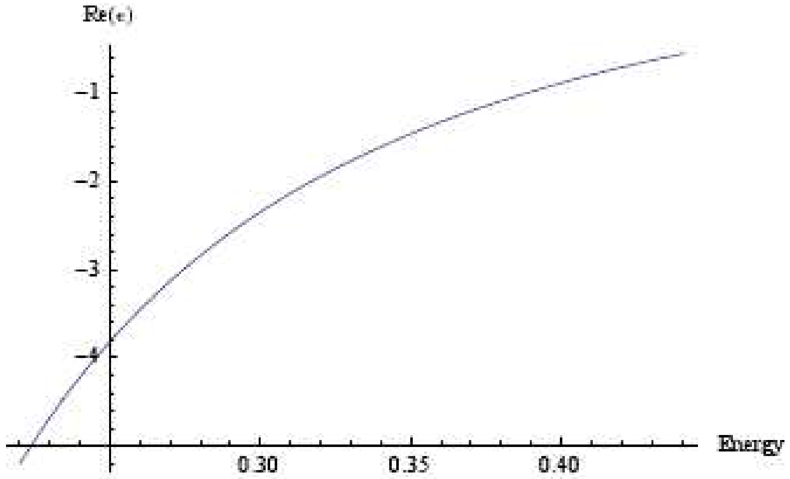

Figure 5.20.: Real part of the dielectric function for aluminium in the Drude-model. The energy axes is given in eV.

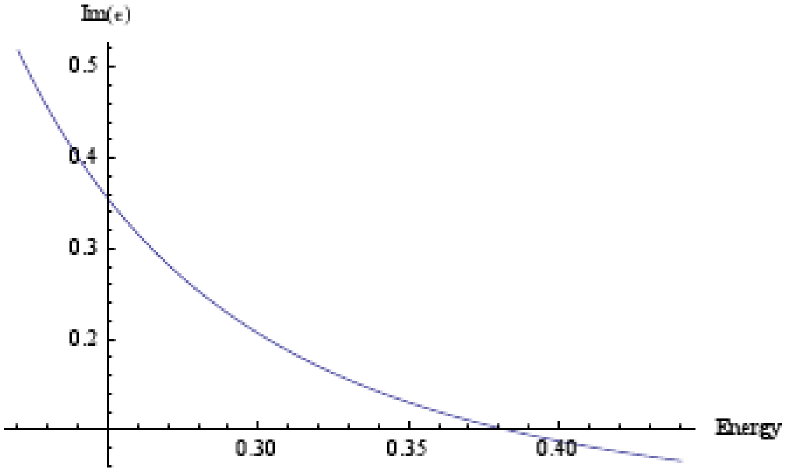

Figure 5.21.: Imaginary part of the dielectric function for aluminium in the Drude-model.

Figures 5.22 (imaginary part) and 5.24 (real part) show the same but this time for gold. The experimental values for gold can be found in [46]. In chapter 4 we present numerical results using a Drude dielectric function and a dielectric function interpolated from the experimental values of [46]. In [46] the analysis was done in terms of the complex index of refraction

$$\tilde{n} = n + ik \tag{5.2}$$

where n and k are the optical constants. The dielectric function is

$$\varepsilon = \varepsilon_1 + i\varepsilon_2 = \tilde{n}^2 \tag{5.3}$$

The experimental data for gold and silver have been taken from [46].

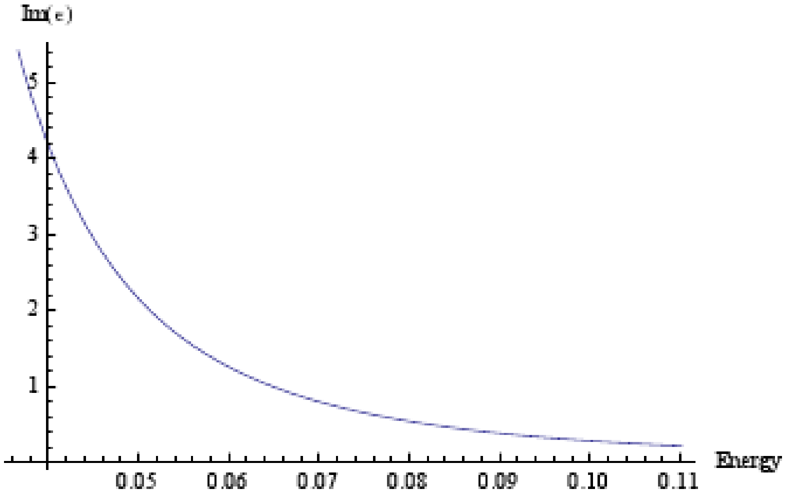

Figure 5.22.: Imaginary part of the dielectric function for gold in the Drude-model.

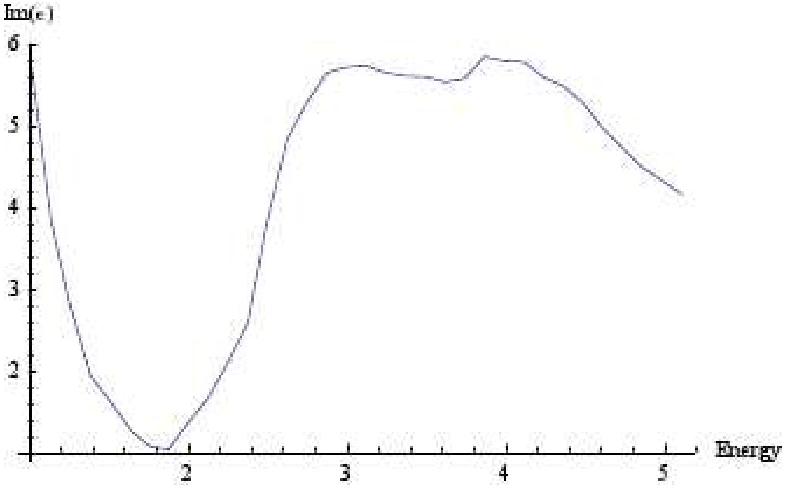

Figure 5.23.: Imaginary part of the experimental dielectric function for gold.

A comparison with the data from [46] shows that for the imaginary part of the dielectric function of gold the agreement with the experimental data is good for energies lower than 2.5 eV [9]. For the real part of the dielectric function the Drude form of the dielectric function is a very good approximation.

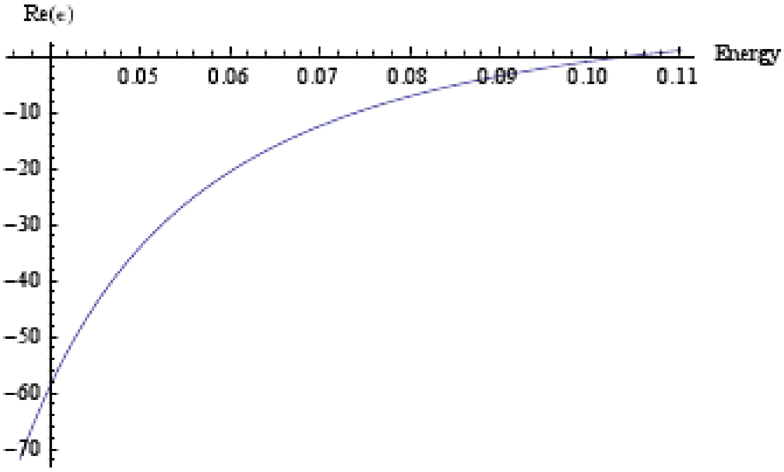

Figure 5.24.: Real part of the dielectric function for gold in the Drude-model.

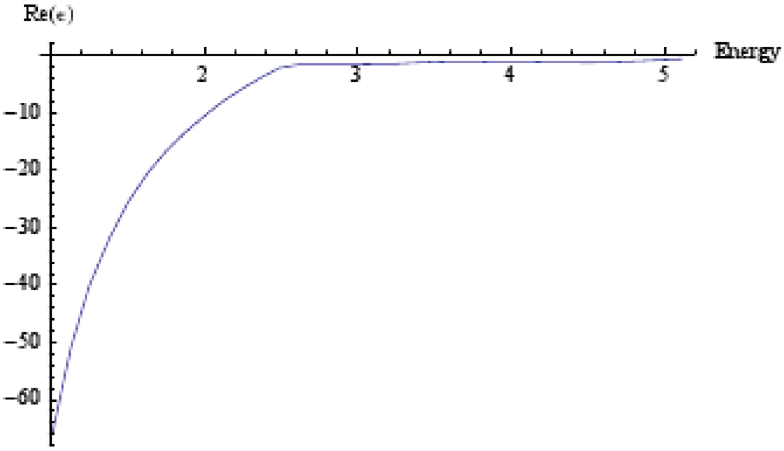

Figure 5.25.: Real part of the experimental dielectric function for gold.

For silver the real parts of the dielectric functions agree very well.

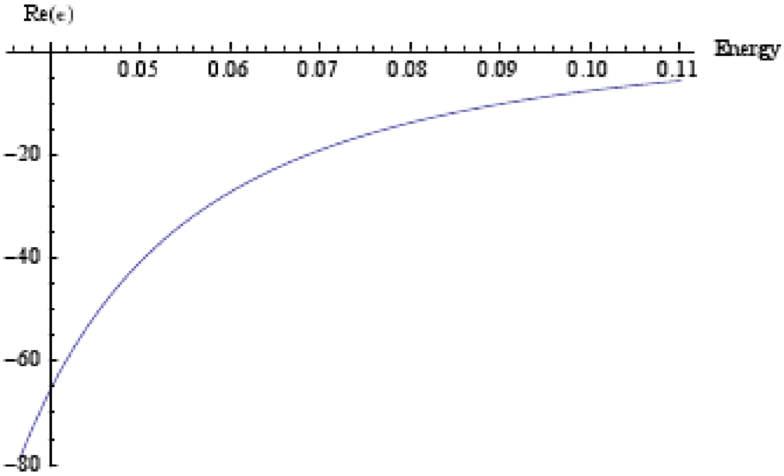

Figure 5.26.: Real part of the Drude dielectric function for silver.

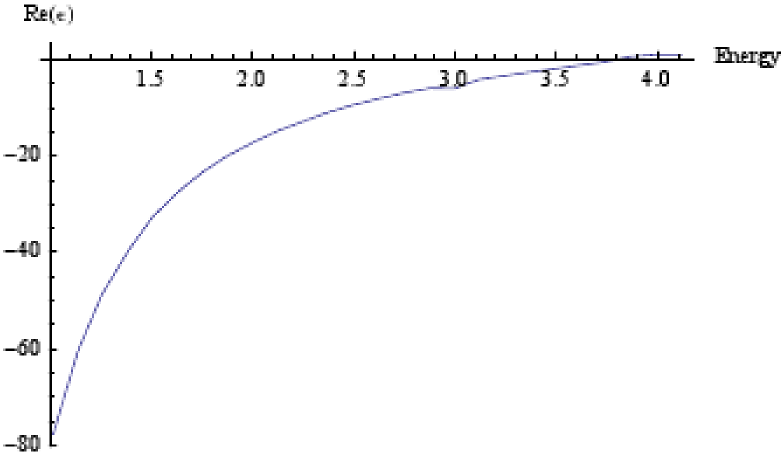

Figure 5.27.: Real part of the experimental dielectric function for silver.

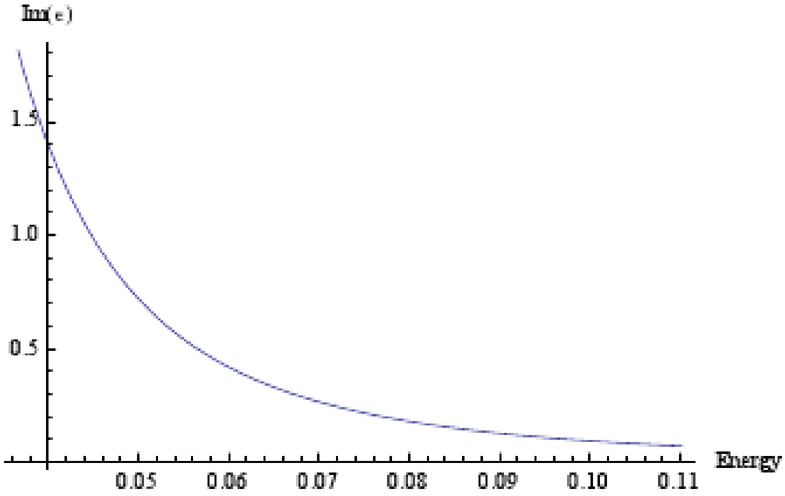

Figure 5.28.: Imaginary part of the Drude dielectric function for silver.

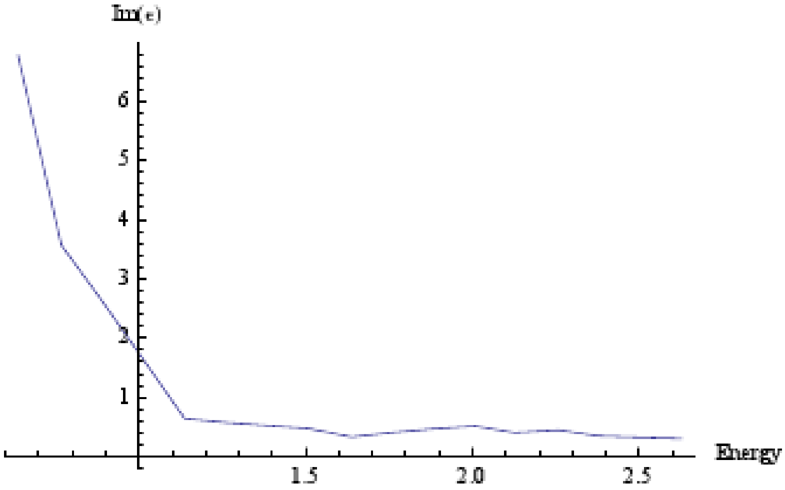

Figure 5.29.: Imaginary part of the experimental dielectric function for silver.

6. Summary and Outlook

In this diploma thesis we have been concerned with electron energy loss spectra (EELS) of metallic nanoparticles. We have discussed them for two cases:

- Electron beam passing by the metallic nanoparticle
- Electron beam penetrating the metallic nanoparticle

The main aim of the thesis was to obtain spectra for the second case. For this we used two methods:

1. Analytical method: We used Mie-theory to obtain the electron energy loss probability
2. Numerical method: We used the Boundary element method (BEM) to obtain the loss probability

In the comparison of the data we saw a good agreement for gold nanospheres using the classical Drude model for the description of the response of the system, i.e. its dielectric function. Especially the plots of the electron energy loss probability $P(\omega)$ against the impact parameter b were most important. We saw that the curve was not as smooth for the numerical results which can be explained by the "technique" we have used to handle the potential values at the triangles which are penetrated by the electron beam. We just took the potential values for these two triangles and its next neighbours and formed the average value of them. An improvement of the results could be obtained by considering more l-values. Furthermore we neglected the momentum dependence of ε throughout and used the Drude dielectric function in order to obtain all the results. The next important steps would be to consider the results for a "full" experimental dielectric function and the case of momentum dependence $\varepsilon(\boldsymbol{k}, \omega)$.

A. Appendix

A.1. Laplace equation in spherical coordinates

The following calculations are based mainly on [9] and [26]. Certain problems in physics have special types of symmetry. Many of these problems contain the Laplace operator Δ. One encounters it for instance in solving the Laplace or the Poisson equation. Depending on the type of symmetry one will use an adequate set of coordinates to solve them. For spherical symmetry one will use spherical coordinates denoted by (r, θ, ϕ). The Laplace equation in spherical coordinates with the Laplace operator acting on a scalar potential Φ is:

$$\Delta\Phi = \frac{1}{r}\frac{\partial^2}{\partial r^2}(r\Phi) + \frac{1}{r^2 \sin\theta}\frac{\partial}{\partial\theta}\left(\sin\theta\frac{\partial\Phi}{\partial\theta}\right) + \frac{1}{r^2\sin^2\theta}\frac{\partial^2\Phi}{\partial\varphi^2} = 0 \tag{A.1}$$

We make the following ansatz:

$$\Phi = \frac{R(r)}{r}P(\theta)Q(\varphi) \tag{A.2}$$

The aim of this ansatz is to separate the Laplace equation into three parts, namely three differential equations for the three variables r, θ and φ. Equation A.1 becomes:

$$PQ\frac{d^2R}{dr^2} + \frac{RQ}{r^2\sin\theta}\frac{d}{d\theta}\left(\sin\theta\frac{dP}{d\theta}\right) + \frac{RP}{r^2\sin^2\theta}\frac{d^2Q}{d\varphi^2} = 0 \tag{A.3}$$

We multiply this equation by $\frac{r^2\sin^2\theta}{RPQ}$ and get

$$r^2\sin^2\theta\left[\frac{1}{R}\frac{d^2R}{dr^2} + \frac{1}{Pr^2\sin\theta}\frac{d}{d\theta}\left(\sin\theta\frac{dP}{d\theta}\right)\right] + \frac{1}{Q}\frac{d^2Q}{d\varphi^2} = 0 \tag{A.4}$$

Only the last term on the left hand side depends on φ and so it has to be equal to a constant, denoted by $(-m^2)$. So the differential equation for φ is:

$$\frac{1}{Q}\frac{d^2Q}{d\varphi^2} = -m^2 \tag{A.5}$$

This is a wave equation and its solution is

$$Q = e^{\pm im\varphi} \tag{A.6}$$

m has to be an integer because otherwise Q is not unique.
The equation for the θ-part, namely for $P(\theta)$ is:

$$\frac{1}{\sin\theta}\frac{d}{d\theta}\left(\sin\theta\frac{dP}{d\theta}\right)+\left[l(l+1)-\frac{m^2}{\sin^2\theta}\right]P=0 \tag{A.7}$$

This is the differential equation for the spherical functions, namely it has the form of the associated Legendre differential equation. Its solution has the form of the associated Legendre polynomials $P_l^m(\cos\theta)$. $l(l+1)$ is another real constant.
For $R(r)$ we get:

$$\frac{d^2R}{dr^2}-\frac{l(l+1)}{r^2}U=0 \tag{A.8}$$

This is the radial equation. The solution is:

$$U=Ar^{l+1}+Br^{-l} \tag{A.9}$$

A.2. Associated Legendre functions and spherical harmonics

We start from equation (A.7). In this equation we introduce the parameter $x = \cos\theta$. Then it takes the form:

$$\frac{d}{dx}\left[(1-x^2)\frac{dP}{dx}\right]+\left[l(l+1)-\frac{m^2}{1-x^2}\right] \tag{A.10}$$

This is the associated Legendre differential equation. For $m^2 = 0$ we get the ordinary Legendre differential equation with the Legendre polynomials of the order l, $P_l(x)$, as solutions. For the 5 lowest orders they are:

$$P_0(x) = 1 \tag{A.11}$$
$$P_1(x) = x \tag{A.12}$$
$$P_2(x) = \frac{1}{2}(3x^2-1) \tag{A.13}$$
$$P_3(x) = \frac{1}{2}(5x^3-3x) \tag{A.14}$$
$$P_2(x) = \frac{1}{8}(35x^4-30x^2+3) \tag{A.15}$$

They fulfill an orthogonality relation:

$$\int_{-1}^{1} P_{l'}(x)P_l(x)dx=\frac{2}{2l+1}\delta_{l'l} \tag{A.16}$$

We are searching for the solutions of the associated Legendre differential equation, i.e. solutions for arbitrary l and m. We get the so-called associated Legendre functions or polynomials, respectively, as solutions. They also form a set of orthogonal functions:

$$\int\limits_{-1}^{1} P_{l'}^{m}(x)P_{l}^{m}(x)dx = \frac{2}{2l+1}\frac{(l+m)!}{(l-m)!}\delta_{l'l} \tag{A.17}$$

In the previous section we split the Laplacian equation into a product of functions, each depending only on one of the variables r, θ, and φ. The solution for the angular part, i.e. for the part depending on θ and φ is:

$$Q(\varphi)P(\theta) = e^{\pm im\varphi}P_l^m(\cos\theta) \tag{A.18}$$

The Qs form a complete set of orthogonal functions on the interval $0 \leq \varphi \leq 2\pi$ with respect to m and the P_l^m form such a set for each value of m with respect to l on the interval $-1 \leq \cos\theta \leq 1$. Therefore the product of these functions above also forms a complete set of orthogonal functions with respect to l and m on the surface of the unit sphere. From (A.17) we can derive the convenient normalisation factor and we get the so-called spherical harmonics $Y_{lm}(\theta,\varphi)$:

$$Y_{lm}(\theta,\varphi) = \sqrt{\frac{2l+1}{4\pi}\frac{(l-m)!}{(l+m)!}}P_l^m(\cos\theta)e^{im\varphi} \tag{A.19}$$

A.2.1. Orthogonality relation, completeness and symmetry of the spherical harmonics

A symmetry relation of the spherical harmonics concerning complex conjugation is

$$Y_{l-m} = (-1)^m Y_{lm}^{\star}(\theta,\varphi) \tag{A.20}$$

Their orthogonality relation reads as follows:

$$\int\limits_{0}^{2\pi} d\varphi \int\limits_{0}^{\pi} \sin\theta d\theta Y_{l'm'}^{\star}(\theta,\varphi)Y_{lm}(\theta,\varphi) = \delta_{l'l}\delta_{m'm} \tag{A.21}$$

And the completeness relation is

$$\sum_{l=0}^{\infty}\sum_{m=-l}^{l} Y_{lm}^{\star}(\theta',\varphi')Y_{lm}(\theta,\varphi) = \delta(\varphi-\varphi')\delta(\cos\theta-\cos\theta') \tag{A.22}$$

For the special case of $m = 0$ we get

$$Y_{l0}(\theta,\varphi) = \sqrt{\frac{2l+1}{4\pi}}P_l(\cos\theta) \tag{A.23}$$

For the first three values of l and $m \geq 0$ the spherical harmonics are:

$l=0$	$Y_{00} = \frac{1}{4\pi}$
$l=1$	$Y_{11} = -\sqrt{\frac{3}{8\pi}} \sin\theta e^{i\varphi}$
	$Y_{10} = \sqrt{\frac{3}{4\pi}} \cos\theta$
$l=2$	$Y_{22} = \frac{1}{4}\sqrt{\frac{15}{2\pi}} \sin^2\theta e^{2i\varphi}$
	$Y_{21} = -\sqrt{\frac{15}{8\pi}} \sin\theta\cos\theta e^{i\varphi}$
	$Y_{20} = \sqrt{\frac{5}{4\pi}} (\frac{3}{2}\cos^2\theta - \frac{1}{2})$
$l=3$	$Y_{33} = -\frac{1}{4}\sqrt{\frac{35}{4\pi}} \sin^3\theta e^{3i\varphi}$
	$Y_{32} = \frac{1}{4}\sqrt{\frac{105}{2\pi}} \sin^2\theta\cos\theta e^{2i\varphi}$
	$Y_{31} = -\sqrt{\frac{21}{4\pi}} \sin\theta(5\cos^2\theta - 1)e^{i\varphi}$
	$Y_{11} = \sqrt{\frac{7}{4\pi}} (\frac{5}{2}\cos^3\theta - \frac{3}{2}\cos\theta)$

A.2.2. Expansion of functions in spherical harmonics

An arbitrary function can be expanded in a series of spherical harmonics:

$$f(\theta,\varphi) = \sum_{l=0}^{\infty} \sum_{m=-l}^{l} A_{lm} Y_{lm}(\theta,\varphi) \tag{A.24}$$

The expansion coefficients A_{lm} are given by

$$A_{lm} = \int d\Omega Y^{\star}_{lm}(\theta,\varphi) f(\theta,\varphi) \tag{A.25}$$

The general solution of a boundary value problem in spherical coordinates can be expanded in spherical harmonics and powers of r:

$$\Phi(r,\theta,\varphi) = \sum_{l=0}^{\infty} \sum_{m=-l}^{l} \left[A_{lm} r^l + B_{lm} r^{-(l+1)}\right] Y_{lm}(\theta,\varphi) \tag{A.26}$$

The coefficients are determined by the boundary conditions.

A.3. The law of Gauss

This section is mainly based on [26].
To derive the law of Gauss we define the electrical flow first:

$$\Psi = \int d\boldsymbol{A} \cdot \boldsymbol{E} \tag{A.27}$$

where $d\boldsymbol{A} = dA \cdot \boldsymbol{n}$ and $\boldsymbol{n}$ is the normal to the surface $\boldsymbol{A}$ pointing outwards and A is a closed surface surrounding a volume V. The law of Gauss describes the relation between the electric flow through a surface and the charges contained in the volume which has this surface A as its boundary. One considers a surface A which surrounds the origin of the coordinate system.
The following relation holds:

$$\cos\vartheta dA = r^2 d\Omega \tag{A.28}$$

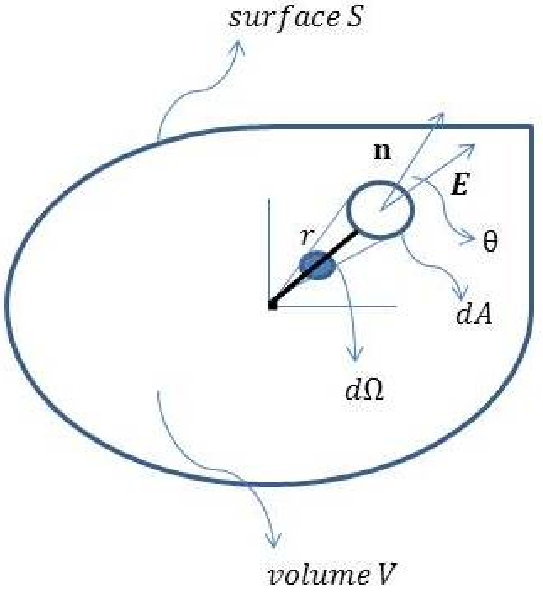

Figure A.1.: Plot of the surface S enclosing the volume V. $\boldsymbol{n}$ is the normal vector to the surface A. The normal component of the electrical field is integrated over the closed surface S. The space angle $d\Omega$ over the charge q yields 4π if the charge lies within the surface and 0 otherwise.

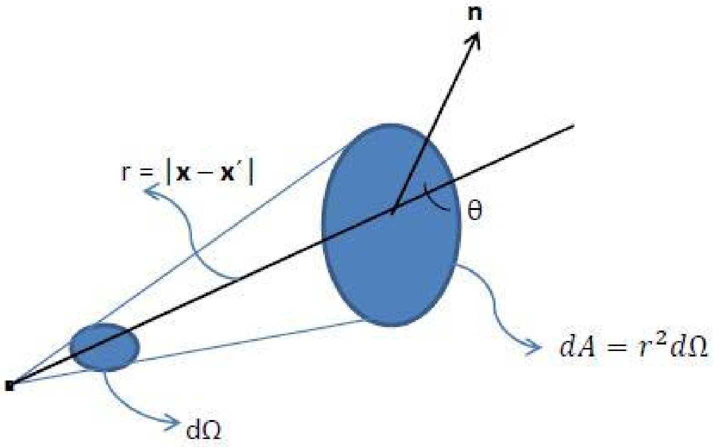

Figure A.2.: Graphical illustration of the formula $\cos\vartheta dA = r^2 d\Omega$.

The electric flow through the surface element dA is $\boldsymbol{E}\cdot\boldsymbol{n}dA$ and with

$$\begin{aligned}\boldsymbol{E} &= q\frac{\boldsymbol{r}}{|\boldsymbol{r}|^3} && \text{(A.29)}\\ |\boldsymbol{E}| &= q|\frac{\boldsymbol{r}}{|\boldsymbol{r}|^3}| && \text{(A.30)}\\ E &= q\frac{1}{r^2} && \text{(A.31)}\end{aligned}$$

where $r = |\boldsymbol{r}|$ is the absolute value of $\boldsymbol{r}$, the flow becomes:

$$\begin{aligned}\boldsymbol{E}\cdot\boldsymbol{n}dA &= |\boldsymbol{E}||\boldsymbol{n}|\cos\theta dA = && \text{(A.32)}\\ &= q\frac{1}{r^2}\cos\theta dA = qd\Omega && \text{(A.33)}\end{aligned}$$

Furthermore we have $\int_S d\Omega = 4\pi$ or $4\pi r^2$ but $r = 1$. $4\pi r^2$ is the surface of a sphere. This means that our volume is a sphere. Using this result we get for the electric flow:

$$\oint_S \boldsymbol{E}\cdot\boldsymbol{n}dA = \oint_S \boldsymbol{E}d\boldsymbol{A} = 4\pi\cdot q \qquad \text{(A.34)}$$

The **law of Gauss** is in words: The electric flow going through a closed surface is 4π times the charge contained in the surrounded volume. If the charge lies *outside* of the sphere we have no contribution to the electric flow. So we have the following form of Gauss law for a single charge in the volume:

$$\oint_S d\boldsymbol{A}\cdot\boldsymbol{E} = 4\pi q \text{ if } q \text{ lies within } A \tag{A.35}$$

$$\oint_S d\boldsymbol{A}\cdot\boldsymbol{E} = 0 \text{ otherwise} \tag{A.36}$$

We can generalize this equation for a continuous charge distribution $\rho(\boldsymbol{r})$:

$$\oint d\boldsymbol{A}\cdot\boldsymbol{E} = 4\pi\int_V d\boldsymbol{r}\rho(\boldsymbol{r}) \tag{A.37}$$

For several point charges we get:

$$\oint d\boldsymbol{A}\cdot\boldsymbol{E} = 4\pi\sum_i q_i \tag{A.38}$$

Now we use the integral relation of Gauss which we know from vector analysis:

$$\oint_{\partial V} d\boldsymbol{A}\cdot\boldsymbol{G} = \int_V dr\boldsymbol{\nabla}\cdot\boldsymbol{G} \tag{A.39}$$

where $\boldsymbol{G}$ is an arbitrary vector field.
We use this equation for A.37 and get:

$$\oint d\boldsymbol{A}\cdot\boldsymbol{E} = \int_V d\boldsymbol{r}\boldsymbol{\nabla}\cdot\boldsymbol{E} \tag{A.40}$$

This is the differential form of Gauss law. Since V is arbitrary we get the first Maxwell equation:

$$\boldsymbol{\nabla}\cdot\boldsymbol{E} = 4\pi\rho(\boldsymbol{r}) \tag{A.41}$$

Since $\boldsymbol{E} = -\boldsymbol{\nabla}\Phi$ we immediately get the Poisson equation

$$\Delta\Phi(\boldsymbol{r}) = -4\pi\rho(\boldsymbol{r}) \tag{A.42}$$

which becomes the Laplace equation if $\rho = 0$.

A.4. Maxwell equations

Coulomb´s law	$\boldsymbol{\nabla}\cdot\boldsymbol{D} = 4\pi\rho$
Ampere´s law	$\boldsymbol{\nabla}\times\boldsymbol{H} = 4\pi\boldsymbol{j}$
Faraday´s law of induction	$\boldsymbol{\nabla}\times\boldsymbol{E} + \frac{\partial \boldsymbol{B}}{\partial t} = 0$
There exist no free magnetic charges	$\boldsymbol{\nabla}\cdot\boldsymbol{B} = 0$

These are the macroscopic Maxwell equations (i.e. the Maxwell equations in matter for the presence of external sources $\boldsymbol{j}$ and ρ) in atomic units. The microscopic Maxwell equations (i.e. the Maxwell equations in vacuum) are just these equations with $\boldsymbol{j} = 0$ and $\rho = 0$.

Bibliography

[1] **J. A. Iriazabal**, *Coupling of Electrons and Electromagnetic Surface Modes in Scanning Transmission Electron Microscopy*, Doctoral thesis at the University of the Basque Country, (October 1998).

[2] **C. Davisson and L. H. Germer**, Phys. Rev. **30**, 705 (1927).

[3] **G. Rutherman**, Ann. Phys. **2**, 113 (1948).

[4] **J. Hillier, R. F. Baker**, *Microanalysis by Means of Electrons*, J. Appl. Phys. **15**, 663-675.

[5] **G. E. Leithäuser**, *Über den Geschwindigkeitsverlust, welchen die Kathodenstrahlen beim Durchgang durch dünne Metallschichten erleiden, und über die Ausmessung magnetischer Spektren*, Ann. Phys. **15**, 283-306 (1904).

[6] **F.J. Garcia de Abajo**, *Optical Excitations in Electron Microscopy*, Reviews Of Modern Physics, Volume **82**, (January-March 2010).

[7] **A. Rivacoba, N. Zabala, J. Aizpurua**, *Image Potential in Scanning Transmission Electron Microscopy*, Progress in Surface Science **65**, (2000).

[8] **P. Hollister, J.-W. Weener, C. R. Vas, T. Harper**, *Nanoparticles*, Cientifica, Technology White Papers Nr. 3 (October 2003).

[9] **A. Trügler**, *Strong Coupling Between a Metallic Nanoparticle and a Single Molecule*, Diploma thesis at the Karl-Franzens University Graz (2007).

[10] *Nanopartikel - Mächtige Waffen gegen den Krebs*, Stand: 14.4.2010, `http://www.welt.de/gesundheit/article7175834/Nanopartikel-Maechtige-Waffen-gegen-den-Krebs.html` (abgerufen am 21.8.2011).

[11] *Nano-Cocktail tötet Krebszellen binnen 24 Stunden*, Stand: 19.4.2011, `http://www.welt.de/gesundheit/article13213129/Nano-Cocktail-toetet-Krebszellen-binnen-24-Stunden.html` (abgerufen am 10.10.2011).

[12] **Anja Scholzen**, *Nano-Gold im Schwangerschaftstest*, Stand: 29.3.2003, `www.welt.de/print-welt/article551132/Nano_Gold_im_Schwangerschaftstest.html` (abgerufen am 21.8.2011).

[13] **H. Hildebrand, K. Mackenzie, F.-D. Kopinke**, *Einsatz von Nano-Katalysatoren zur Abwasserreinigung*, Chem. Ing. Tech. **79** (9), 1461-1462.

[14] **Martin Brinkmann**, *Hightech in der Haut - Autolack von morgen*, Stand: 1.12.2005, `http://www.spiegel.de/auto/aktuell/0,1518,387405,00.html` (abgerufen am 21.8.2011).

[15] **Franziska Badenschier**, *Interview: Nanopartikel in Lebensmitteln*, Stand: 30.6.2010, `http://www.planet-wissen.de/natur_technik/forschungszweige/nanotechnologie/interview_vengels.jsp` (abgerufen am 21.8.2011).

[16] **Annett Klimpel**, *Nanoteilchen im Milchshake*, Stand: 22.1.2008, `http://www.welt.de/welt_print/article1579891/Nanoteilchen_im_Milchshake.html` (abgerufen am 21.8.2011).

[17] **Andreas Braun, Gabor Paal**, *Nanotechnologie: Fortschritt mit Risiken*, Stand: 21.10.2009, `http://www.swr.de/auto/contra/-/id=7612/nid=7612/did=5518658/1bxvgrg/index.html` (abgerufen am 21.8.2011).

[18] **Daniel Münter**, *Nano-Sonnencreme*, Stand: 6.8.2002, `http://www.wdr.de/tv/quark/sendungsbeitraege/2002/0806/006_nano.jsp.html` (abgerufen am 21.8.2011).

[19] **Wolfgang Löhr** *Sonnencreme könnte Hirn aufweichen*, Stand: 11.7.2008, `http://www.taz.de/1/archiv/archiv/?dig=2006/07/11/a0108` (abgerufen am 21.8.2011).

[20] **R. F. Egerton**, *Electron Energy Loss Spectroscopy in the TEM*, Rep. Prog. Phys. **72** (2009).

[21] **W. Demtröder**, *Experimentalphysik Band 2: Elektrizität und Optik*, (Springer 2004).

[22] **R. H. Ritchie**, *Plasmon Losses by Fast Electrons in Thin Films*, Phys. Rev. **106**, 874–81 (1957).

[23] **S. A. Maier**, *Plasmonics - Fundamentals and Applications*, Springer (2007).

[24] **N. W. Ashcroft, N. D. Mermin**, *Festkörperphysik*, (Oldenbourg, München, 2001).

[25] **C. Kittel**, *Einführung in die Festkörperphysik*, (Oldenbourg, München, 1999).

[26] **J. D. Jackson**, *Classical Electrodynamics*, Wiley, New York (1999, third edition).

[27] **U. Hohenester, A. Trügler**, *MNPBEM - A Matlab Toolbox for the Simulation of Plasmonic Nanoparticles*, (2011).

[28] **D. J. Griffiths**, *Introduction to Electrodynamics*, Prentice Hall, New Jersey (1999, third edition).

[29] **R.Goloskie,T.Thio,L.R. Ram-Mohan**, Computers in Phys. **10**, 477 (1996).

[30] **E. Fermi**, *The Ionization Loss of Energy in Gases and in Condensed Materials*, Phys. Rev. **57**, 485-493.

[31] **R. H. Ritchie, A. Howie**, Philos. Mag. A **58**, 753, (1988).

[32] **C. Meffert**, *Mie-Streuung an sphärischen Partikeln*, (Hauptseminar WS 2004/05).

[33] **G. Mie**, *Beiträge zur Optik trüber Medien, speziell kolloidaler Metalllösungen*, Ann. Phys. **25**, 377 (1908).

[34] **F. J. Garcia de Abajo**, *Relativistic Energy Loss and Induced Photon Emission in the Interaction of a Dielectric Sphere with an External Electron Beam*, Phys. Rev. B **59**, (1998).

[35] **T. L. Ferrell, P. M. Echenique**, *Generation of Surface Excitations on Dielectric Spheres by External Electron Beam*, Phys. Rev. Letters **55**, (1985).

[36] **A. Rivacoba and P.M. Echenique**, *Surface Corrections to Bulk Energy Losses in Scanning Transmission Electron Microscopy of Spheres*, Scanning Microscopy, Vol. **4**, No. 1 (1990).

[37] **W. Nolting**, *Grundkurs Theoretische Physik 3: Elektrodynamik*, Springer (2007).

[38] **N. Zabala, A. Rivacoba**, *Electron Energy Loss Near Supported Particles*, Phys. Rev. B, Volume **48**, (1993).

[39] **T. L. Ferrell, R. J. Warmack, V. E. Anderson, P. M. Echenique**, *Analytical calculation of Stopping Power for Isolated Small Spheres*, Phys. Rev. B **35**, (1987).

[40] **P. M. Echenique, J. Bausells, A. Rivacoba**, *Energy-loss Probability in Electron Microscopy*, Phys. Rev. B **35**, (1987).

[41] **A. Rivacoba, J. Aizpurua, N. Zabala**, *Target Geometry Dependence of Electron Energy Loss Spectra in Scanning Transmission Electron Microscopy (STEM).*

[42] **F. J. Garcia de Abajo, A. Howie**, *Retarded Field Calculation of Electron Energy Loss in Inhomogeneous Dielectrics*, Phys. Rev. B **65**, (2001).

[43] **Wolfram Math World**, *Modified Bessel function of the second kind*, Stand: 30.9.2011, `http://mathworld.wolfram.com/ModifiedBesselFunctionoftheSecondKind.html` (abgerufen am 3.7.2011).

[44] **M. Abramowitz, I. A. Stegun**, *Modified Bessel functions I and K*, in Handbook of Mathematical Functions with Formulas, Graphs, and Mathematical Tables, 9th printing. New York: Dover, pp. 374-377, 1972.

[45] **P. M. Echenique, A. Howie, D. J. Wheatley**, *Excitation of Dielectric Spheres by External Electron Beam*, Phil. Mag. B **56**, (1987).

[46] **P. B. Johnson, R. W. Christy**, *Optical Constants of the Noble Metals*, Phys. Rev. B **6**, (1972).

[47] **T. Fließbach**, *Allgemeine Relativitätstheorie*, Spektrum Akademischer Verlag, (1995).

[48] **Andreas Trügler**, *Optical Properties of Metallic Nanoparticles*, Doctoral thesis at the Karl-Franzens University Graz (2011).

[49] **D. Meschede**, *Gerthsen Physik*, (Springer, 2002).

[50] **O. Madelung**, *Introduction to Solid State Theory*, Springer (1996).

[51] **P. E. Batson**, *Damping of Bulk Plasmons in Small Aluminium Spheres*, Solid State Community **34**, (1980).

[52] **P. E. Batson**, *Inelastic Scattering of Fast Electrons in Clusters of Small Spheres.*

[53] **Carsten Sönnichsen**, *Plasmons in Metal Nanostructures*, Doctoral thesis at the Ludwig-Maximilians-University München (2001).

[54] **U. Hohenester, A. Trügler**, *Interaction of Single Molecules with Metallic Nanoparticles*, (2007).

[55] **S. Kirkup, J. Yazdami**, *A Gentle Introduction to the Boundary Element Method in Matlab/Freemat*, www.boundary-element-method.com (2008).

[56] **W. Nolting**, *Grundkurs Theoretische Physik 5/1: Quantenmechanik*, Springer (2007).

[57] **W. Nolting**, *Grundkurs Theoretische Physik 5/2: Quantenmechanik*, Springer (2007).

[58] **U. Hohenester, H. Ditlbacher, J. R. Krenn**, *Electron-Energy-Loss Spectra of Plasmonic Nanoparticles*, Phys. Rev. Letters **103** (2009).

[59] **C. B. Lang, N. Pucker**, *Mathematische Methoden in der Physik*, (Spektrum Akademischer Verlag, Heidelberg, Berlin, 1998).

[60] **J. Nelayah, M. Kociak, O. Stéphan, F. J. Garcia de Abajo, M. Tence, L. Henrard, D. Taverna, I. Pastoriza-Santos, L. M. Liz-Marzán, C. Colliex**, *Mapping Surface Plasmons on a Single Metallic Nanoparticle*, Nature (2007).

[61] **B. Schaffer, U. Hohenester, A. Trügler, F. Hofer**, *High-resolution Surface Plasmon Imaging of Gold Nanoparticles by Energy-filtered Transmission Electron Microscopy*, Phys. Rev. B **79**, (2008).

[62] **J. Nelayah, L. Gu, W. Sigle, C. T. Koch, I. Pastoriza-Santos, L. M. Liz-Marzán, P. A. van Aken**, *Direct Imaging of Surface Plasmon Resonances on Single Triangular Silver Nanoprisms at Optical Wavelength Using Low-loss EFTEM Imaging*, Optic Letters **34**, (2009).

[63] **H. Ditlbacher, A. Hohenau, D. Wagner, U. Kreibig, M. Rogers, F. Hofer, F. R. Aussenegg, J. R. Krenn**, *Silver Nanowires as Surface Plasmon Resonators*, Phys. Rev. Letters **95**, (2005).

[64] **M. N´Gom, J. Ringwald, J. F. Mansfield, A. Agarwal, N. Kotou, N. J. Zaluzec, T. B. Norris**, *Single Particle Plasmon Spectroscopy of Silver Nanowires and Gold Nanorods*, Nanoletters **20**, (2008).

[65] **F. J. Garcia de Abajo, M. Kociak**, *Probing the Photonic Local Density of States with Electron Energy Loss Spectroscopy*, Phys. Rev. Letters **100**, (2008).

[66] **N. Barberan, J. Bausells**, *Plasmon Excitation in Metallic Spheres*, Phys. Rev. B **31**, (1985).

[67] **M. Achèche, C. Colliex, H. Kohl, A. Nourtier, P. Trebbia**, *Theoretical and Experimental Study of Plasmon Excitations in Small Metallic Spheres*, Ultramicroscopy **20**, (1986) 99.

[68] **U. Hohenester, J. Krenn**, *Surface Plasmon Resonances of Single and Coupled Metallic Nanoparticles: A Boundary Integral Method Approach*, Phys. Rev. B **72**, (2005).

[69] **F. J. Garcia de Abajo, J. Aizpurua**, *Numerical Simulation of Electron Energy Loss Near Inhomogeneous Dielectrics*, Phys. Rev. B **56**, (1997).

[70] **L. Novotny, B. Hecht**, *Principles of Nano-optics*, (Cambridge University Press, 2006).

[71] **H. Raether**, *Surface Plasmons on Smooth and Rough Surfaces and on Gratings*, (Springer, 1988).

[72] **J. M. Pitarke, J. B. Pendry, P. M. Echenique**, *Electron Energy Loss in Composite Systems*, Phys. Rev. B **55**, (1997).

[73] **J. Aizpurua, A. Rivacoba, N. Zabala, F. J. Garcia de Abajo**, *Collective Excitations in an Infinite Set of Aligned Spheres*, Surface Science 402-404 (1998) 418-423.

[74] **Z. L. Wang**, *Transmission Electron Microscopy and Spectroscopy of Nanoparticles*, Characterization of Nanophase Materials (Wiley-VCH Verlag GmbH 2000).